IDENTIFICATION OF NOVEL MOLECULAR PLAYERS IN GBM CELL DISPERSAL

by

Fidan ŞEKER

A dissertation submitted to the

Graduate School of Health Sciences

in Partial Fulfillment of the requirements

for the Degree of

Doctor of Philosophy

in

Cellular and Molecular Medicine

KOÇ ÜNİVERSİTESİ

December 26, 2019

Identification of Novel Molecular Players in GBM Cell Dispersal

Koç University

Graduate School of Health Sciences

This is to certify that I have examined this copy of a doctoral dissertation by

Fidan ŞEKER

and have found that it is complete and satisfactory in all respects,

and that any and all revisions required by the final

examining committee have been made.

Committee members:

_____

Assoc. Prof. Tuğba Bağcı Önder (advisor)

_____

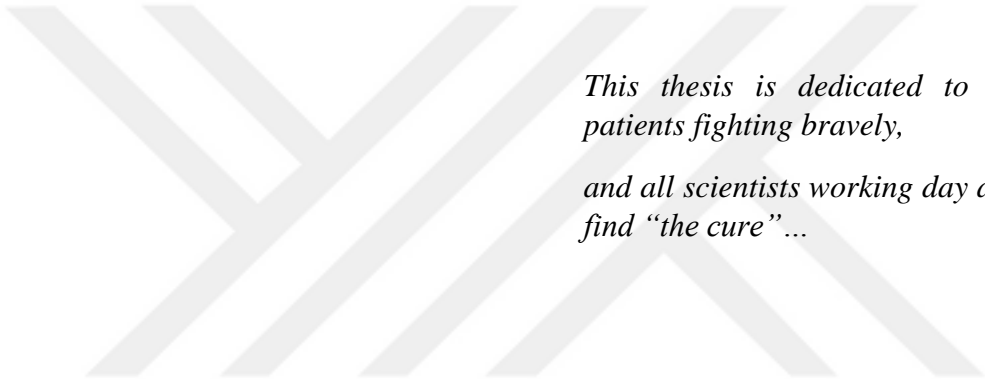Assoc. Prof. Tamer Önder

_____

Prof. İhsan Solaroğlu

_____

Assoc. Prof. Bilal Ersen Kerman

_____

Assoc. Prof. Halil Bayraktar

Date: December 26, 2019

This thesis is dedicated to all cancer patients fighting bravely,

and all scientists working day and night to find "the cure"…

ABSTRACT

Identification of Novel Molecular Players in GBM Cell Dispersal

Fidan ŞEKER

Doctor of Philosophy in Cellular and Molecular Medicine

December 26, 2019

GBM is the most common and malignant primary brain tumor. Despite the advances in diagnosis and treatment, GBM is still one of the deadliest human cancers. In case of highly aggressive tumors as GBM, tumor cells infiltrate and invade to normal neural tissue. Despite tumor removal, invasive GBM cells remain embedded into CNS which is resistant to chemo-radiotherapy and responsible from recurrence of the disease. Dissemination of invasive GBM cells results failure of the current therapeutic strategies in long term. High mortality rates of GBM patients are partly attributed to the invasive behavior of tumor cells, which show extensive infiltration into adjacent brain tissue leading to rapid and almost inevitable recurrence. Given the additional chemo- and radio-resistant characteristics of these invasive cells "left behind" after surgical resection, conventional therapies remain ineffective. Therefore, understanding the mechanisms of GBM cell invasiveness is of utmost priority to develop successful therapeutic approaches.

In this study, we analyzed the dynamic changes in transcriptome of motile (dispersive) and non-motile (core) GBM cells and identified *SERPINE1* as a dramatically induced gene in the dispersive cell populations. We showed that genetic or pharmacological inhibition of SERPINE1 led to reduction of dispersal, attributing a functional role for SERPINE1 in dispersal. Furthermore, we demonstrated that SERPINE1 regulates cell-substrate adhesion and directional movement of GBM cells, and that its expression is regulated by TGFβ signaling. Together, our results suggest that SERPINE1 is a key player in GBM dispersal providing insight into the future design of anti-invasive therapies.

ÖZETÇE

GBM Hücre Dağılmasında Rol Oynayan Özgün Moleküler Faktörlerin Keşfi

Fidan ŞEKER

Hücresel ve Moleküler Tıp, Doktora

26 Aralık 2019

GBM en sık görülen ve en kötü huylu primer beyin tümörüdür. Teşhis ve tedavideki gelişmelere rağmen GBM hala en ölümcül insan tümörlerindendir. GBM gibi oldukça agresif tümörlerde tümör hücreleri normal nöral dokuya hücum eder ve sızarlar. Tümörün ameliyatla alınmasına rağmen, kemoterapi ve radyoterapiye dirençli invazif tümör hücreleri merkezi sinir sistemine gömülü halde kalır ve tümörün nüksetmesine sebep olur. Invazif GBM hücrelerinin beyne dağılması güncel tedavi strajilerinin uzun zaman diliminde işe yaramaması ile sonuçlanır. GBM hastalarında görülen yüksek ölüm oranlarının önemli sebeplerinden biri de hücrelerin yakın beyin dokularına yüksek oranda hücum ederek, hızlı ve neredeyse kaçınılmaz bir şekilde tümörün nüksetmesine sebep olan invazif davranışlarıdır. Tümör ameliyat ile alındıktan sonra "geri kalan" invazif hücrelerin kemoterapi ve radyoterapiye dirençli olmalarından dolayı alışılagelmiş tedaviler etkili olmamaktadır. Bu nedenle GBM hücre invazyon mekanizmalarını anlamak başarılı tedavi yaklaşımları geliştirmek için en önemli önceliktir.

Bu tez çalışmasında hareketli (dağılan) ve hareketsiz (dağılmadan merkezde kalan) GBM hücrelerinin transkriptomlarındaki dinamik değişiklikler analiz edilmiştir ve *SERPINE1* geninin dağılan hücrelerde çarpıcı şekilde indüklenerek ifade edildiği saptanmıştır. SERPINE1'in genetik ya da farmakolojik olarak kısıtlanmasının, hücre dağılımını azalttığı saptanmıştır. Ayrıca SERPINE1'in, hücrelerin substrata bağlanmasını düzenlediği, hücrelerin yönelimli hareketlerini etkilediği ve SERPINE1 ifadesinin TGFβ sinyali ile düzenlendiği gösterilmiştir. Sonuç olarak çalışmamızın sonuçları SERPINE1'in GBM hücre dağılmasında kilit bir rol oynadığını ve geliştirilecek anti-invazif tedaviler için önemli bir hedef olabileceğini göstermiştir.

ACKNOWLEDGEMENTS

TABLE OF CONTENTS

LIST OF TABLES

LIST OF FIGURES

NOMENCLATURE

2-OG	2-oxyglutarate
2-HG	2-hydroxyglutarate
ADAM	A Disintegrin And Metalloproteinase
ALT	Alternative Lengthening of Telomeres
BBB	Blood-Brain-Barrier
CAR-T	Chimeric Antigen Receptor T
CHAT	Cancer Hallmarks Analytics Tool
CNS	Central Nervous System
ECM	Extracellular Matrix
EGFR	Epidermal Growth Factor Receptor
ERK	Extracellular Signal Regulated Kinase
EMT	Epithelial to Mesenchymal Transition
FAK	Focal Adhesion Kinase
FDA	Food and Drug Administration
FGF	Fibroblast Growth Factor
GBM	Glioblastoma Multiforme
GSC	Glioma Stem Cell
G-CIMP	Glioma CpG Island Methylator Phenotype
HGF	Hepatocyte Growth Factor
HIF	Hypoxia Inducable Factor
IDH	Isocitrate Dehydrogenase
JHDM	Jumonji C domain containing Histone Demethylase
KDM	Lysine Demethylase

MAPK	Mitogen-Activated Protein Kinase
MET	Mesenchymal to Epithelial Transition
MGMT	Methyl Guanine Methyl Transferase
MMP	Matrix Metalloproteinase
MMR	Mismatch Repair
PA	Plasminogen Activator
PAI-1	Plasminogen Activator Inhibitor 1
PDGFR	Platelet Derived Growth Factor Receptor
PTEN	Phosphatase and Tensin
RTK	Receptor Tyrosine Kinase
SERPINE1	Serine Protease Inhibitor Clade E
TCGA	The Cancer Genome Atlas
TGFβ	Transforming Growth Factor β
TERT	Telomerase Reverse Transcriptase
TMZ	Temozolomide
tPA	Tissue Plasminogen Activator
uPA	Urokinase Plasminogen Activator
uPAR	Urokinase Plasminogen Activator Receptor

1. INTRODUCTION

1.1. Glioblastoma Multiforme (GBM)

The most common type of brain cancer is malignant glioma, which arises from the glial cells present in the central nervous system[1]. Gliomas include astrocytomas, oligodendrogliomas and ependymomas with infiltrating astrocytomas. Within each glial cell lineage, gliomas are divided into grades of increasing aggressiveness from grade I to grade IV by World Health Organization based on histopathological criteria[2]. Grade IV tumors are referred as Glioblastoma multiforme (GBM) which is the most common and malignant primary brain tumor[3]. Glioblastoma may develop in different ways: a primary (or *de novo*) glioblastoma may arise rapidly without any evidence of a prior lesion; whereas a secondary glioblastoma may arise by progressing from a lower grade astrocytoma[2]. These aggressive brain tumors are characterized by high cellular proliferation, diffuse infiltration of tumor cells to the central nervous system, high levels of angiogenesis, nuclear atypia and presence of necrotic areas[1] as given in **Figure *1.1*** and **Figure *1.2***. GBM affects 20000 patients per year and the peak age is 50-60. GBM is still one of the deadliest human cancers, despite the advances in diagnosis and treatment, life expectancy still remains at approximately 12-18 months[4].
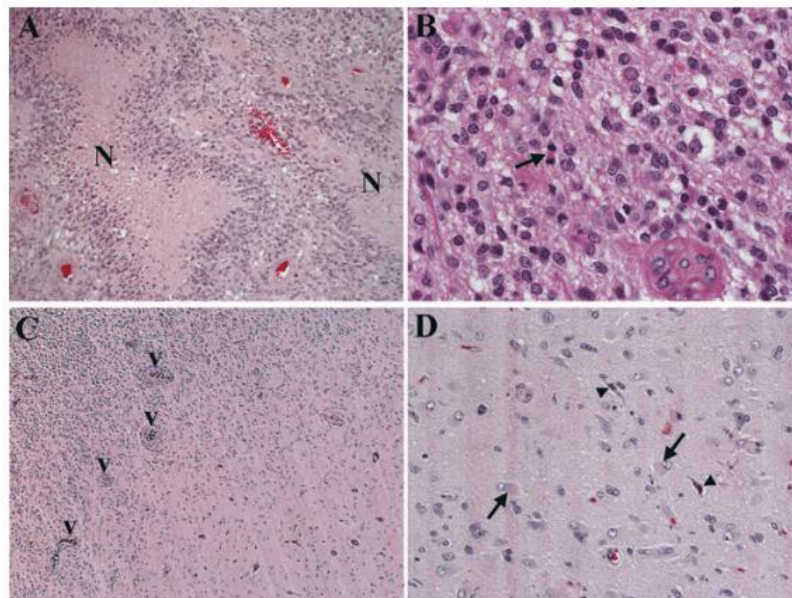
Figure 1.1. Histology of GBM. A. Sample tumor core shows tumor necrosis (N) with pseudopalisading glioma cells. B. High magnification image from tumor core sample indicates pleomorphic and nuclear atypical glioma cells. C. Sample from tumor border shows microvascular proliferation (V). The unclear border indicates that tumor cells have invaded into

brain diffusely. D. Sample from tumor rim demonstrates invading glioma cells (arrowhead) which are elongated and have atypical nuclei. These cells are surrounded by reactive astrocytes (arrow)[5].
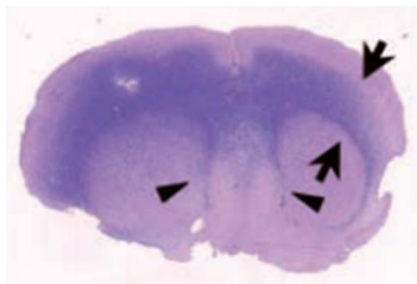
Figure 1.2. Growth characteristics of GBM. Invasive GBM cells infiltrate into brain tissue, these cells may extend through corpus callosum to contralateral brain as shown with the arrows. This butterfly-like growth pattern is the characteristic of human GBM[6].

1.1.1. Molecular Genetics and Molecular Subtypes of GBM

To better understand the biology of GBM tumors, molecular gene signatures were identified which are directly or indirectly responsible for the aggressiveness of this tumor type. Based on The Cancer Genome Atlas (TCGA) which is a cancer genomics program that provides molecular information for different cancer types including GBM, mutations were increased in the leading aberrant pathways in GBM. These mutations and the de-regulations in related pathways are the main pillars that contribute to the therapy resistance, poor patient survival and aggressive disease progression[7–9].

There are some mutation signatures in more specific to primary GBM, not seen commonly in secondary GBM. In primary GBM, one of the most common mutations is telomerase reverse transcriptase (TERT) promoter mutation which is associated with increased telomerase expression and amplified telomerase activity[10]. Aberrations of epidermal growth factor receptor (EGFR) is seen in 57% of GBM, which can arise as EGFR mutation, rearrangement, altered splicing and/or amplification[11] which highlights the key role of this receptor in GBM. Loss of NF1 is seen in primary mesenchymal GBM, highlighting its role in driver of mesenchymal transition[12,13]. Since NF1 is a tumor suppressor and a Ras-GTPase, NF1 exerts its affects in deregulations of MAPK pathway[14]. PDGFRA amplification is the second common alterations dysregulating RTK signaling in GBM and results in constitutively active RTK signaling[15].

Chapter 1: Introduction

The molecular signature of secondary GBM is IDH mutation. Isocitrate dehydrogenase, IDH, is an enzyme works in the Crebs cycle and responsible from turning isocitrate to 2-oxogluterate (2-OG). A point mutation in IDH1 (R132H) changes the enzymatic activity of IDH1 and results in accumulation of an oncometabolite, 2-hydroxygluterate (2-HG) instead of 2-OG[16]. 2-HG accumulation causes a methylation phenotype by inhibiting TET enzymes that de-methylate DNA and KDM/JHDM enzymes that de-methylate histones[17], together generates a glioma CpG island methylator phenotype (G-CIMP)[4,18]. These mutations change gene expression and further oncogenic transformation[19]. ATRX mutation or loss is another secondary GBM signature affecting genome integrity by promoting non-telomerase-dependent telomere lengthening mechanism named alternative lengthening of telomeres (ALT)[20–22].

Some aberrations are commonly seen in both primary and secondary GBMs. Loss of cyclin-dependent kinase inhibitor 2A (CDKN2A) is a mutation which is seen both primary and secondary GBMs and affecting Rb pathway[14]. PTEN loss in PI3K signaling is one of the main drivers of GBM cell proliferation. PI3K pathway induces cellular proliferation responding the presence of growth factors. PTEN is a negative regulator of PI3K pathway[23], loss of PTEN results in elevated activity of PI3K pathway, leading increased proliferation. Similarly, PI3K mutations leading the increased activity of this pathway is also very common, but interestingly, commonly seen in only primary GBM. TP53 mutation is another very commonly seen mutations in GBM, these mutations are generally gain-of-function mutations of oncogenic p53 protein variants. Deregulations in p53 pathway is linked with almost malignant properties of GBM as invasion, proliferation and evasion from apoptosis and cancer cell stemness[24]. RB1 loss results in dysregulation of cell cycle since its phosphorylation induces E2F phosphorylation and G1 to S phase transition[25].

The genetic abnormalities and affected signaling pathways are summarized in

Table *1.1*.

Table 1.1. Genetic abnormalities and altered signaling pathways in Glioblastoma. Adapted from Li et.al., 2016[14].

Genetic abnormalities	Frequency	Altered Signaling Pathways
Primary GBM		
TERT promoter mutation	60-80%	Telomere maintenance
CDKN2A loss	31-78%	Rb pathway
EGFR amplification	36-60%	RTK signaling
EGFR vIII	25-50%	RTK signaling
PTEN loss	36-41%	PI3K signaling
TP53 mutation	28-35%	P53 pathway
PI3K mutation	15-25%	PI3K signaling
NF1 loss	10-18%	MAPK signaling
RB1 loss	14%	Rb pathway
PDGFRA amplification	10-13%	RTK signaling
FGFR3-TACC3 fusion	3%	RTK signaling
Secondary GBM		
IDH mutation	60-80%	Metabolism
TP53 mutation	65%	P53 pathway
ATRX mutation or loss	57%	Genome integrity
RB1 loss	43%	Rb pathway
CDKN2A loss	19%	Rb pathway
PTPRZ1-Met fusion	15%	RTK signaling
PTEN loss	4%	PI3K signaling

Molecular information available from TCGA data also revealed that GBM can be subclassified since different subtypes carry distinctive molecular signatures and different disease progression. GBM has 4 subtypes as classical, mesenchymal, proneural and neural as described in **Figure *1.3***. Tumors that has a molecular signature fit to classical subtype are more proliferative while the ones fit to mesenchymal subtype are more invasive. Also, recurrent and therapy resistant tumors are enriched in mesenchymal subtype[26–28]. These two subtypes are associated with poor prognosis compared to the proneural and neural subtypes[29].

Molecular signature of classical subtype is linked to epidermal growth factor receptor (EGFR) amplification. Mesenchymal subtype is linked to MET and CD44 overexpression, nuclear factor-kappaB signaling is and neurofibromatosis type 1 (NF1) loss or mutation. On the other hand, Isocitrate dehydrogenase 1 (IDH1) mutations and platelet-derived growth factor receptor alpha (PDGFRα) amplification is a signature for proneural subtype. However, cells from the neural subtype tumors are generally associated with normal brain tissue and express neuronal markers[30].
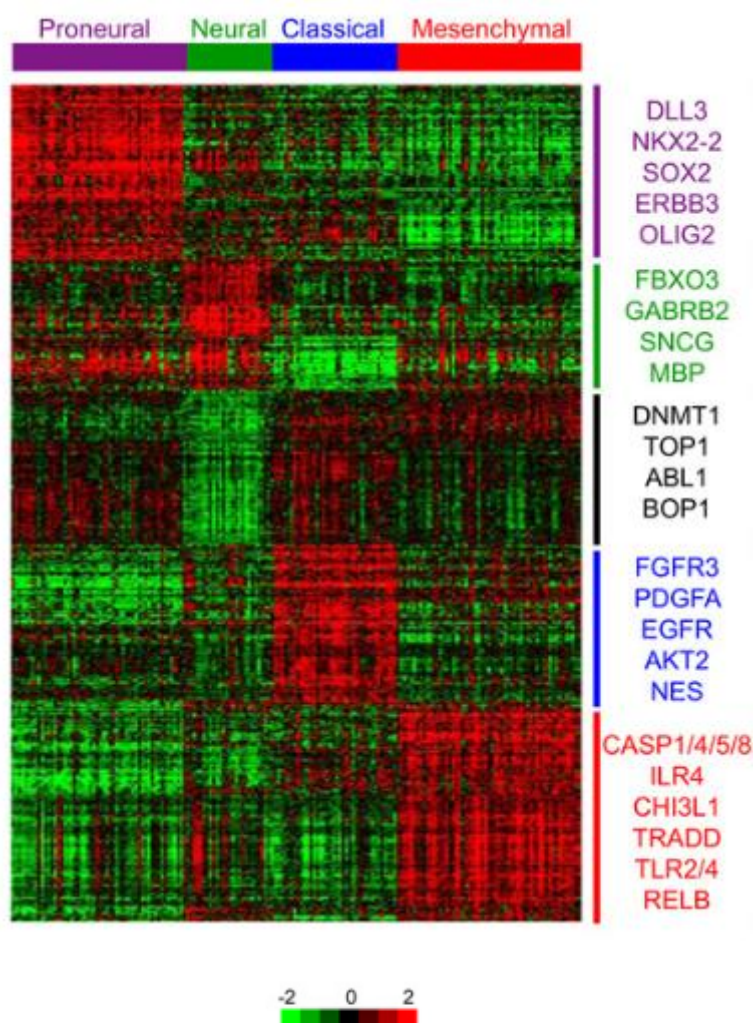
Figure 1.3. Gene expression data of GBM subtypes. GBM has 4 subtypes which has different gene expression signatures; these subtypes are proneural, neural, classical and mesenchymal[4].

1.1.2. Current Treatment of GBM and Developments in GBM Therapy

The current treatment for GBM patients is the maximal safe tumor resection followed by the Stupp protocol, which is radiotherapy combined with concurrent daily temozolomide followed by adjuvant temozolomide treatment[8]. TMZ (Temodar; FDA approval: 1997) is a

Chapter 1: Introduction

DNA alkylating agent that delivers a methyl group on specific sites of purine bases of DNA at the O6 and N7 positions of guanine and N position of adenine[31]. O6 methylguanine is the main cause of TMZ toxicity[32,33] which mispairs with thymidine instead of cytosine. This mispairing induces MMR pathway which can excise mispaired thymidine but cannot remove O6 methylguanine. These repeated cycles cause DNA double strand breaks, cell cycle arrest at G2/M phase and induces apoptosis toxicity[34]. The differential response that GBM patients have for TMZ treatment and radiotherapy is linked to the MGMT (O6-methylguanidine DNA methyltransferase) methylation status[35]. MGMT encodes for a DNA repair protein that inhibits DNA repair after TMZ treatment; as a result, the patients whose tumor cells have methylated MGMT promoter have a better response to TMZ treatment and have longer overall survival. This makes MGMT promoter methylation both a predictive factor for TMZ response and a prognostic factor for survival[35].

Other than TMZ, 2 other FDA approved oncology drugs are routinely used for GBM treatment; biodegradable carmustine (BCNU) wafers (Gliadel; FDA approval: 1995) and bevacizumab (Avastin; FDA approval: 2009 for recurrent GBM). Despite the increasing molecular and clinical knowledge, GBM treatment options have not advanced. Even though these standard therapies increases the median overall survival time of GBM patients, the tumor recurs in nearly all cases[36]. For this reason, designing new therapeutics by comprehending the aggressive and complex nature of GBM cells is an urgent need[37]. Immune checkpoint inhibitors, especially the ones targeting PD-1 and CTLA-4 are currently being examined in clinical trials for GBM treatment. CAR T cells, which is constructed from patients' tumor by examining antigens of these tumors and identifying the ones that is specific to tumor, is another immunotherapy approach in clinical trials for GBM. In these trials, several GBM antigens related with GBM development and progression are being targeted. Dendritic cell therapy is another personalized medicine application, which aims to target multiple GBM antigens by using tumor lysates, RNA, peptides and products of cancer stem cells. Vaccination with neo-antigens derived from tumor specific protein coding mutations is another immunological strategy. Gliovac vaccine is a promising treatment option in clinical trials[38]. Virotherapy uses genetically engineered oncolytic viruses to target GBM[39]. An example trial is using Aglatimagene besadenovec adenovirus vector to deliver herpes simplex virus thymidine kinase gene followed by valacyclovir which inhibits DNA replication and induces apoptosis[40]. Another strategy is to use neural stem cells loaded with engineered viruses to increase targeted efficiency[37].

Considering the low efficacy of golden standard of GBM treatment, current developments in GBM treatment are inclined towards the problems causing failure of traditional treatment options. Even though a drug can show efficacy *in vitro*, delivery of this drug to tumor site and providing a blood-brain-barrier passage is one of the biggest challenges[41]. To this end, several drug delivery methods are being developed with the help of biomaterial sciences Even though chemotherapy approaches could seem to be useful at first treatment, resistance to chemotherapy limits the usage of drugs since cells no longer respond to particular therapies by developing resistant populations or by over-population of innately resistant cells[42]. To this end, sensitization to chemotherapy approaches are studied. Similarly, innovations in radiotherapy are focused on increasing the efficacy of radiotherapy[43–45]. Another approach is destroying tumor locally, in site[46]. Cell therapy using CAR-T cells is a hot immunological approach[47] and a promising strategy in addition to immunological studies and clinical trials described above. Current developments in GBM treatment is listed in **Figure** *1.4*.
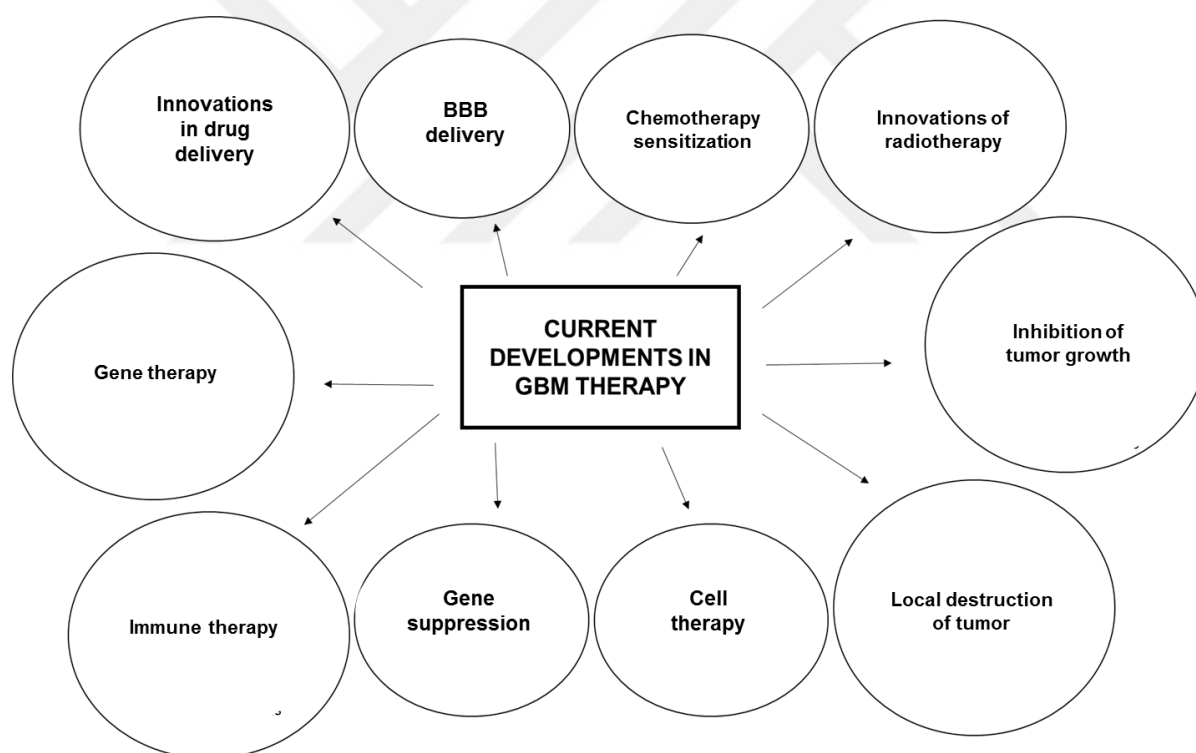
Figure 1.4. Current developments in GBM therapy. Developments are inclined towards the problems causing failure of traditional treatment options. Figure adapted from Jain et.al.[48].

Unfortunately, neither the golden standard for GBM therapy nor the current and innovative developments target the invasive cells of GBM. Despite invasive nature of GBM cells is mainly responsible from the poor therapy response and high recurrence rates, there is

no specific treatment targeting invasive cells[49]. Therefore, understanding the mechanisms of GBM cell invasion and developing anti-invasive therapies are required for successful eradication of GBMs.

1.2. Invasion in Glioblastoma

1.2.1. Current Models to Study GBM Invasion

Glioblastoma invasion is studied several by different models as *in vitro* 2D, *in vitro* 3D, *ex vivo* and *in vivo*. The study model should be chosen by considering advantages and disadvantages of each model and hypothesis and purpose of the study. However, it is important to test the hypothesis and confirm the finding using *ex vivo* organotypic brain slice models and/or *in vivo* models to expose the cells to original microenvironment. Another thing to consider is validation of findings using GSC (cultures, which would closely mimic genotypic and phenotypic characteristics of GBM.

For 2D migration studies, most preferred technique is monolayer wound healing or scratch assay. After cells are grown on plastic, a scratch is made and the time that cells take to migrate and fill the gap or the distance of gap after a certain time period is measured. In this case, it should be noted that this model is not very suitable to distinguish proliferative or migratory properties of the cells[50–52]. This model also fails to reflect brain microenvironment[53]. 2D studies have a limitation to provide cell-cell and cell-ECM interactions, to this end, these studies do not reflect true physiological conditions. While stroma cells are one of the most important players in cancer concept, lack of the cues from stromal cells and microenvironment is the biggest challenge for 2D studies[54].

3D models of invasion better mimic brain structures in culture. Discrepancies have been reported between studies conducted using 2D or 3D cultures derived from the lack or presence of different substrates and matrices[55]. One of the mostly used techniques is Boyden chamber assays, which allows to evaluate invasion through a porous insert. In this assay, cells are seeded on top of the insert which could be coated with 3D matrices and invasion of the cells to bottom compartment is measured. In this assay, generally an attractant as serum, growth factors, ECM proteins and paracrine signals from relevant cells is added[51,56,57].

Another 3D model to assess invasion is spheroid model. In this model, spheroids are prepared from cell of interest and then embedded into matrices including different type of ECM proteins. These spheroids are tumor nodules without vascularization[58]. Cell spheroids can be

generated using hanging drops method, spinner cultures, cell repulsive substrates and entrapment in hydrogel matrices[59,60]. Spheroid model is advantageous for modeling invasiveness by providing a 3D ECM structure, having the control on cell concentration and spheroid size and suitability for *in vivo* implantation. In addition, if spheroids are generated from cancer cells and stromal cells together or with proper ECM components, this system would mimic the tumor interactions better[61–63]. Analysis of the protein and gene expression profiles using spheroids have shown that this model can recapitulate clinical and in vivo gene expression profiles better than 2D culture profiling studies[58]. Drawback of this model is that not all the cell lines are suitable for generating compact spheroid structures[64].

Bioengineered scaffolds have the capacity to recapitulate the brain ECM better than most of the models, however, these scaffolds fail to include various cell types in the brain environment[65,66]. Microfluidic co-culture platforms can resolve this limitation as they allow different types of cells to a gel scaffold[67,68]. These devices also allow for generating the gradients of chemoattractant molecules[69]. Cerebral organoids are advantageous as they involve co-culture with endothelial cells; however, these systems lack vasculature[70].

In the case of *ex vivo* models, organotypic brain slice cultures are a good combination as they provide relevant *in vivo* brain environment with throughput applications of *in vitro* models[50,71,72]. In these cultures, slices are prepared from postmortem animal brains and cultured on porous inserts in transwell plates. Tumor cells are seeded adjacent to the slices and their depth of penetration is measured. Compared to in vivo models, brain slice cultures have technical advantages as imaging is simple and requires small number of animals, however, deterioration of tissue viability brings along a time limitation for the culture[73–75].

In vivo orthotopic xenograft models mimic tumor development in complex brain microenvironment[71,76,77]. In addition to fixed data point assessment by histology and imaging, intravital imaging allows dynamic analysis of tumor cell behavior[78–80]. Limitations are ethical concerns, inter-animal variability and difficulty in high-scale experiments[78,81].

Advantages and disadvantages of several models are listed in

Table *1.2*.

Table 1.2. Comparison of current models of invasion. Adapted from Gooijer et.al., and Katt et.al.[82,83]

Model	Advantages	Disadvantages
Scratch assay	Technically easy Low cost High throughput Real-time cell tracking	Low physiological relevance Only for assessing migration Lacks 3D environment Scratch width and cell proliferative properties affect the results
Boyden Chamber	Technically easy Low cost High throughput If coated, allows studying matrix interactions	Only for assessing migration Chemoattractant can affect the results Endpoint assay Lacks tumor complexity
Cell spheroids	Spheroids can be generated with different methods Migration and invasion can be studied Control on spheroid size Suitable for in vivo implantation High throughput Real-time cell tracking	Lacks tumor complexity Not suitable for all cell types Lacks tumor-stroma interactions
3D bioscaffolds	High throughput 3D microenvironment Real-time cell tracking Recapitulates migration and invasion	Lacks tumor complexity Lacks tumor-stroma interactions Lacks brain structure
Microfluidic co-culture	3D microenvironment Real-time cell tracking Allows interactions between different cell types Recapitulates invasion routes	Does not fully recapitulate tumor complexity Lacks native brain microenvironment Expensive
Organotypic brain slices	Native microenvironment Real-time cell tracking Allows interactions between different cell types Recapitulates invasion routes	Ethical issues Limited tissue stability Intra- and inter- animal variability Lacks blood flow
Orthotopic xenograft	Native microenvironment with all cell types Recapitulates invasion routes	Ethical issues Time-consuming and expensive Difficult to scale up Limited image resolution

1.2.2. Routes of GBM Cell Invasion

Invasive cells of GBM diffusely infiltrate into normal brain tissue, which limits the therapeutic options and increases recurrence rates by inducing formation of secondary tumors. The invading cells generally follow the existing anatomical structures and move along the structures as white matter tracts, the brain parenchyma, perivascular space and leptomeningeal space[84] as shown in **Figure *1.5*.**; more specifically myelinated fiber tracts like corpus callosum and the internal capsule, meninges, ventricular lining and basement membrane of blood vessels, subependymal space-perivascular regions and glia limitans externa. White matter tracts are

composed of myelinated axons, corpus callosum is the biggest source of tracts and invasive GBM cells use this structure to invade into contralateral hemisphere[82].

Active migration in the brain is mediated by cell surface receptors. The dissemination is facilitated by passive flow of cerebrospinal fluid within perivascular space and in ventricular linings[85,86].

GBM rarely disseminates out of the CNS. The reasons that limits dissemination outside of CNS is that leptomeninges to act as a barrier[87] or short survival time of GBM to limit the spread[88].
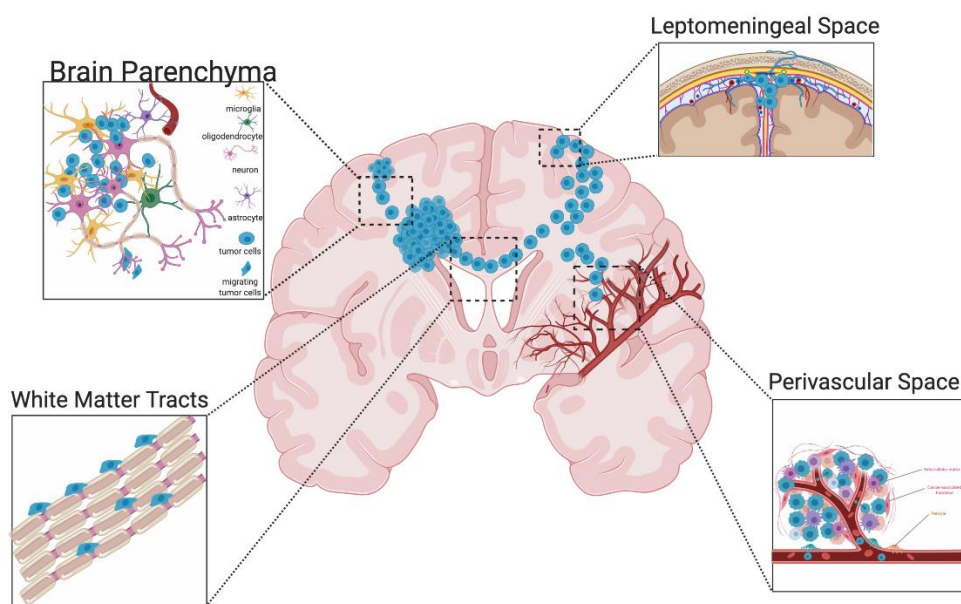
Figure 1.5. Routes of GBM invasion. Accordingly, GBM cells generally invade using tracts in parenchyma, white matter tracts, leptomeningeal and perivascular spaces. Adapted from Gooijer et.al. [82]. *Figure generated with Nareg Pınarbaşı.*

1.2.3. Modes of GBM Cell Invasion

Tumor cells may have different invasion mechanisms, they may migrate as individual cells or move together collectively. Extracellular matrix (ECM) composition, mechanical properties as stiffness or porosity and topography are the factors that affect migration and invasion properties of the cells[89]. At a single cell level, invasion may be mesenchymal or amoeboid. While amoeboid mode of invasion is based on the propulsive movement without proteolytic ECM remodeling, mesenchymal mode involves focal interactions with ECM and

movement in a traction-dependent manner due to cytoskeletal contractility. Due to the focal cell-ECM interactions, ECM-degrading proteolytic enzymes are recruited. These enzymes remodel ECM and generate a path for the invading cells[90].

GBM cells show unique invasion features as they invade locally inside the brain instead of generating distant organ metastasis. GBM cells generally invade as single cells and the cells exhibit mesenchymal mode of invasion; so called saltatory migration[91]. During invasion, GBM cells generate a strong adhesion force at the focal contacts on ECM by concentrating integrins. At the same time, they produce proteolytic enzymes like matrix metalloproteinases (MMPs) to degrade the local ECM components by pulling and contracting the actin cytoskeleton to propel toward newly generated invasion path[49].

In 3D collagen gels, a "leader" glioblastoma cell reorganizes the collagen and creates a track for invasive glioblastoma cells to follow[5]. These cells generate leading pseudopodia which are short-lived, actin-rich membrane protrusions and filopodia which are long-lived, finger-like protrusions. Generation of these extensions that explore the environment is thought to be the mechanism in vivo to find and move along the white matter tracts and blood vessels. Formation of these protrusions are followed by front-edge of the cells to form focal adhesions and rear-edge of the cells to detach from these adhesions[92]. Regulation of dynamic adhesion turn-over is critical for cell movement. On the other hand, GBM cells generate an interconnected network in the brain and facilitate their infiltration using tumor micro-tubes[93].

1.2.4. Molecular Mechanisms of GBM Cell Invasion

Role of Extracellular Matrix in Invasion

Tumor cell invasion is regulated by biophysical and biochemical stimuli coming from the complex extracellular matrix networks[94]. GBM cells infiltrate into brain tissue by interacting with various brain microenvironment components. Attachment to ECM, detachment from ECM, and dynamic remodeling of ECM are major drivers of cell invasion[49] which will be discussed in detail.

Well-defined ECM of brain is constructed by mesoderm-derived endothelial cells[95]. ECM is in the form of a true basement membrane around all cerebral blood vessels and at the glia limitans externa[96]. ECM composition is controlled in healthy conditions, but the tumor formation and invasion results in loss of ECM control.

Healthy brain ECM mainly consists of non-protein-bound, space filling hyaluronic acid and also different types of proteoglycans and glycoproteins which organizes extracellular space by their interactions[97]. The vascular and subpial basement membranes contain ECM proteins collagen IV, laminin, fibronectin and vitronectin. The basement membrane of glia limitans externa and subependymal space consists of collagen I, III, IV, fibronectin, laminin and several proteoglycans[98].

On the other hand, cultured GBM cells generate basement membrane components as laminin[99], vitronectin[100], fibronectin[29,101], collagen I[29,30], collagen IV[29,102] or collagen VI[103]. GBM cells disseminate within the brain by moving along myelinated axons ,vascular basement membrane and externa composed of fibrous proteins as collagens, fibronectin, laminins and vitronectin[97,104]. Accordingly, vitronectin and fibronectin expression is correlated with increasing invasiveness[105]. ECM proteins as hyaluron, tenascin C, osteopontin, SPARC and laminin expression is upregulated at the invasive edge of GBM cells[99] and vitronectin is found to surround invaded tumor cells[106].

Role of Adhesion Proteins in Invasion: Attachment to & Detachment from ECM

Cells need to regulate their ECM interactions in order to coordinate their movement. In case of cancer cell invasion, cells first detach from ECM and invading cells re-attach to ECM to retain their movement. Indeed, local detachment of tumor cells from the primary tumor and their interaction with the adjacent parenchymal tissues facilitate their distant movement[107]. Glioma cell adhesion is enhanced in ECM rich regions of the brain, further supporting that ECM interactions and increased adhesion facilitates glioblastoma invasion[91]. Adhesive properties of cancer cells are significant determinants of their invasive potential; and many adhesion-related proteins have been proposed as potential targets to inhibit invasion[108].

Cells first need to detach from tumor mass in order to invade. In this stage of invasion, cell adhesion molecules CD44, neural cell adhesion molecule (NCAM), cadherin and L1 proteins have a significant role. CD44 is a transmembrane glycoprotein and an adhesion molecule interacting with hyaluronic acid. Hyaluronic acid is a significant portion of brain ECM and this increases the significance of CD44 in physiological and pathological cases[109]. A CD44 variant is detected in metastatic tumors[110] and cleaved CD44 is seen in 60% of gliomas[111]. NCAM is a glycoprotein classed in immunoglobulin receptor superfamily. In the case of glioma invasion, NCAM has a role as paracrine inhibitor by interacting with cell surface receptor and with other NCAM expressing cells[112]. Its role in ECM degradation has been shown by previous

studies[113]. Cadherins are calcium dependent transmembrane cell adhesion molecules and they mediate cell to cell adhesion. E and N cadherins bind to β-catenins. In turn, β-catenins bind to α-catenins and act as a bridge to bind cadherin complex to actin cytoskeleton. Switch from E-cadherin to N-cadherin has been associated with cell motility and transition to more invasive phenotype[114]. It has been hypothesized that instability and disorganization of cadherin mediated junctions increases invasion in GBM[115]. A variant of another neural cell adhesion molecule L1 has also been shown to facilitate invasion[116].

For the invading cells to re-attach to ECM, key proteins as Tenascin-C and integrins have an important role. Tenascin-C is an ECM protein known to induce filopodia formation and over-expressed in gliomas[117,118]. Integrins are the most important class of adhesion molecules interacting with ECM proteins and other adhesion molecules as ICAM-1, ICAM-2 and VCAM-1. Integrins are mainly responsible from cell to ECM interactions[119]. Focal adhesion kinase (FAK) which is a close interactor of integrins, recruits cytoskeletal proteins and activates Rho GTPases; finally, integrates adhesion process with cytoskeleton assembly and rearrangement. FAK is overexpressed in many types of cancer including gliomas[120]. Integrin clusters aggregate together with cytoskeletal proteins as vinculin and FAK to generate adhesion complexes[121].

Role of Proteinases in Invasion: Remodeling of ECM

Remodeling of ECM is crucial for the invading cells to generate a path to move along. In addition to generating paths, active degradation also release growth factors and matrix proteins in ECM which promotes invasion further[122]. Invading cells express proteinases and/or proteinase activators at their leading edge. ECM degradation by proteinases as matrix metalloproteinases, ADAM, PA system and cathepsin is an important feature for GBM invasion. MMP activity is shown to be significant for GBM invasion because MMP-2, MMP-9 and MT-MMPs can together degrade almost all types of ECM, they are specifically activated in tumor tissues and their activation correlates with poor prognosis and invasion[123]. MMP2 activity is highly increased in GBM tumors compared to normal brain tissue and expression levels correlate with malignant progression[124,125]. MMP9 expression is generally detected at tumor margins and at the endothelial proliferation sites which relates its expression with angiogenesis and invasion[126]. Inhibition of MMP2 or MMP9 activity or downregulation of MMP2 and MMP9 protein levels decreases invasion in GBM cell lines and mice model[124,125]. Similarly, ADAM family contains metalloproteinase domains homologous to MMPs.

ADAM12m and ADAMTS-5 are overexpressed in GBM[127,128]. Plasminogen activator (PA) system will be discussed below in more details, but briefly, this system generates active plasmin which in turn degrades ECM and activates MMPs and growth factors. Cathepsin is a lysosomal acid hydrolase which associates with tumor cell plasma membrane and is able to activate MMPs and uPA[129,130].

Cytoskeletal Changes during Invasion

Cytoskeleton rearrangement is crucial for the movement of the cells. For cells to move forward, large degree of actin polymerization followed by depolymerization is needed in addition to myosin contraction. During this movement, microtubules and intermediate filaments maintain cell structure and hold the organelles in place[131]. Protrusions from the cell body called podosomes and invadopodia are crucial for invasion. These structures release high amounts of matrix degradation enzymes and form the leading structure for invasion[132].

Role of Other Motility Factors in Invasion

Motility factors which operate through autocrine and/or paracrine signaling have significant roles for invasion. In the context of GBM invasion, scatter factor/hepatocyte growth factor (SF/HGF) and epidermal growth factor receptor (EGFR) act on cell motility. SF/HGF and its receptor c-Met which is a proto-oncogene product and has tyrosine kinase activity promoting cell motility in GBM[133]. EGFR amplification and overexpression is one of the most frequently seen signatures in GBM[134]. Amplification of EGFRvIII, which is the constitutively active form of EGFR is associated with poor prognosis since EGFR signaling both enhances proliferation, migration and invasion and blocks apoptosis of GBM cells[135,136].

Other class of molecules involved in GBM invasion is extracellular secreted proteins as insulin-like-growth-factor-binding protein family (IGFBPs), cysteine-rich 61/connective tissue growth factor/nephroblastoma overexpressed (CCN) family (Cyr61), angiopoietin 2 (Ang2), YKL40 and autotaxin (ATX)/lysophospholipase D.

There are also membrane-type proteins as Fn14/TWEAK, EphB2/ephrin-B3 and CD155 associated with GBM invasion. Especially ephrins and ephrin receptors have an important role in bi-directional signaling in GBM invasion. Ephrins mediate cell to cell signaling and control tissue organization. Ephrin pathway is over-activated in GBM invasive cells compared to stationary ones[137]. This over-activation, especially for EphA2 and EphA3, has been associated with invasiveness and poor patient outcome[115,137]. The Rho family of GTPases from Ras

superfamily is divided into Rho-A, Rac1 and Cdc42 and they are responsible from spatial regulation of GBM invasion. They control actin-mediated cytoskeleton rearrangements that facilitate cell movement[119]. In glioblastoma, Rho GTPase pathway is deregulated, increased activity of Rac1, Cdc42, RhoA and RhoG is associated with invasiveness of GBM cells[138–140].

Intracellular proteins Bcl-2 family, Rac GTPases Rac1 and Rac3, synaptojanin2, P311, FAK and proline-rich tyrosine kinase 2, CrkI and myosin II are also known to be actors of GBM cell invasion[5].

Role of Transcriptional Regulators in Invasion

Even though understudied, transcriptional regulators have important roles in GBM invasion. Interferon regulatory factor 3 (IRF3) represses the expression of collagens and collagen interacting proteins and has a repressive role for invasion[75]. IRF3 repression is negatively regulated by CK2 which is a master regulator in several cellular processes [141]. Another factor mediates GBM invasion named promyelocytic leukemia protein (PML) which is a scaffold protein induced by Ras. PML expression is enriched in mesenchymal subtype of GBM, which is highly invasive[142,143]. Associated with these transcriptional regulators, NF-κB and Jak/Stat pathways have a significant part in mediating GBM cell invasion. NF-κB is already constitutively activated in most cases of GBM and this pathway promotes conversion to mesenchymal subtype of GBM by inducing the expression of the genes associated with mesenchymal program as STAT3, CCAAT-enhancer binding protein β (C/EBPβ)[144,145]. Jak/Stat pathway regulates migration by controlling focal adhesions and regulates the expression of ECM remodelers as MMPs[146].

Role of Microenvironment during Invasion

Invasion by cancer cells depends on crosstalk between invading cells and normal tissue-remodeling mechanisms of host. Hypoxia is one of the micro-environmental features in GBM. While glioma tumor is growing rapidly, this brings along increased oxygen needs. Lack of oxygen causes intra vascular thrombosis and hemorrhage and eventually necrosis of tumor and tissue. To evade hypoxic environment, tumor cells migrate from the hypoxic area to reach oxygen as well as they produce angiogenic factors to induce blood vessel formation and show anaerobic glycolysis. Eventually, they re-model tissue microenvironment by accumulating lactate that generates a low pH environment that further induces invasion[36].

Another determinant in the role of microenvironment during invasion is the paracrine signaling of the cells present in the brain. Factors secreted by different cell types have a significant role in inducing invasion. Invasive GBM cells secrete autocrine motility factors to maintain motility and several cell types in CNS express receptors for these motility factors. On the other hand, the factors secreted by parenchymal cells may also induce invasion of tumor cells. Astrocytes, oligodendrocytes, microglia, glial progenitors, neurons, neural progenitors, neural stem cells and vascular endothelium are known to express receptors to secrete ligands and motogens that induces invasiveness in GBM[147].

Considering all the molecular mechanisms discussed in this section summarized in **Figure *1.6***, understanding molecular mechanisms of GBM invasion has the potential to open up new approaches for GBM treatment. Therapeutics targeting invasion mechanisms would be useful to eradicate the population left behind after surgical removal and would make the GBM tumor more manageable in clinic especially with combination of complementary therapies that target other features of GBM.
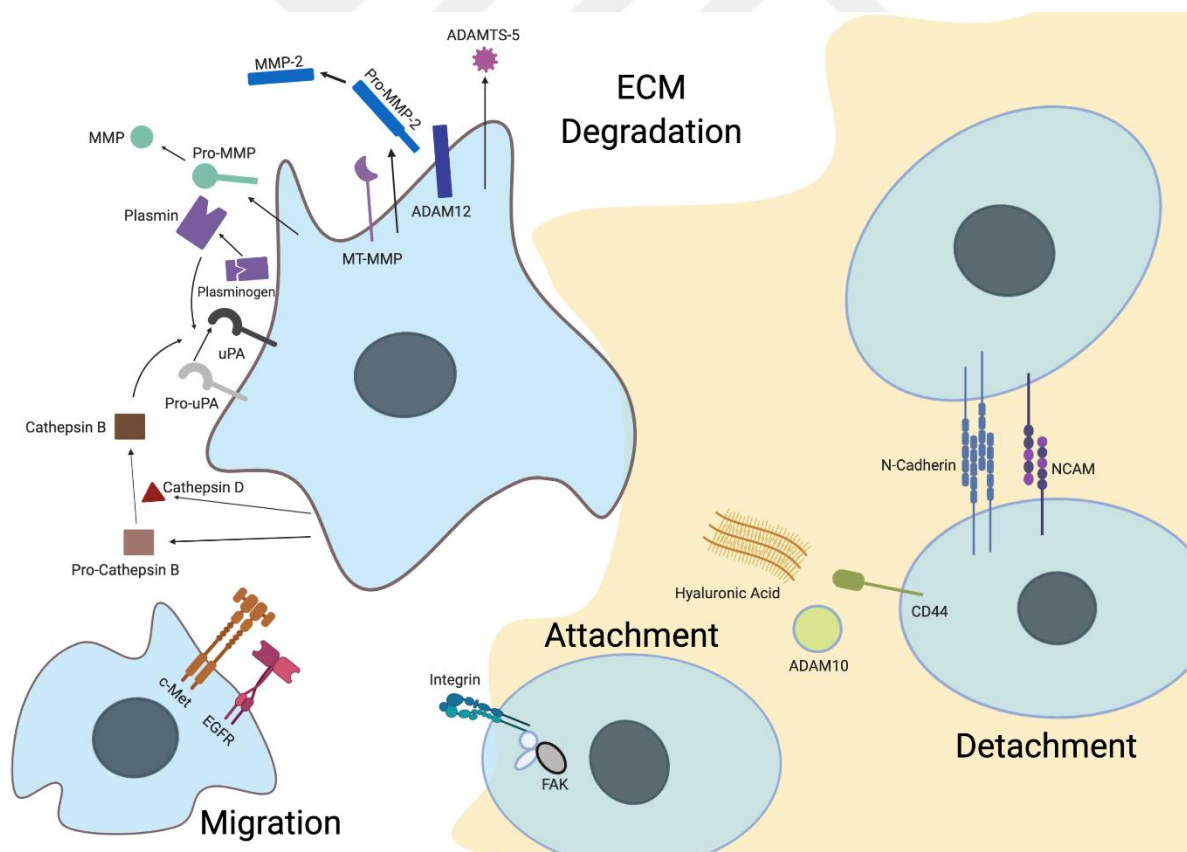
Figure 1.6. A summary of molecular mechanisms regulating GBM cell invasion. Molecules having significant roles in cell attachment-detachment, ECM degradation and migration are indicated. Adapted from Nakada et.al.[5] *Figure generated with Nareg Pınarbaşı.*

1.2.5. Epithelial-to-Mesenchymal Transition and Invasion

Epithelial to mesenchymal transition (EMT) has an important role in cancer progression, where it controls the transcriptional programs operating during the transition between tumor growth and metastasis. This transition brings along the changes in the gene expression and functional behavior which affects phenotype. Proliferative tumors generally exhibit epithelial-like morphology with tight cell junctions and E-cadherin overexpression on the cell membrane. When these cells undergo EMT; cells become more fibroblast-like, tight junctions disappear and E-cadherin expression is majorly lost. The cells that undergo EMT degrade the ECM and become more invasive. With this increased invasiveness, they can now enter into circulation (intravasation) easily and survivors can leave the blood or lymphatic vessels (extravasation). After extravasation, the cells reverse the EMT program and undergo mesenchymal to epithelial transition (MET). This is a strategy for cancer cells to metastasize and generate secondary tumors in distant area[36].

As opposed to most carcinomas, GBM tumors show local invasion and dispersal within the brain tissue instead of distant metastasis. However, invasive GBMs share common molecular features with metastatic cancers[148] and some essential regulators of EMT, such as TGFβ, strongly stimulates GBM invasion[36]. Zeb1 transcription factor, which is a key regulator of EMT is also a driver of GBM invasion[149].

1.2.6. Clinical Targeting of GBM Cell Invasion

Invasion ability toward surrounding tissue is a determinant for the malignant tumor progression[150]. In the case of GBM, high mortality of patients is mostly caused by the invasive behavior of GBM cancer cells, which show extensive infiltration from primary tumor site into healthy adjacent tissue and result in rapid and almost inevitable recurrence. **Figure *1.7.*** depicts the MRI scans of a GBM patient before surgery, right after surgical removal and 18 months following surgery. Despite tumor removal, the tumor has recurred in the contralateral hemisphere as a consequence of invasive cells infiltrating into brain parenchyma.
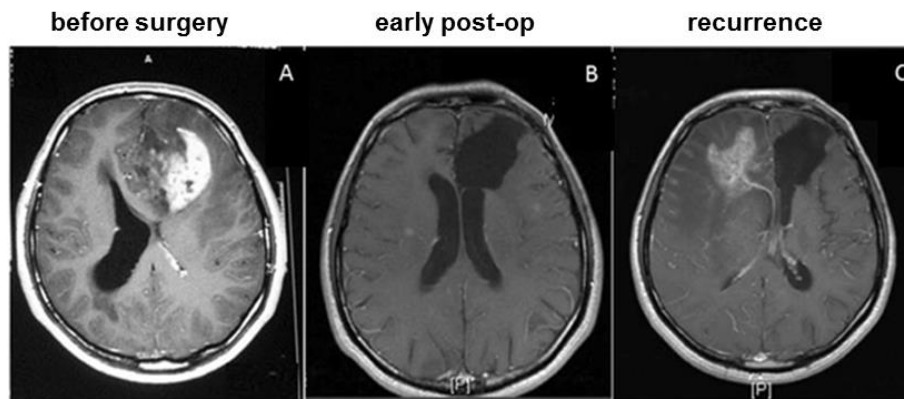
Figure 1.7. MRI scans of a GBM patient. Images showing tumor right before surgery, right after operation and recurrence in contralateral hemisphere. *Image courtesy: Prof. Dr. I.Solaroglu, KUTTAM.*

Invasive nature of GBM cells limits the therapy options in GBM. Invasion of cells to the brain tissue limits tumor resection as tumor borders are diffuse and individual cells that have infiltrated into the healthy parenchyma are not easily detectable[49]. As a result, the infiltrative cells can escape from surgery and re-colonize. Disseminated cells are less effected by radiotherapy because radiotherapy is restricted to the area surrounding the GBM tumor to prevent radiation-induced injury to normal brain tissue.

Despite the fact that invasive nature of GBM cells has drastic results on therapy resistance, very high recurrence rates and poor survival rates, there is no directed therapy against these population[49]. In return, studies showed that current therapeutic strategies further increase invasiveness of the cells. In some cases, resection has been shown to increase tumor malignancy through a stem cell proliferation effect termed repopulation. While chemotherapy causes further variations and mutations, low dose radiation increases invasiveness of glioma cells[151,152].

On the other hand, considering that highly invasive cells have already disseminated to other locations than the primary tumor area and formed tumor seeds in secondary locations, preventing only the invasion would not kill these cells and change the patient survival considerably. To this end, anti-invasive therapies should be combined with other treatments. Offering this kind of combinations would hopefully result in more compact tumors with drug-penetrable-BBB and cells to switch to more proliferative mode that would sensitize them to anti-proliferative therapies.

GBM invasion pathways and signaling networks offer druggable targets as TGFβR1, Ephrin receptors, FAK, ROCK, CK2, AKT, JAK, NF-κB, STAT3 and EZH2. In spite of having these targets, targeting not all of them is specific to GBM invasion signaling. Among these, using inhibitors of TGFβR1, Ephrin receptors, FAK, ROCK and CK2 would more specifically target invasive GBM cells.

Several TGFβ inhibitors as Vactosertib and Galunisertib are in clinical development. Galunisertib is being tested in glioblastoma (clinicaltrials.gov identifier: NCT01220271, NCT01682187, and NCT01582269)[153]. An ongoing Phase I/II trial is combination of Galunisertib with temozolomide and ionizing radiation (NCT01220271). For Ephrin receptors, an ongoing Phase I study is investigating KB004, a monoclonal antibody targeting EphA3 in GBM (NCT03374943). FAK inhibitors have not been tested in glioma yet, but Phase II trials are ongoing for defactinib and GSK2256098 (NCT01951690 and NCT02523014)[82]. Other than these trials, targeting glutamate signaling and ion receptors are ongoing studies and trials[154].

In addition to these ongoing trials, other elements linked to invasion have already been tested. Targeting MMPs to reduce the glioblastoma tumor invasion evoked severe normal tissue effects in patients and did not improve patient survival when combined with temozolomide[155]. Targeting integrins were more promising, but unfortunately it was found that patients with newly diagnosed GBM and methylated MGMT promoter did not have prolonged survival when combined with chemoradiotherapy[156]. Even though targeting proteases have restricted the dissemination of tumors inside the brain, this approach did not improve patient survival[155].

1.2.7. High Throughput Approaches for Invasion

Considering the role of invasion in cancer and poor patient prognosis, many previous reports have searched for invasion reports have searched for invasion related signatures or targets (

Table *1.3*).

Mariani et. al. compared the mRNA expression profiles of tumor core and invasive rim in GBM tumors by laser capture microdissection and identified P311 gene as an upregulated gene in invasive cells[157]. Hoelzinger et.al. conducted a microarray analysis of patient tumor cores and white matter invading cells using laser capture microdissection[158]. Demuth et.al. conducted a microarray screen in order to identify gene signatures in stationary and migratory populations in ten GBM cell lines and found 22 gene signatures classifying GBM cultures based on migration rate[159].

Gumireddy et.al. conducted a screen in mice using a retroviral cDNA library and introducing this library to a non-metastatic cell line. These cells were orthotopically transplanted to mouse mammary fat pads and observed for lung metastasis. They identified ERp5 and β-catenin as genes promote breast cancer invasion and metastasis[160]. Seo et.al. used a retroviral mouse brain cDNA library to fibroblasts cells and assessed migration using 3D culture inserts and identified CHCHD2 has a cell migration promoting activity[161].

Gobeil et.al. identified GAS1 gene as a novel melanoma metastasis suppressor gene performing an shRNA screen[162]. Collins et.al conducted an siRNA screen using ovarian carcinoma cell line and identified MAP4K4[163]. Another siRNA screen conducted by Roosmalen et.al. performed an siRNA screen for 1500 genes encoding kinases/phosphatases and adhesome which are migration related proteins and identified SRPK1 as a driver in breast cancer[164]. Bagci et.al. identified Neuropilin-1 and its ligand Semaphorin3A as mediator of GBM invasion using fluorophore-assisted light inactivation and functional proteomics[165].

Li et.al. utilized a miRNA screen in two distinct types of brain tumors; slow-growing, diffusely infiltrating glioma and non-invasive primitive neural tumors. This study identified miRNA-449a as a suppressor of migration via suppression of GPR158[166].

Table 1.3. High Throughput Approaches for Invasion.

Study	Screen Method	Technique	Cell/Tissue Type	Advantages	Disadvantages
Mariani et.al., 2001	Differential display of mRNA	Laser capture microdissection	GBM tumor tissue	Usage of patient sample, native tumor properties	High incidence of false positives because of screen method Usage of LCM in not-well-defined tumor border
Hoelzinger et.al., 2005	Microarray	Laser capture microdissection	GBM tumor and white matter invasive cells	Usage of patient sample, native tumor properties Invasive cells from a natural invasion route	Data limited with only the genes included in microarray Usage of LCM in not-well-defined tumor border
Demuth et.al., 2008	Microarray	Manual collection	GBM cell lines	High number of replicates Statistic method	Manual collection Usage of cell lines
Gumireddy et.al., 2006	Retroviral introduction of cDNA library	*in vivo* screen	Non-metastatic cell line	Analyzing the metastasis of a non-metastatic cell line to lung	Data limited with only the genes included in cDNA library
Seo et.al, 2010	Retroviral introduction of cDNA library	3D culture inserts	Fibroblast	Analysis of the metastasis-promoting genes for a non-metastatic cell line	3D culture insert limitations, lack of native microenvironment Data limited with only the genes included in cDNA library
Gobeil et.al, 2008	shRNA screen	3D culture	Weakly metastatic melanoma cells	Unbiased, genome-wide screening	3D culture limitations, lack of native microenvironment
Collins et.al., 2005	siRNA screen	Wound-healing assay	Highly motile ovarian carcinoma cells	Inclusion of only phenotype-related genes to library, focusing on related mechanisms	Data limited with only the genes included in siRNA library High off-target rate
Roosmalen et.al., 2015	siRNA screen	Phagokinetic track assay	Migratory breast cancer cells	Inclusion of only phenotype-related genes to library, focusing on related mechanisms	Data limited with only the genes included in siRNA library
Bagci et.al., 2009	FALI	Transwell invasion assay	GBM cells	Usage of a novel method for functional proteomics analysis	3D culture insert limitations, lack of native microenvironment
Li et.al., 2018	miRNA screen	*in vivo* screen	Glioma and neural tumors	Usage of patient sample, native tumor properties, Comparison of diffuse and non-invasive tumors	Lack of assessment in all targets of candidate miRNA, miRNAs have several targets that may reverse the effects if targeted

1.3. SERPINE1 (PAI-1)

SERPINE1 gene is located on chromosome 7 (7q21.3-q22) and encodes PAI-1 protein[167]. PAI-1 is a 45 kDa, single chain glycoprotein[168]. Serpin family members, including PAI-1 has a reactive central loop (RCL) in C-terminal region which contains site of proteolytic cleavage. PAI-1 may be found in three forms based on state of RCL; active, latent and cleaved forms. In the active form, RCL is exposed at the surface of the molecule, in the latent form, RCL is internalized, and in cleaved form, N terminal of RCL remains inside. PAI-1 carries three domains to bind different molecules; uPA, somatomedin B domain of vitronectin and LRP1 or LRP2. The uPA binding domain is located in RCL and upon binding, uPA is cleaved and N-terminal portion of RCL is re-located at the opposite site. Binding of somatomedin B domain of vitronectin stabilizes the structure, delays its internalization in latent form and shown to inhibit cell adhesion to vitronectin. LRP binding and interaction occurs following binding of

uPA and its receptor uPAR which results in internalization of the complex and promoting cell migration[169–171].

PAI-1 is produced by tumor cells and non-malignant cells such as endothelial cells, macrophages and adipocytes in tumor microenvironment. Therefore, in the context of cancer, PAI-1 is in both paracrine and autocrine signaling networks.

1.3.1. PAI-1 and Plasminogen Activator System

PAI-1 is a serine protease inhibitor (serpin) which has a central role in plasminogen activator system (PA). PA system is a key player in ECM remodeling which is a crucial step for tumor invasion and spreading[172]. Main components of PA system are plasminogen activators urokinase plasminogen activator (uPA) and tissue plasminogen activator (tPA), the cell membrane receptor for uPA named uPAR, plasminogen activator inhibitors PAI-1 and PAI-2 and plasmin[173]. Active plasmin generated by this system degrades ECM directly or indirectly via activation of MMPs[174] and facilitates cell migration and invasion in the context of cancer. This focal proteolysis carried out by PA system reorganizes ECM, changes cell-ECM interactions via integrin receptors and releases molecules in matrix which can further induce migration[175](**Figure *1.8***).
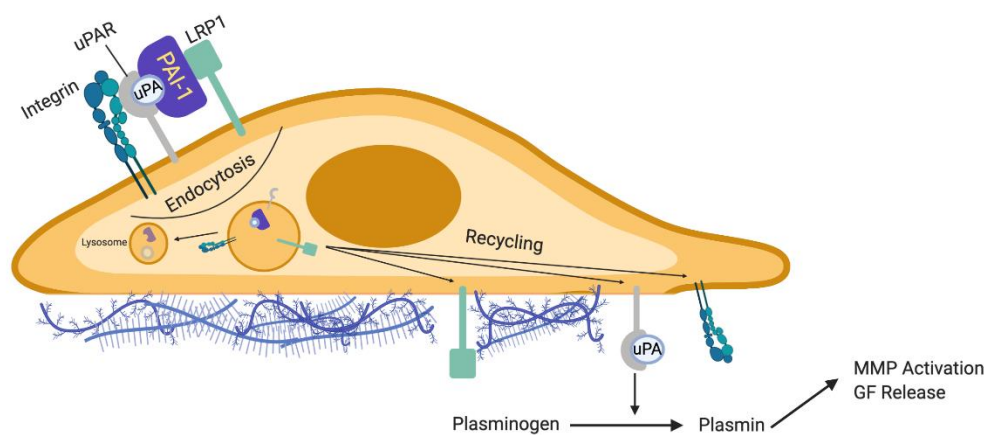
Figure 1.8. Regulation of PA system during cell invasion. Accordingly, this system has an important activity driving cell invasion, especially in the leading edge of the migrating cells. Aadpted from Czekay et. al.[176]. *Figure generated with Nareg Pınarbaşı.*

Considering the fact that plasminogen activation support cancer progression and metastasis, and PAI-1 acts as an inhibitor for plasmin generation, PAI-1 would be predicted to

have antitumor functions. However, PAI-1 is upregulated in many types of cancer and elevated PAI-1 levels correlate with poor patient outcome in several cancer types including breast, gastric and ovarian cancers[177,178]. The central tumor-promoting role of PAI-1 in cell migration, cancer invasion and tumor vascularization has been shown in some cancer types[179]. This paradox may point to the fact that PAI-1 has other ligands than PAs, as ECM components, heparin and LRP1[180] and PAI-1 exerts its invasion-promoting role through several pathways. It should also be noted that all three forms of PAI-1 can induce cell motility in LRP1 dependent manner; while active PAI-1 has a routine turn-over, latent and inactive forms remain embedded in matrix to act as a reservoir for motility induction[176].

Other than cancer, PAI-1 has a role in thrombosis. PAI-1 is upregulated in several pathologies as vascular diseases, wound healing problems, obesity and metabolic syndrome[177].

1.3.2. PAI-1 as a Prognostic Indicator in Cancer

PAI-1 is expressed in different levels in diverse cancer cell lines (**Figure *1.9***).
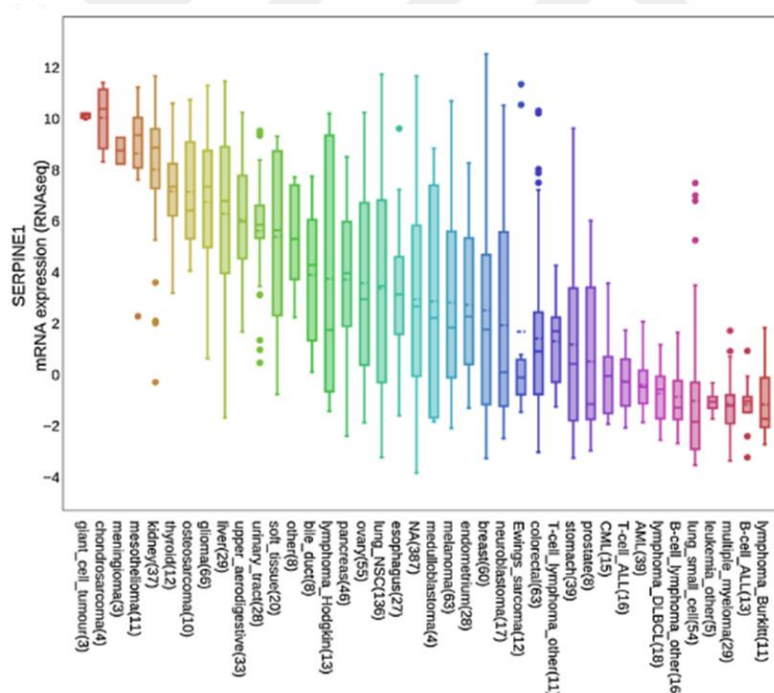
Figure 1.9. *SERPINE1* expression in diverse cancer cell lines. The data is from the Cancer Cell Line Encyclopedia (CCLE) website (https://portals.broadinstitute.org/ccle).

PAI-1 expression is significantly upregulated in cancers such as stomach adenocarcinoma, head and neck squamous carcinoma, esophageal carcinoma, thymoma, bladder urothelial carcinoma and testicular germ cell tumors compared to their normal matched

tissues (The data are from TCGA, http://cancergenome.nih.gov/). PAI-1 expression positively correlates with poor clinical outcome in breast, ovarian, bladder, colon and non-small cell lung cancer patients[181–188]. In addition, PAI-1 plasma levels are significantly elevated in patients with acute leukemia or several solid tumors such as breast cancer, colorectal cancer and hepatocellular carcinoma; and elevated plasma levels indicate poor outcome in different cancer types[189–193]. In glioma, overexpression of PAI-1 has been shown to correlate with poor prognosis and reduced survival[194] and PAI-1 plasma level is a predictive marker of glioma grade[195].

1.3.3. Functional Roles of PAI-1 in Cancer

Based on Cancer Hallmarks Analytics Tool (CHAT), which is tool provides analysis of strength of association between genes and hallmarks of cancer, PAI-1 has multiple roles in cancer progression resulting in poor prognosis PAI-1 has a significant role in inducing angiogenesis, generating tumor promoting inflammation, sustained proliferative signaling and immortalization and invasion and metastasis as given in **Figure *1.10*** and **Figure *1.11***.
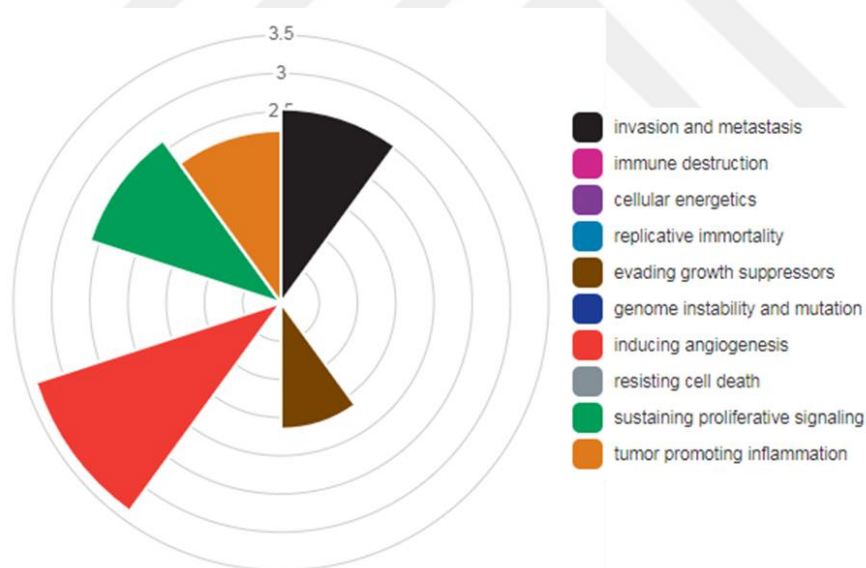
Figure 1.10. Roles of PAI-1 in cancer progression. The data are from Cancer Hallmarks Analytics Tool (http://chat.lionproject.net/).
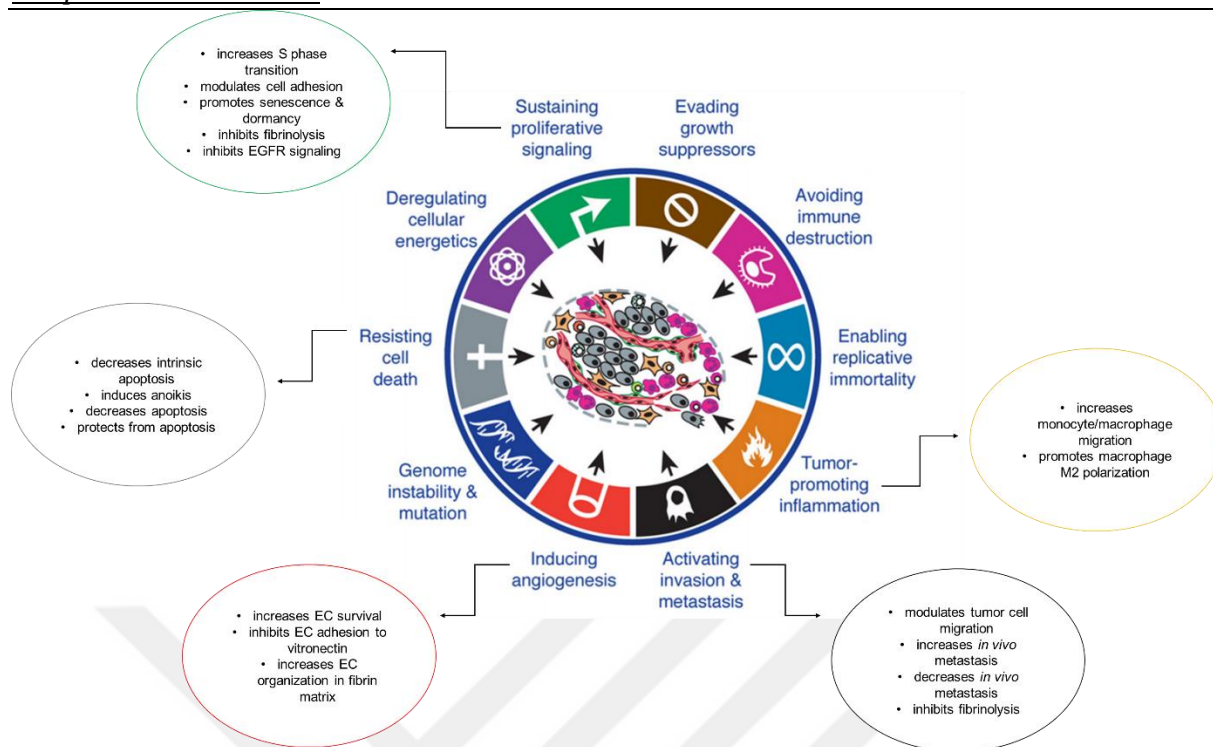
Figure 1.11. Role of PAI-1 in different hallmarks of cancer. PAI-1 has several roles in cancer progression including inducing angiogenesis, generating tumor promoting inflammation, sustained proliferative signaling and immortalization and invasion and metastasis.

1.3.4. Role of PAI-1 in Invasion and Metastasis

Although there is no consensus about role of PAI-1 in invasion and metastasis for all cancer types[196,197], several groups, including our group, have showed that PAI-1 induces tumor cell invasion and metastasis. Induction of cancer cell invasion by PAI-1 has been reported in osteosarcoma lung metastasis via promoting MMP-13 expression and secretion in osteosarcoma cells[198]. High PAI-1 expression has been shown to induce head and neck cancer cell migration and eventually metastasis via activation of PI3K-Akt pathway[199]. Another study demonstrated that PAI and CCL5 signaling induced endothelial cells to enhance EMT-induced triple negative breast cancer[200].

In addition to the role of elevated PAI-1 levels in inducing ECM degradation, PAI-1 has been shown to be a downstream effector of EMT induced by TGFβ in several cancer types such as lung cancer, gastric cancer and colorectal carcinoma[201,202]. Another study reported that PAI-1/PIAS3/Stat3/miR-34a axis induced EMT-mediated metastasis in non-small cell lung cancer[203].In some cancer types including advanced melanoma and colorectal cancer lung metastasis, elevated plasma levels of PAI-1 has been correlated with increased metastasis[192,204].

Overall, PAI-1 induces metastasis by activating signaling mechanisms that induces invasion. In addition, several studies noted that pro-migratory effect of PAI-1 is associated with LRP1 interaction and this interaction leads to activation of Jak/Stat pathway[205]. Also, correlation of elevated PAI-1 plasma levels with metastasis explained by the binding of PAI-1 with plasma vitronectin, which is a cofactor of PAI-1 via extending PAI-1 lifetime and stabilizing cancer cell to ECM adhesion[206]. Another mechanism of PAI-1 in inducing invasion and metastasis is that PAI-1 forms a specialized ECM around cancer cell by inducing fibrin deposition and this specialized ECM induces angiogenesis and migration[207].

1.3.5. Role of PAI-1 in Proliferation

As there are conflicting reports about role of PAI-1 in cancer proliferation and tumor growth, role of PAI-1 seems to be cell and cancer type specific. PAI-1 has been shown to inhibit proliferation in hepatocellular carcinoma and prostate cancer[208,209] and overexpression of PAI-1 induced growth of HeLa xenografts. In contrast, down-regulation of PAI-1 inhibited cell proliferation and tumor growth in some xenograft models and this inhibition induced apoptosis[210]. Similarly, inhibition of PAI-1 with chemical inhibitor induced intrinsic apoptosis of ovarian cancer cells[178]. Anti-apoptotic effects of PAI-1 have been also shown in head and neck carcinoma and breast cancer via activation of PI3K/Akt and ERK1/2 signaling[178,199,211]. Overall, role of PAI-1 in cell viability depends on the cell and cancer type.

1.3.6. Regulators of PAI-1 in Cancer

PAI-1 is regulated by several mechanisms in normal and cancer cells including growth factors, cytokines, miRNAs, hormones and environmental stress as summarized in **Figure *1.12***.
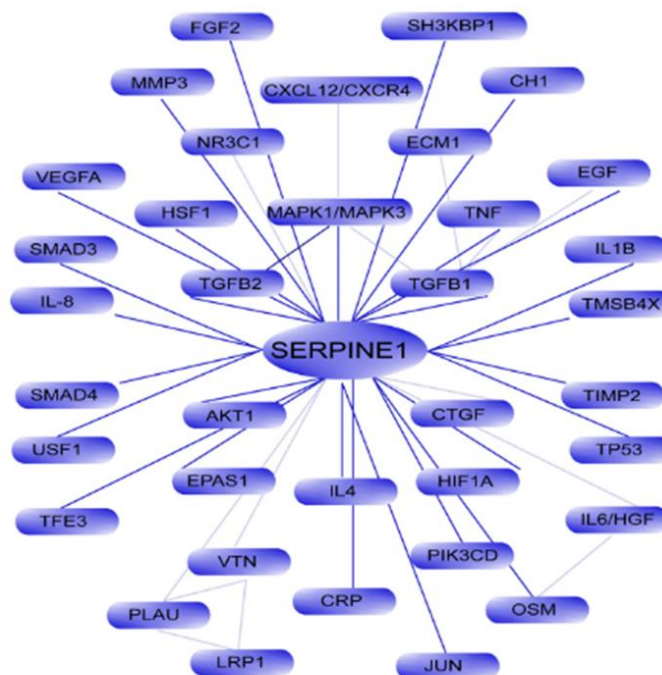
Figure 1.12. Regulators of PAI-1. The information is from Information Hyperlinked Over Protein (iHOP, http://www.ihop-net.org/UniPub/iHOP/).

PAI-1 is regulated by several growth factors including epidermal growth factor (EGF) and TGFβ. In glioblastoma, EGF induces PAI-1 expression by a signaling cascade of protein kinases c-Src, protein kinase c delta and sphingosine kinase 1[210]. In ovarian and breast cancers, EGF mediates PAI-1 regulation via transcription factors NF-κB or Elk-1[212]. Other studies have also reported that PAI-1 is regulated by EGF in cutaneous squamous cell carcinoma, hepatocellular carcinoma and astrocytoma[213–215]. On the other hand, TGFβ has been shown to regulate PAI-1 expression via inducing the interaction between Smads and p53 in hepatoma and via inducing the interaction between Smad2/3 and AP-1 signaling components c-Jun, JunB and Fra1 in breast cancer[216,217]. This regulation is mediated via p38MAPK, ERK1/2 and Smad 2/3 pathways in ovarian cancer[218]. Regulation of PAI-1 by TGFβ was also demonstrated in chorciocarcinoma, oral squamous cell carcinoma, melanoma, prostate cancer and pancreatic cancer[219–224]. Other growth factors regulating PAI-1 are HGF, bFGF and and IGF-1[225–227].

Cytokines are also central regulators of PAI-1 expression. Oncostatin M induces PAI-1 expression via activation of MEK1/2 pathway in lung carcinoma[228]. While CXCL12/CXCR4 axis induces PAI-1 expression in glioma cells via MAPK signaling in glioma cells, IFN-Ƴ is the mediator for astrocytoma cells[229,230]. In addition, TNFα in colon carcinoma and hepatoma and leptin in breast cancer have been demonstrated as regulators[231,232].

In previous studies, it has been shown that PAI-1 is regulated by several miRNAs in different types of cancer. miR-143 and miR-145 regulates PAI-1 in osteosarcoma, breast cancer and bladder cancer[198,233,234], miR-93/106b in leiomyoma[235], miR-486 in myxioid liposarcomas[236] and miR-30b in gastric cancer[237]. In addition, miR-34a, miR-192 and miR-126 are another regulators of PAI-1 in cancer[203,238].

Another important regulator of PAI-1 is HIF-1α, induction of PAI-1 by hypoxia has been studied in lung and gastric cancers[210]. Hormones also regulate PAI-1 expression. Insulin induces PAI-1 in hepatoma[239,240] and glucocorticoids as dexamethasone regulates PAI-1 in ovarian cancer and hepatoma[241]. Sex steroids, irradiation and free fatty acids are another regulators of PAI-1[242–244].

Pathways regulating PAI-1 is summarized in **Figure *1.13***.
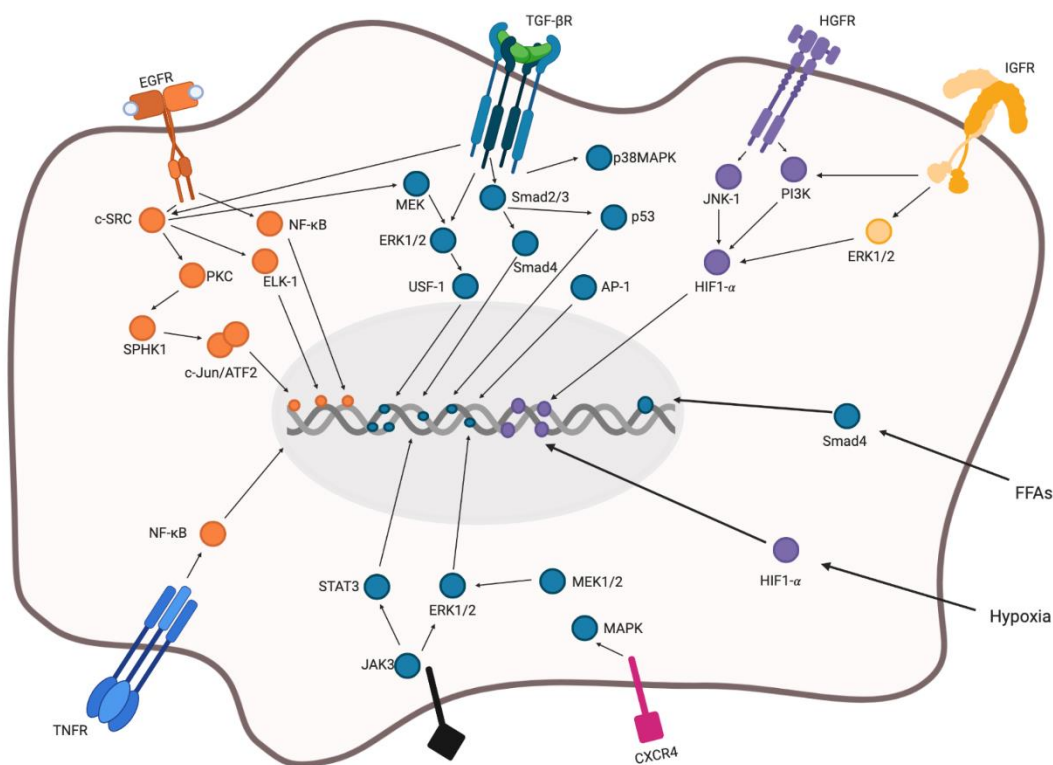
Figure 1.13. Pathways regulating PAI-1 expression. Adapted from Li et.al.[210]. EGFR, TGFβ, HGFR, IGFR, TNFR, CXCR4 signaling pathways and effect of hypoxia and FFAs are shown. *Figure generated with Nareg Pınarbaşı.*

1.3.7. PAI-1 Inhibitors

Considering its central role in tumor cell invasion and tumor progression, PAI-1 has been studied as a therapeutic target in several cancer types. Different types of inhibitors targeting PAI-1 has been developed for cancer research.

A chemical synthesis inhibitor of PAI-1 named PAI-039 or tiplaxtinin has been studied as a promising cancer targeting drug in lung cancer, HeLa, bladder cancer and head and neck cancer cell lines and shown to induce apoptosis and inhibit cell adhesion and angiogenesis[245]. Effects of other PAI-1 inhibitors SK-216 and SK-116 inhibits tumor progression and invasion/metastasis in lung cancer and pleural mesothelioma[246–248] and XR5967 is effective in fibrosarcoma[249]. A more recently developed PAI-1 inhibitor IMD-4482 reduced the invasion of ovarian cancer cells by affecting adhesion to vitronectin and exerted its effects by inhibiting FAK phosphorylation[250]. PAI-1 specific RNA aptamers have also been effective in vitro in breast cancer cells[251,252]. However; none of the inhibitors addressed have been tested in cancer clinical trials. Limitations for clinical testing are the lack of activity against vitronectin-bound stable form of PAI-1, very short half-life and need for high concentrations as a single agent[253].

In this thesis, we analyzed the dynamic changes in transcriptome of motile (dispersive) and non-motile (core) GBM cells and identified *SERPINE1* as a dramatically induced gene in the dispersive cell populations. We showed that genetic or pharmacological inhibition of SERPINE1 led to reduction of dispersal, attributing a functional role for SERPINE1 in dispersal. Furthermore, we demonstrated that SERPINE1 regulates cell-substrate adhesion and directional movement of GBM cells, and that its expression is regulated by TGFβ signaling. Together, our results suggest that SERPINE1 is a key player in GBM dispersal providing insight into the future design of anti-invasive therapies.

2.   MATERIALS AND METHODS

2.1.   Cell Culture and Reagents

A172, U373, LN18, LN229, T98G and U87MG GBM cell lines, human embryonic kidney 293T cells and SUM149 epithelial breast cancer cells were obtained from American Tissue Type Culture Collection (USA). GBM cell lines and 293T cell line were cultured in DMEM medium (Gibco, USA) supplemented with 10% fetal bovine serum and 1% Penicillin-Streptomycin (Gibco, USA). SUM149 breast cancer cell line was cultured in Ham's F12 Nutrient Mix (Gibco, USA) supplemented with 5% fetal bovine serum (Gibco, USA), 5 µg/mL insulin (Sigma-Aldrich, USA), 1 µg/mL hydrocortisone (Sigma-Aldrich, USA) and 10 mM HEPES (ThermoScientific, USA). GBM8, GBM4 and MGG119 cells[6,155] were cultured in neurobasal medium (Gibco, USA) supplemented with 3 mM L-Glutamine (Mediatech, USA), B27 (Invitrogen, USA) and N2 (Invitrogen, USA) supplements, Pen-Strep (Gibco, USA), 2 µg/mL heparin (StemCell Technologies/Fisher Scientific, USA), 20 ng/mL human EGF (R&D Systems, USA), and 20 ng/mL human FGF-2 (PeproTech, Germany) (EF media). All cells were grown in 37°C, 5% CO_2 in a humidified incubator. Vitronectin (Gibco, USA), Collagen (Gibco, USA), recombinant human TGFβ1 (Peprotech, Germany), Tiplaxtinin (Selleckchem PAI-039, USA), Repsox (Tocris, USA), and SB431542 (Stemcell Technologies, USA) were used for dispersal experiments. D-luciferin was used for in vivo imaging (Biotium, USA).

2.2.   Generation of Tumor Cell Spheroids

For generating A172 and U373 spheroids, cell suspensions of 1,000 cells/µL were generated in DMEM medium with 10% FBS and 1% Pen-Strep; and 20,000 cells/20 µL drops were placed on the cover of a 10 cm culture plate. Covers were flipped to allow for hanging drop formation, which were incubated at 37 °C incubator for 3 days in order to generate spheres. To provide humidification, PBS was added to plate. Formed spheroids were washed in PBS. For GBM8, GBM4, and MGG119 primary cell neuro-spheres, EF media was used and spheres were naturally generated in suspension.

2.3.   Shape Coefficient Analysis

After generating spheroids, they were transferred to 24-well plates and individual spheres were imaged. Shape coefficients of spheres were determined using ImageJ software (NIH Image, Bethesda, MD, USA) circularity coefficient tool.

2.4. Dispersal Assays

After spheroids were generated and washed, they were manually transferred to 24-well plates using 200 µL pipette tips for dispersal experiments. Tumor spheres were allowed to settle and attach to 24-well plates in culture medium. Cells were allowed to disperse out of sphere for 24 hours if otherwise stated.

For assays with *SERPINE1* pharmacological inhibition, U373 spheres and primary cell line spheres (GBM8, GBM4, and MGG119) were treated with 300 µM or 25 µM tiplaxtinin, respectively at the beginning of 24 hours of dispersal.

For assays with vitronectin coating, vitronectin was diluted 1:1000 with PBS, surface was coated at 37 °C for 2 hours. Spheres were placed on coated surface after surface was washed with PBS. For assays with collagen coating, collagen was diluted 1:60 with 0.02 N acetic acid, and surface was coated at 37 °C for an hour. Spheres were placed on coated surface after surface was washed twice with PBS.

For assays testing TGFβ signaling, spheres were treated with TGFβ (50 ng/mL), Repsox (1 µM for U373, 5 µM for A172) or SB431542 (2.5 µM) for 24 hours after attachment. Images were taken using Nikon Eclipse TS100 Inverted Fluorescence Microscope (Nikon Instruments Inc., USA) at time 0 (right after spheres were transferred to wells) at 24 hours (which is the end point of dispersal assays for A172 and U373 cell line spheroids) or 5 hours which is the end point of dispersal assays for GBM4, GBM8 and MGG119 primary cell line spheroids if otherwise stated.

2.5. Dispersal Area Analysis

Dispersal area analysis was performed using paint.net software (USA). Images (an image corresponding to each sphere) were analyzed using a Lasso tool. Total area of dispersal and remaining spheroid area were measured for the endpoint of dispersal, and overall dispersal was determined by normalization to starting area of individual spheres using the following equation:

$$\text{normalized dispersal} = \frac{[\text{total area(end point)} - \text{sphere area(end point)}]}{[\text{sphere area(time 0)}]}$$

Normalized dispersal value was calculated for each individual sphere (**Figure 2.1**) in the experimental condition, then an average value for condition was calculated.

Figure 2.1. Representative images of an individual spheroid for normalized dispersal area calculation. *left:* endpoint total area, *middle:* endpoint sphere area, *right:* time zero sphere area.

2.6. Wound Healing Assays

For wound healing experiments, 400,000 cells/well were seeded on 6-well plates. Cells were scratched using a 200 µL tip, washed with PBS and media was refreshed. Images were taken using Nikon Eclipse TS100 Inverted Fluorescence Microscope (Nikon Instruments Inc., USA). Multiple images were collected from the wound at time 0 right after scratch was generated and 24 hours after scratching (**Figure 2.2**). Distance of the cells from each side of the wound were analyzed using ImageJ ($n = 35$ areas were analyzed for each condition).
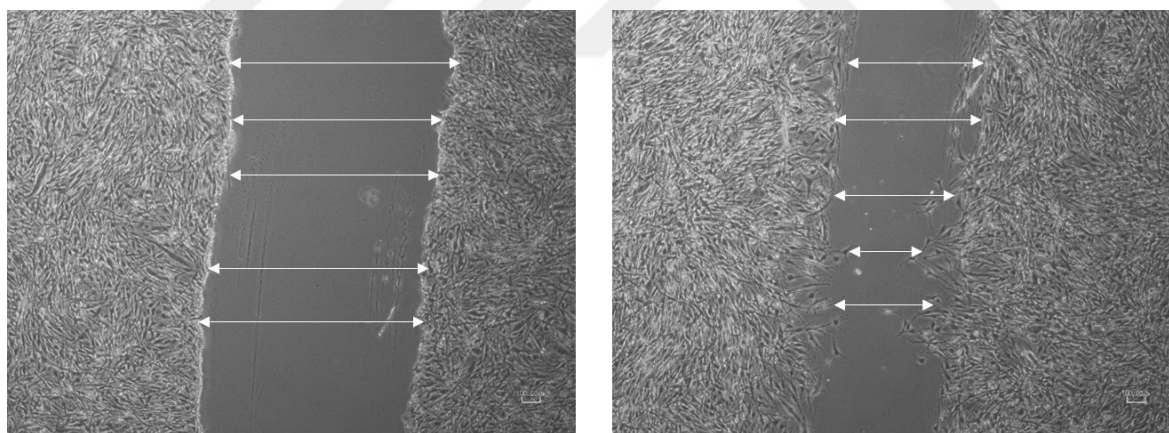
Figure 2.2. Representative images of wound healing assay. Images taken from wound for wound healing analysis. Arrows depict the data points collected from these individual images. *left:* wound at time zero, *right:* wound after 24 hours of migration.

2.7. RNA Sequencing (RNA-seq) and Transcriptome Profiling of Core and Migratory Cells

For RNA-sequencing, 360 spheroids for each replicate were generated. After spheroids were formed, they were transferred to plates and were allowed to disperse for 24 hours. Core and dispersive populations were collected by manual dissection. **Figure 2.3** shows

representative images taken right after manual collection of spheroids, note that dispersive cells are still intact after spheroids were removed.

Separately collected dispersive cells and cores were pelleted by centrifugation and RNA was isolated using Macharey–Nigel RNA kit (Germany) following manufacturer's instructions. Library preparation, sequencing, and raw data processing were performed at the Epigenomics Core at Weill Cornell Medical School, Genomics Core Facility (New York, NY, USA).
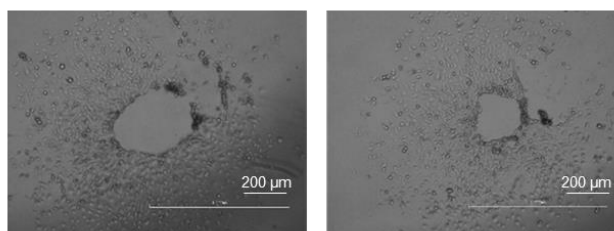
Figure 2.3. Representative images of dispersive cells after manual spheroid collection. Images show that dispersive cells are still intact after spheroids were removed.

Briefly, RNA-seq libraries were prepared using established Illumina methods (Part #RS-122-2001), using HiSeq2500 (Illumina, San Diego, CA, USA). Single end 50 bp reads were generated with 2 biological replicates for each condition. Primary processing of sequencing images was done using Real-Time Analysis software (RTA) (Illumina, San Diego, CA, USA). CASAVA 1.8.2 software (Illumina, San Diego, CA, USA) was then used to demultiplex samples, generate raw reads and respective quality scores, as well as to perform image capture, base calling, and demultiplexing.

For RNA sequencing analysis, single-end reads were aligned to human genome GRCh38 using an HISAT2[254] aligner using prebuilt indexes that were downloaded from the official website of HISAT2. The resulting sam format files were converted to bam and sorted using SAMtools[255]. The aligned reads were counted using FeatureCounts[256]. Differentially expressed genes were identified based on negative binomial distribution using DESeq2 (v.1.18.1)[257]. The RNA-seq data have been deposited in NCBI's Gene Expression Omnibus (GEO), with accession number GSE130857.

Enrichment of gene sets and functions were analyzed using Ingenuity Pathway Analysis (IPA)[258] and Gene Set Enrichment Analysis (GSEA) software (GSEA V4.0.2, Cambridge, MA, USA).

Chapter 2: Materials and Methods

2.8. qRT-PCR Experiments

RNA isolation from samples were conducted using Nucleospin RNA isolation kit (Macharey-Nagel, Germany) following manufacturer's instructions. Concentrations of isolated RNA samples were measured with NanoDrop in absorbance-based method.

For cDNA synthesis, required amount of RNA was mixed with 2.5 µL of 2nM dNTPs (Life Technologies, USA) and 1 µL of random hexamers (Invitrogen, USA) for each sample. Total volume or reactions was completed to 16.5 µL with nuclease-free H_2O. Following incubation at 65^oC for 5 minutes, RT mix composed of 5 µL of First Strand Buffer (Invitrogen, USA), 2 µL of 0.1 M DTT (Invitrogen, USA) and 0.5 µL of RNasin (Promega, USA) was added to each tube and incubated at room temperature for 10 minutes. Finally, 1 µL of MMLV-RT enzyme (Invitrogen, USA) was added. Reactions were incubated at 37^oC for 1 hour and inactivated at 70^oC for 15 minutes. Reactions were diluted by adding 75 µL of nuclease-free H_2O in order to be used in qRT-PCR experiments.

For qRT-PCR reaction, 10 µL of 2X LightCycler®480 SYBR Green I Master Mix (Roche, Switzerland), 1 µL of 5 µM primer (Roche, Switzerland), 1 µL of 5 µM primer mix which contains forward and reverse primer together and 7 µL of RT-PCR grade together and 7 µL of RT-PCR grade H_2O was mixed for each well of 96 well opaque white plate (Roche, Switzerland). 2 µL of plate (Roche, Switzerland). 2 µL of diluted cDNA was added to each well. C_P values were obtained for each reaction using obtained for each reaction using Roche LightCycler 480. The primers used in qRT-PCR experiments were listed in

experiments were listed in

Table *2.1*. EMT-related primers (Slug, Wnt5A, N-cadherin, Col3A1, Zeb1, Twist, Sparc, Snail, E-cadherin, Tcf4 and FoxC2) were kindly gifted by Dr. Tamer Önder[259].

Table 2.1. qRT-PCR primer sequences.

Gene Name	Forward primer (5'-3')	Reverse primer (5-3')
GAPDH	AGCCACATCGCTCAGACAC	GCCCAATACGACCAAATCC
SERPINE1	TCGAGGTGAACGAGAGTGGCA	AAGGACTGTTCCTGTGGGGTTGT
CYR61	CCAAGAAATCCCCCGAACCA	GAAACGCTGCTTCATTGGCA
CCND1	AAGATCGTCGCCACCTGGAT	AGCTCCATTTGCAGCAGCTC
CTGF	CACCCGGGTTACCAATGACA	GGATGCACTTTTTGCCCTTCTTA
CSF2	GCTGAGATGAATGAAACAGTAGAAG	CTGGGTTGCACAGGAAGTT
INHBA	GAAGAGTGGGGACCAGAAAGAGAAT	GCAGCGTCTTCCTGGCTGTT
CXCL8	TTGGCAGCCTTCCTGATTTCT	ATTCTCAGCCCTCTTCAAAAACTTC
ANKRD1	ACGCCAAAGACAGAGAAGGAGAT	AGATCCATCGGCGTCTTCCCA
NAV3	CATCCTCCCAAAGATCTTCGCATCA	TCAGCTCACTTCCTCTAGAGTTCAC
RAD51	TGCGGACCGAGTAATGGCA	TCCTTCTTTGGCGCATAGGCA
HAP1	AGCTGGCTTCGGAGAAGGAAA	AAATCATACCTTAGGCTGGATGTGT
EFNA1	AGTTCCAGCGCTTCACACCTT	TGGGTCATCTGCTGCAAGTCTCT
YPEL4	GGAGCAGACCTCAAGGTGACTT	TGAAGCAGCGGAGCAGGTTG
BMF	GAGCCATCTCAGTGTGTGGAG	GCCAGCATTGCCATAAAAGAGTC
RGS16	TCAGAGCTGGGCTGCGATACT	TTCAGGAAAGCGTGGAAGGCA
PTP4A3	CCGGTGGAGGTGAGCTACAA	GCCAGTCCACAACGGTGAT
PCK1	GACACAGTGCCCATCCCCAAA	CGTCAGCTCGATGCCGATCTT
PTX3	CAGACGCGAGCCGACCTG	TGGTCTCACTGGATGCACGCT
NTM	TGGTACAAGGATGACAAAAGACTGA	GGGGTCAGGGCTGTAGTTTTCA
CDC45	TGACAGTGATGGGTCAGAGCCT	GTTCACTCCCAGAGCCACTCC
MCM3	AGGTAGTTCTTTGGCAGCGG	AAATTCCCTGGTCTTCCTCGT

2.9.   Cloning and Packaging of Silencing Vectors

shRNA sequences were designed using an RNAiCodex program[260]. shRNA sequences targeting related genes are given in **Table 2.2**. Oligos were PCR-amplified by using following primers having compatible restriction ends with backbone vector, pSMP.   Forward: 5′ GATGGCTGCTCGAGAAGGTATATTGCTGTTGACAGTGAGCG-3′,   Reverse: 5′-CCCTTGAACCTCCTCGTTCGACC-3′. PCR products were cloned into an pSMP retro-viral backbone as described[261]. All vectors were verified by sequencing.

Table 2.2. shRNA oligo sequences.

shRNA	oligo sequence (5'-3')
shSERPINE1 #1	TGCTGTTGACAGTGAGCGAGGACACCCTCAGCATGTTCATTAGTGAAGCC ACAGATGTAATGAACATGCTGAGGGTGTCCCTGCCTACTGCCTCGGA
shSERPINE1 #2	TGCTGTTGACAGTGAGCGCCCATACAATTTCATCCTCCTTTAGTGAAGCC ACAGATGTAAAGGAGGATGAAATTGTATGGTTGCCTACTGCCTCGGA
shCDC45	TGCTGTTGACAGTGAGCGACCAGTCAATGTCGTCAATGTATAGTGAAGCC ACAGATGTATACATTGACGACATTGACTGGCTGCCTACTGCCTCGGA
shMCM3	TGCTGTTGACAGTGAGCGACCACAGATGATCCCAACTTTATAGTGAAGCC ACAGATGTATAAAGTTGGGATCATCTGTGGCTGCCTACTGCCTCGGA
shCTGF	TGCTGTTGACAGTGAGCGCCGCCTCCTGCAGGCTAGAGAATAGTGAAGC CACAGATGTATTCTCTAGCCTGCAGGAGGCGTTGCCTACTGCCTCGGA
shCYR61	TGCTGTTGACAGTGAGCGACCTGTGAATATAACTCCAGAATAGTGAAGCC ACAGATGTATTCTGGAGTTATATTCACAGGGTGCCTACTGCCTCGGA

Sequenced vectors were packaged into retroviral particles as described[261,262]. Briefly, 800.000 293T cells were seeded on 6 cm culture dish with complete DMEM. Next day, viral plasmid DNA (1µg) and packaging plasmids (pUMVC (1 µg) and VSVG (110 ng)) were mixed and transfected to cells using Fugene HD reagent (Promega, USA). Media was changed after 16 hours of transfection. Virus containing media was collected 48 and 72 hours after transfection, filtrated by 0.45 μm filters.

If collected viruses were to be used in GBM8 cells, viruses were concentrated in order to protect GBM8 cells from the effect of serum. 50% PEG (Sigma Aldrich, USA) was added as 1:5 volume ratio on collected viruses and left overnight. Viruses were centrifuged at 1500 g for 30 minutes at 4°C and then for 5 minutes again to remove supernatant. Collected viral particles were dissolved in PBS to make a total 100X concentration.

Viral transductions were carried out using fresh viruses. Cells reached to 70-80% confluency were transduced with virus containing media with 10 µg/mL protamine sulfate (Sigma Aldrich, USA) addition. 16 hours post-transduction, viral medium was replaced by fresh media. Next day, transduced cells were selected by 2 µg/mL Puromycin (Sigma Aldrich, USA) antibiotic for 3 days.

2.10. Western Blotting

Conditioned medium (CM) or cell lysates derived from A172, U373, or GBM8 cells were used to examine SERPINE1 protein levels. For CM collection, media on cells growing in culture were refreshed with serum-free DMEM. After 48 hours of incubation, CM and cell lysates were obtained. GBM8 cells were seeded with EF media and cultured for 48 hours before CM and lysate collection. CM was added to a 10 kDa ultrafiltration tube (50 mL, Millipore,

France) and centrifuged at 3500× *g* in 4 °C, for 30 min for enrichment. Protein extraction and Western blotting was performed as described[263]. The following primary antibodies were used: SERPINE1 (Santa Cruz Biotechnology sc-5297, USA), GAPDH (Abcam ab9485, USA), Beta-tubulin (Abcam ab6046, USA). To control the equal loading of CM PVDF membranes were stained with Panceu. Secondary antibodies against corresponding antibodies were horseradish peroxidase coupled goat anti-rabbit IgG (Abcam ab97051, USA) and or goat anti-mouse IgG (Abcam ab97023, USA). Blots were incubated with Clarity™ Western ECL Substrate (Biorad, USA) and visualized using an Odyssey Scanner (LiCor Biosciences, USA).

2.11. Cell Viability and Cell Cycle Experiments

Cell viability was measured with ATP based Cell Titer-Glo® (CTG) Luminescent Cell Viability Assay (Promega, USA) according to the manufacturer's instructions using a plate reader (BioTek's Synergy H1, USA) at 560 nm. 1000 cells/well were seeded to 96-well plates (Corning Costar, clear bottom black side, USA) as triplicates for each condition and cell growth was determined by repeated measurement of cell viability on days 3, 5 and 7 after seeding. Before reading viability results, media was removed and replaced with CTG mixture diluted 1:10 with media for the attached cells. For suspension cells, CTG reagent was directly transferred to media as 1:10.

For cell cycle analysis, cell pellets were collected and washed in ice-cold PBS. Pellets were resuspended with ice-cold EtOH (70%) and incubated at 4°C for 30 min. Fixed cells were washed with PBS twice. Resuspension was carried out in RNase A (100 µL/mL, Thermo Fisher Scientific, USA) containing PBS and incubated at room temperature for 15 min. PI (50 µL/mL, Sigma Aldrich, USA) was added on samples and incubated at room temperature for 30 min for staining. Stained cells were analyzed by BD Accuri C6 (BD Biosciences, USA) flow cytometer by recording 10.000 events for each sample.

2.12. Immunofluorescence Staining

Cells on coverslips (uncoated or vitronectin coated) were washed and fixed with 3% PFA for 5 minutes. Fixed cells were washed with PBS and permeabilized with 0.1× Triton for 3 minutes. After washing and blocking for 30 minutes, coverslips were incubated with primary antibodies at 4 °C overnight in humidified chamber. Following washing steps to remove excess amount of primary antibody, cells were incubated with secondary antibodies at room temperature for 1 hour. Mounting was performed with VectaShield with DAPI (Vector Laboratories, USA). Antibodies used in the experiments are: anti-vinculin antibody (Abcam

ab73412, USA), rhodamine-phalloidin (Thermo R415, USA) and AlexaFluor488 (Thermo, USA). Images were taken using Leica DMI8 SP8 CS/DLS microscope (Leica Microsystems, Germany) at 63× magnification. At least 20 cells were analyzed for each condition.

2.13. Adhesion Experiments

For adhesion experiments of cells growing as monolayer cultures, cells were washed, trypsinized and counted. For suspension cells, cells were harvested, treated with accutase (Stem Cell Technologies, USA) and counted. Cell suspensions of 100,000 cells/well were prepared. To ensure the seeding of equal number of cells from each group, starting cell suspensions were subjected to viability assays and consistency in the cell number was verified. For both control and SERPINE1 knock-down conditions, cells were transferred to uncoated or vitronectin coated (for attached cells) or collagen coated (for suspension cells) 24-well plates simultaneously and allowed to adhere. For different time points, unattached cells were washed off with PBS and attached cells were fixed with ice-cold methanol at for 5 minutes. Attached cells were stained with crystal violet (Sigma, USA) for 1 hour, washed and left to dry. Plates were scanned and particle mean for each well were analyzed using Adobe Photoshop (Berkeley, CA, USA). Triplicates were used for each condition.

2.14. Single-Cell Tracking and Persistence Analysis

The trajectories of cells on uncoated and vitronectin-coated surfaces were determined by using a custom script written in MATLAB (R2017b, Mathworks, Natick, MA, USA). Single-cell tracking code to determine time-dependent positions of cells was partially adapted from previous studies[264,265]. Briefly, point defects were removed by using a Gaussian filter with a lower bound of 3 pixels. A threshold filter was applied to determine the location of each cell. Centroid position of segmented cells was later determined by comparing intensity values in the neighboring pixels. Mean square displacement of cell position in consecutive frames was computed to associate each cell. Trajectories of cells were displayed on a polar plot. Persistence ratios of cells were analyzed by computing the ratio of direct distance to total displacement. If the ratio approaches to 1, cells tend to move linearly. Low persistence ratios imply a random migration. Direct displacement was measured by an interval of 8 frames while cumulative displacement was computed by an interval of 2 frames to avoid the overestimation of persistence due to the movement of cell centroid positions.

2.15.   Patient Survival Analysis

Gene expression profiles of "glioblastoma multiforme" (GBM) and "brain lower grade glioma" (LGG) tumors were preprocessed by the unified RNA-Seq pipeline of The Cancer Genome Atlas (TCGA) consortium. For both cancer types, HTSeq-FPKM files of all primary tumors from the most recent data freeze (i.e., Data Release 14–December 18, 2018) were downloaded, leading to 703 files total. Clinical annotation files of cancer patients were used to extract their survival characteristics (i.e., days to last follow-up for alive patients and days to death for deceased patients). Clinical Supplement files of all patients from the most recent data freeze were downloaded, leading to 1114 files in total. To perform survival analysis using gene expression profiles, a total of 663 patients with survival information and gene expression profile available were included. The gene expression profiles of primary tumors were first $\log_2$-transformed and then *z*-normalized within each cohort before further analysis. For analyses, 663 samples were grouped into two categories (i.e., low and high) based on comparing each sample's gene expression value compared to the mean expression value of that particular gene. Kaplan–Meier analysis was used to compare the survival of these two groups and the log-rank test performed to obtain the *p*-value. For correlation of SERPINE1 expression with glioma grades or glioblastoma subtypes, the data with gene expression and subtype or grade information were analyzed and Wilcoxon rank sum test was used to compare the groups.

2.16.   Live Cell Imaging Experiments

Live-cell imaging experiments were carried out using a Leica DMI8 inverted microscope Leica Microsystems, Germany) with 10× air objective in a chamber at 37 °C, supplied with 5% CO_2. For *SERPINE1* knock-down in GBM8, time lapse series were captured from randomly selected positions for 5 hours of dispersal, with images taken every 5 minutes. For GBM8 dispersal with tiplaxtinin, time-lapse series were captured from positions for 5 hours of dispersal, with images taken in every 60 minutes. Image stacks were generated for each position and relative increase in dispersal area was measured by dividing final area of each neuro-sphere to initial area of that individual sphere. Results were obtained by calculating average increase for spheres of each experimental group.

2.17.   In Vivo Experiments

Non-obese diabetic/severe combined immunodeficiency (NOD/SCID) mice housed and cared in appropriate conditions of the Koç University Animal Facility were used. All protocols were approved by the institution boards of Koç University (ethical code: 2013.198.IRB2.61 and

date of permission: 27 August 2013). shControl or sh*SERPINE1* transduced GBM8 cells were further transduced with a vector carrying Firefly Luciferase (Fluc) and mCherry. 400,000 cells were injected in 7 µL PBS intracranially using stereotaxic injection, as described with coordinates from bregma, AP: -2 mm, ML: 1.5 mm, V (from dura): 2.5 mm[266]. Presence and progression of tumors were monitored by repeated noninvasive bioluminescence imaging (IVIS Lumina III, PerkinElmer, USA) by injecting D-luciferin (Biotium, USA) intraperitoneally as 150 µg/g body weight. 32 days after injection, mice were perfused with 4% PFA, and brains were dissected. Quantification of tumor progression was performed with GraphPad PRISM software (Graphpad Prism v5, USA). 10-micron thick cryo-sections from tumors were stained with hematoxylin & eosin. Sections were first stained with Hematoxylin (Merck, USA) for 1 minute and immediately washed with dH₂O, then counter-stained with Eosin Y (Electron Microscopy Sciences, USA) for 30 seconds and washed again. Sections were dipped into 70% EtOH, 96% EtOH, 100% EtOH in order and then placed into Xylene (Merck, USA) for 5 minutes. Slides were mounted using Entellan (Merck, USA). Sections were imaged with Leica M205 FA Stereo microscope (Leica Microsystems, Germany).

2.18. Statistical analysis

QPCR results in figures 3.8., 3.13., 3.16., 3.17. and 3.27. were normalized to expression of core sample. Results in Figure 3.14. were normalized to expression of SUM149 cells. Results in Figure 3.18. were normalized to expression of U373 cells. Results in figures 3.19., 3.20., 3.28., 3.32. and 3.52. were normalized to expression of shControl sample. Result in Figure 3.39. was normalized to expression of uncoated condition shControl sample. Result in Figure 3.44. was normalized to expression of untreated condition. Result in Figure 3.45. was normalized to expression of DMSO-treated condition. Result in Figure 3.48. was normalized to expression of DMSO-treated core sample.

Dispersal analysis in figures 3.14., 3.22., 3.30., 3.37. and 3.38. were normalized to dispersal of shControl sample. Dispersal analysis in figures 3.24. and 3.47. were normalized to dispersal of DMSO treated sample. Dispersal analysis in figure 3.36. was normalized to dispersal of uncoated condition sample. Dispersal analysis in figure 3.46. was normalized to dispersal of untreated sample. Dispersal analysis in figures 3.54., 3.55. and 3.56. were normalized to time zero area for sample in each group separately.

Viability analysis in figures 3.25., 3.29. and 3.53. were normalized to time zero viability results for each group separately. Viability analysis in Figure 3.26. was normalized to DMSO treated sample. Cell cycle analysis in Figure 3.31. was normalized to shControl sample.

Chapter 2: Materials and Methods

Focal adhesion analysis in Figure 3.34. was normalized to shControl sample.

Significance was detected by student's t-test or ANOVA, and at p-value <0.05.

3.   RESULTS

3.1.   Fitness of the GBM Cell Lines for the Model was Tested

3.1.1.   Sphere Forming Ability of GBM Cell Lines Were Tested

To assess the fitness of our cell lines to hanging drops spheroid model, we formed tumor spheroids from six different GBM cell lines and compared their sphere forming ability. After forming spheroids, we analyzed circularity coefficients of different cell line spheroids. In this analysis, while circularity shape coefficient value of 1 indicates perfect spheroids, value of 0 means that form is not a spheroid. We observed that LN18, LN229, and T98G cells stayed as multi-centric clumps in the hanging drops and they were unable to form spheroids. On the other hand, A172, U373, and U87MG cells could form single compact spheroids (**Figure *3.1***).
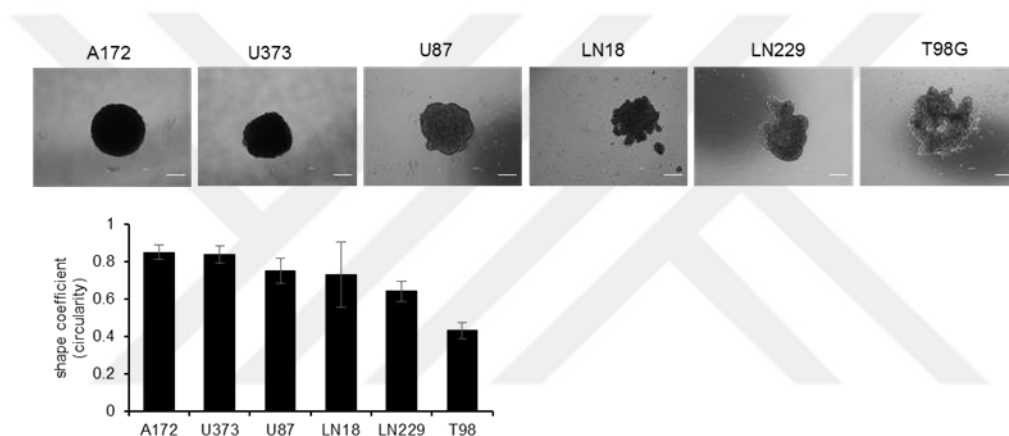
Figure 3.1. Shape coefficient analysis of GBM cell lines. Spheroids of 6 GBM cell lines analyzed for their circularity shape coefficient. Shape coefficient value of 1 indicates perfect spheroids. A172, U373 and U87MG can generate almost perfect spheres ($n = 8$ spheroids for each cell line, scale bar: 250 µm).

3.1.2.   Dispersal Capacity of GBM Cell Line Spheroids Were Tested

To generate an in vitro model that better mimics the dynamics that operate between the tumor core and tumor rim, we tested outward migration ability of the cell lines, here termed dispersal. We formed spheroids and let the spheroids disperse for 24 hours. After dispersal analysis, we found that U373 cells have the highest dispersal capacity among cell lines tested (**Figure *3.2***).
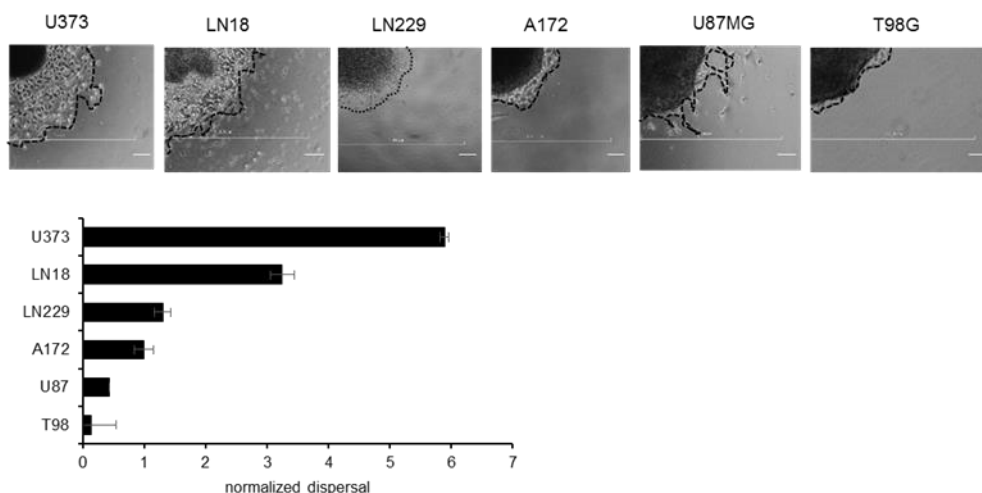
Figure 3.2. Dispersal capacity analysis for spheroids at 24 hours of dispersal. ($n = 8$ spheroids for each cell line, scale bar: 250 µm).

In the light of these experiments, we worked with U373 cells which exhibited the highest dispersal capacity and A172 cells that have a modest dispersal capacity. In order to collect adequate amount of high-quality RNA from the dispersive cells, we used U373 for further experiments such as transcriptome profiling and verified the hits for both cell lines, as well as a primary cell line as described below.

3.2. Transcriptome Profiling of Motile and Non-Motile GBM Cells Reveal Major Changes in Gene Expression

To assess the transcriptional differences between the core (non-motile) and dispersive (motile) cell populations, we first generated U373 cell spheroids and let the spheroids disperse for 24 hours. After 24 hours of dispersal, we manually isolated those cells that have dispersed and those have remained in the tumor cores (**Figure *3.3***). We then extracted high quality RNA from 2 biological replicates of both core and dispersive cells (**Figure *3.4***) and shipped our samples for RNA sequencing to Epigenomics Core at Weill Cornell Medical School, Genomics Core Facility (New York, NY, USA).
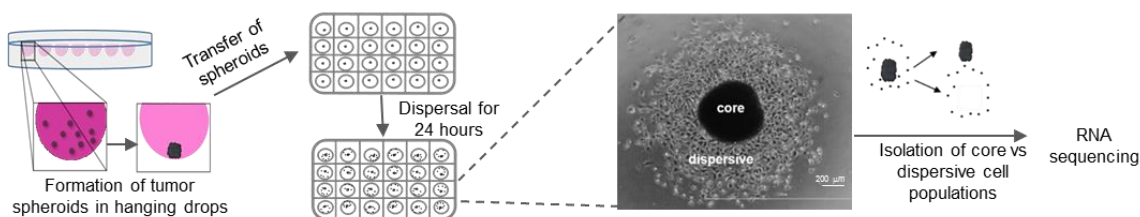
Figure 3.3. Strategy for RNA sequencing experiments. Hanging drops method was used to generate tumor-mimicking spheroids. After formation of tumor spheroids in hanging drops, spheres were transferred to well plates and allowed to disperse for 24 hours. Core and dispersive cells were collected separately for RNA sequencing.

Sample Name	Customer [conc] (ng/ul)	QC1 Qubit OD (ng/ul)	Total Sample (ng)	QC2 Bioanalyzer	QC Status
set1_d1s	50	49.4		10-16-2015/9.7	pass
set1_d1	25.8	26.2		10-16-2015/8.6	pass
set2_d1s	50	58		10-16-2015/8.7	pass
set2_d1	29.2	23.8		10-16-2015/8.6	pass

Figure 3.4. Quality-control of sequencing samples. (d1s: core 24 hours, d1: dispersive 24 hours). Quality control was performed using QC2 Bioanalyzer.

RNA-sequencing of core and dispersive cells pointed to major differences in transcriptome (**Figure *3.7***) with 1627 differentially expressed genes (DEGs) (log2 fold change -1$\leq$ or $\geq$1, *padj* $\leq$ 0.05). Of these DEGs, 985 were upregulated, and 642 were downregulated in dispersive cells (**Figure *3.5*** and **Figure *3.6***).
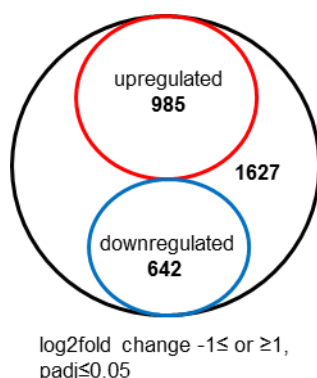
Figure 3.5. Differentially expressed genes in core and dispersive populations. Total 1627 genes were differentially expressed between motile and non-motile cells. (*log2 fold change -1$\leq$ or $\geq$1, padj $\leq$ 0.05*).
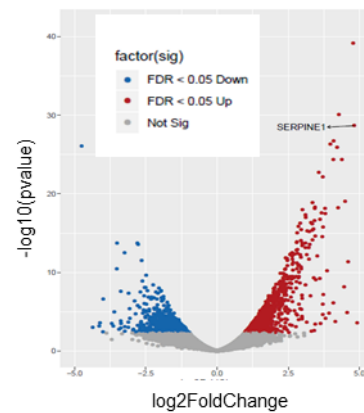
Figure 3.6. Volcano plot for differentially expressed genes. Plot showing the upregulated (red) and downregulated (blue) genes in dispersive cells. *Figure generated by Fırat Uyulur.*
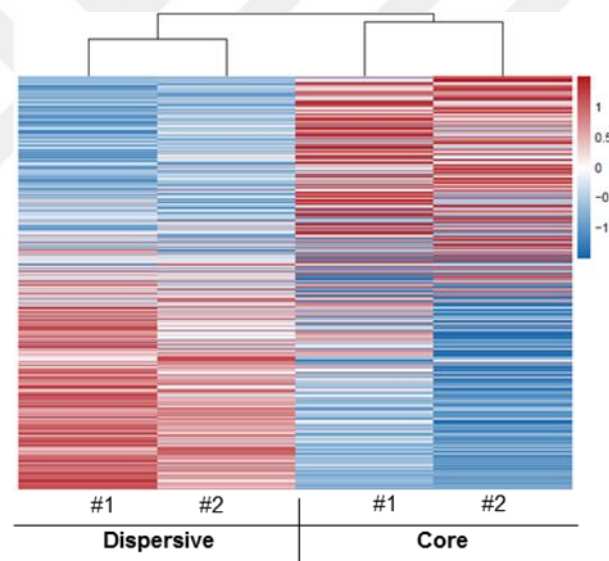
Figure 3.7. Gene expression heatmap for core and dispersive transcriptomes. Transcriptome of core and dispersive cells have major differences. *Figure generated by Fırat Uyulur.*

We validated the differences in gene expression of the most significantly altered genes in core and dispersive cells with qRT-PCR in independently collected samples (**Figure *3.8***). We were able to validate the differential expression of those genes in core and dispersive cells. Accordingly, SERPINE1 (54.69 fold), CYR61 (39.21 fold), CCND1 (28.97 fold), CTGF (27.73 fold), CSF2 (26.29 fold), INHBA (22.32 fold), CXCL8 (18.81 fold), ANKRD1 (11.18 fold),

NAV3 (10.48 fold) and RAD51 (10.15 fold) genes were upregulated; and HAP1 (5.58 fold), EFNA1 (6.23 fold), YPEL4 (9.43 fold), BMF (11.70 fold), RGS16 (12.52 fold), PTP4A3 (13.45 fold) and PCK1 (51.26 fold) genes were downregulated in dispersive cells compared to core.
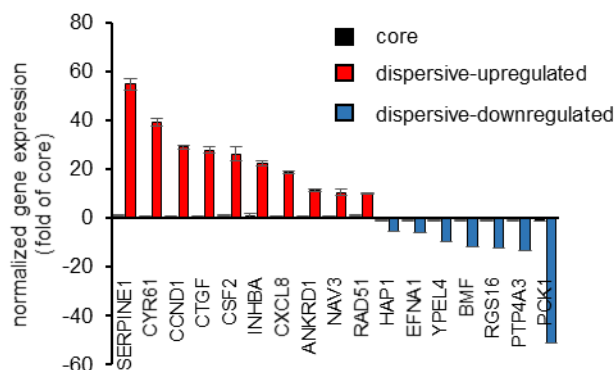
Figure 3.8. **QRT-PCR validation of top differentially expressed genes in core and dispersive cells.** Expression data is normalized as fold of core sample.

3.2.1. Transcriptome Profiling of Motile and Non-Motile GBM Cells Reveal Major Alterations in Cell Movement Pathways

After RNA-sequencing, we first analyzed the function of the genes which were differentially regulated in dispersive cell transcriptome to better understand their roles in the context of cell biology. Functional analysis of RNA-sequencing results with Ingenuity Pathway Analysis (IPA) tool showed that "cell movement" was a majorly activated pathway in dispersive cell transcriptome as it was statistically significant in multiple disease and pathway sets (**Figure *3.9***).
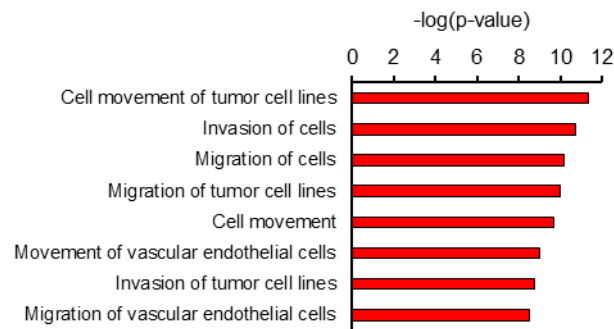
Figure 3.9. IPA analysis of differentially expressed genes. "Diseases and bio functions" from IPA core functional analysis of the differentially expressed genes related to "cell movement" in the dispersive cells. (*z-score* of >|2|).

Similarly, gene set enrichment analysis (GSEA) revealed that, in addition to several gene sets related with cell cycle such as "E2F targets", "G2-M checkpoint", and "Myc targets", a movement related "EMT" gene set was significantly upregulated in dispersive cells (**Figure 3.10** and **Figure 3.11**).
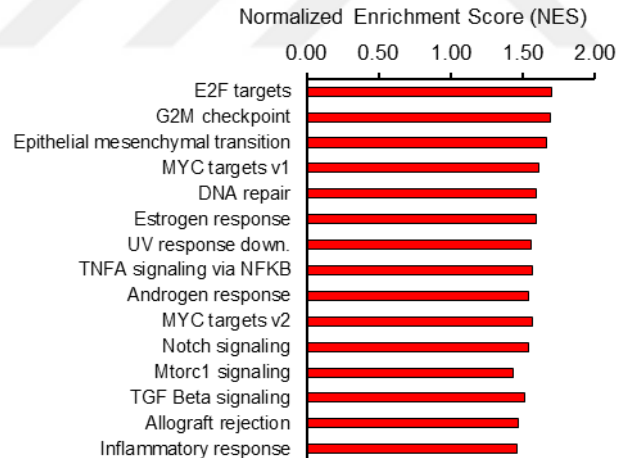
Figure 3.10. Top 15 cancer hallmark gene sets in dispersive cells. These gene sets were enriched in dispersive cell transcriptome in GSEA analysis. (*NOM p* ≤ 0.05). *GSEA analysis performed with Alişan Kayabölen.*
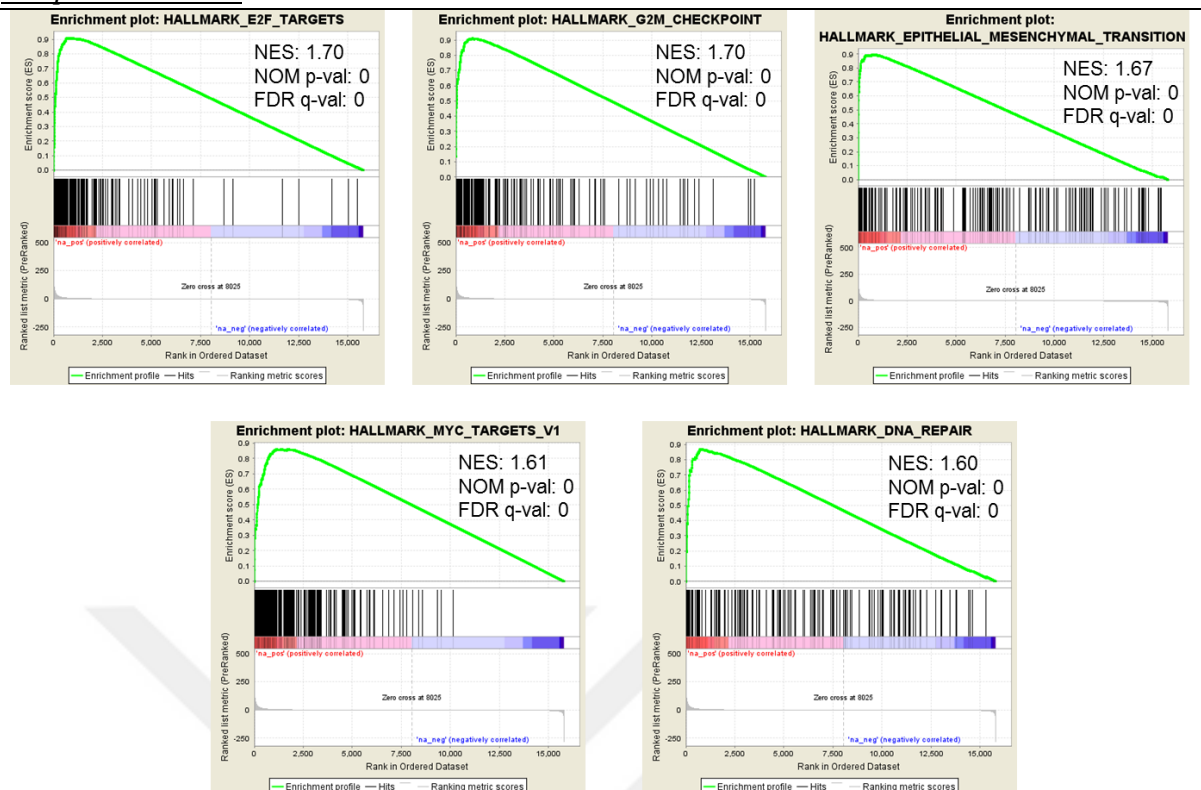
Figure 3.11. Enrichment plots for top 5 enriched gene sets in dispersive cells. Normalized enrichment score (*NES*), nominal p value (*NOM p-val*) and False Discovery Rate q value (*FDR q-val*) were indicated for each enrichment plot. *GSEA analysis performed with Alişan Kayabölen.*

We wanted to focus on EMT gene set genes since these set contains genes related with cell movement and assessed the expression of EMT genes in core and dispersive cells. Accordingly we found that EMT genes were upregulated in dispersive cell transcriptome as expected (**Figure** *3.12*).
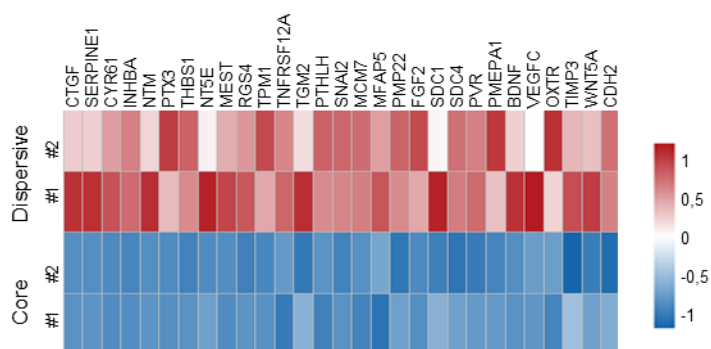
Figure 3.12. Gene expression heat map of EMT genes in core and dispersive cells. (biological duplicates were shown). *Figure generated by Fırat Uyulur.*

Given the marked upregulation of EMT genes in dispersive cells, we compared the expression of these genes in core and dispersive cells by qRT-PCR in independently collected samples (**Figure** *3.13*). We showed that a number of key EMT regulators, such as Slug (5.13 fold), Wnt5A (3.18 fold) and N-cadherin (2.93 fold) were indeed upregulated in dispersive population compared to core population.
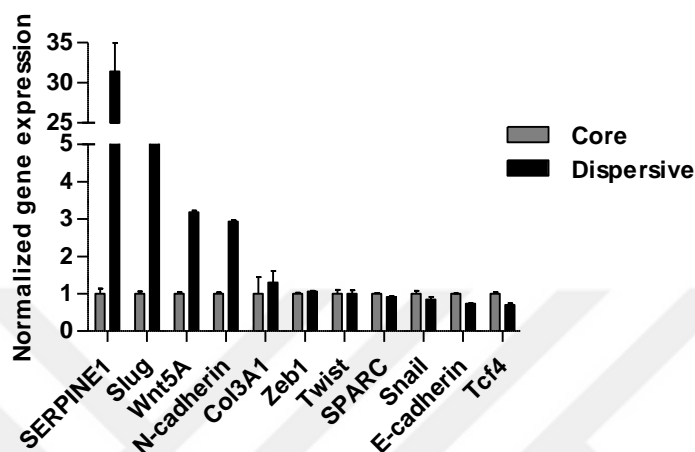
Figure 3.13. Expression levels of EMT genes in core and dispersive populations. Expression data is normalized as fold of core sample.

Among the EMT related genes that were altered, *SERPINE1* was the most upregulated gene in dispersive cells (**Figure** *3.13*). Other top upregulated genes linked with EMT were *CTGF* and *CYR61,* whose relations to GBM cell invasion were previously demonstrated[159], attesting to the strength of our approach for identifying mediators of dispersal. Indeed, downregulation of *CTGF* or *CYR61* reduced the dispersal ability of GBM cells in our spheroid model validating the findings of previous reports (**Figure** *3.14*). Here, knockdown of CTGF and CYR61 with shRNA reduced gene expression levels down to 55% and 59% respectively. This was accompanied by a concomitant decrease in dispersal.
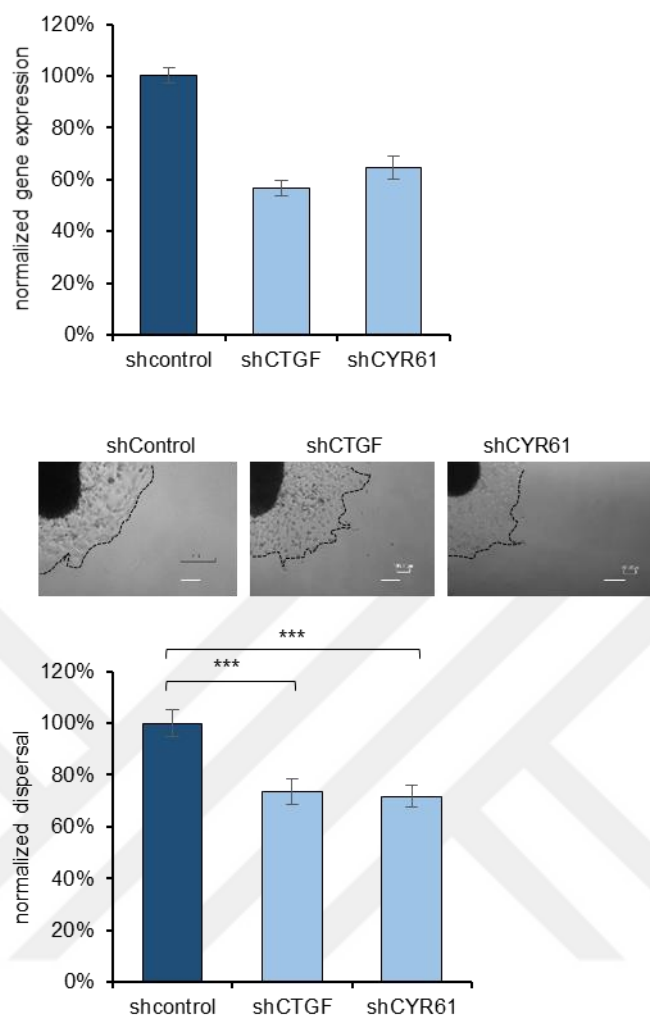
Figure 3.14. Effect of *CTGF* or *CYR61* knock-down on dispersal. Knock-down of CTGF or CYR61 genes reduces the dispersal of U373 spheroids. *top:* mRNA levels after shRNA knock-down of CTGF or CYR61 genes. *bottom:* Knock-down of CTGF or CYR61 genes reduces dispersal of U373 spheroids significantly ($n = 24$ spheroids for each condition, scale bar: 200 µm). (*** denotes $p < 0.001$, two-tailed Student's *t*-test).

In the light of transcriptome analysis of core and dispersive cells, we wanted to examine the role of *SERPINE1* gene in the context of GBM cell dispersal, since *SERPINE1* is the most upregulated gene in dispersive cells and a member of EMT gene set. To our knowledge, SERPINE1 has not been studied in the context of GBM dispersal before.

3.2.2. GBM Cell Lines Used Display Mesenchymal Characteristics

Since we showed the marked enrichment of EMT genes in dispersive cell transcriptome, we wanted to examine the mesenchymal characteristics of GBM cell lines (U373 and A172) and primary cell line (GBM8) used in the experiments. We assessed the expression of select epithelial and mesenchymal genes in addition to endogenous *SERPINE1* expression. For comparison, we used an epithelial cancer cell line, SUM149. Accordingly, expression of *E-cadherin*, an epithelial marker gene, was markedly lower in GBM cell lines compared to SUM159 cells. On the contrary, expression of N-cadherin, a mesenchymal marker gene was markedly higher in GBM cells. Expression of Snail, another gene from mesenchymal signature, was slightly higher (~2 fold) in 2 of the 3 GBM cell lines compared to SUM159 cells. Expression of Wnt5A was slightly lower in 2 of the 3 GBM cell lines compared to SUM159 cells. Overall, we concluded that GBM cell lines and primary GBM cell line display more mesenchymal characteristics compared to the epithelial cancer cell line (**Figure** *3.15*).
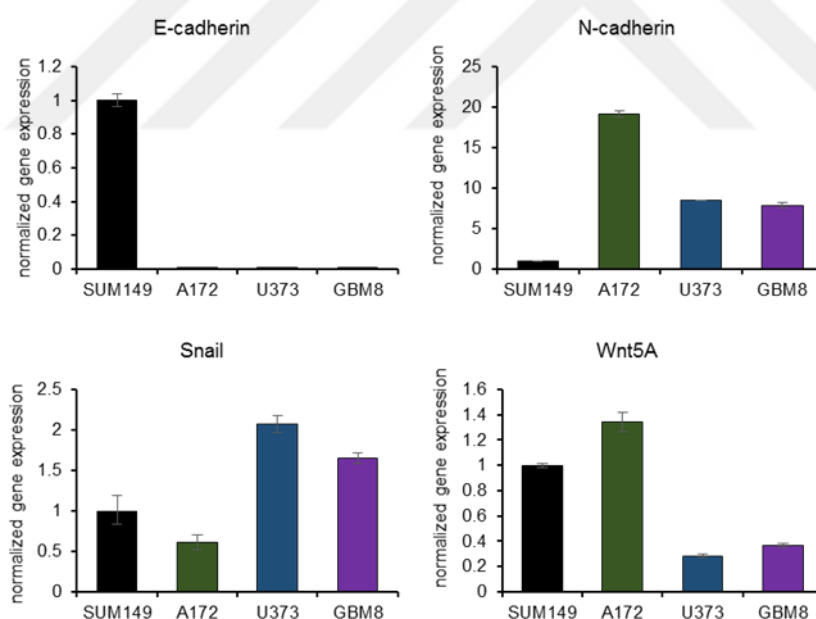
Figure 3.15. Endogenous expression of selected EMT genes for epithelial cancer cell line SUM149 and GBM cells. Expression data is normalized as fold of SUM149 expression.

3.3. *SERPINE1* Expression is Dynamically Regulated and Induced in Dispersive Cells

Given the marked upregulation of *SERPINE1* in dispersive cells, we re-examined its differential expression between core and dispersive cells for GBM cell lines U373 and A172

and showed that both displayed *SERPINE1* upregulation in the dispersive cell population (**Figure** *3.16*).
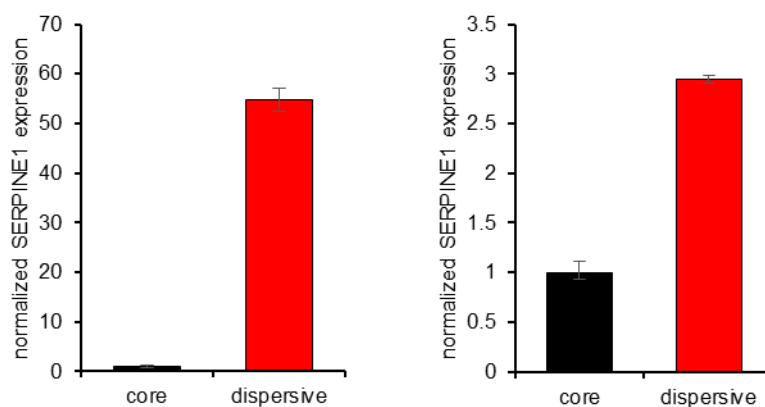
Figure 3.16. *SERPINE1* **expression in core and dispersive populations.** *left:* U373 and *right:* A172 cells.

We also assessed how the SERPINE1 expression changes in cells cultured with normal confluency, cells in core and dispersive populations to better understand its regulation. We have seen that endogenous SERPINE1 expression in cells cultured in normal confluency is dynamically regulated in core and dispersive cells (**Figure** *3.17*).
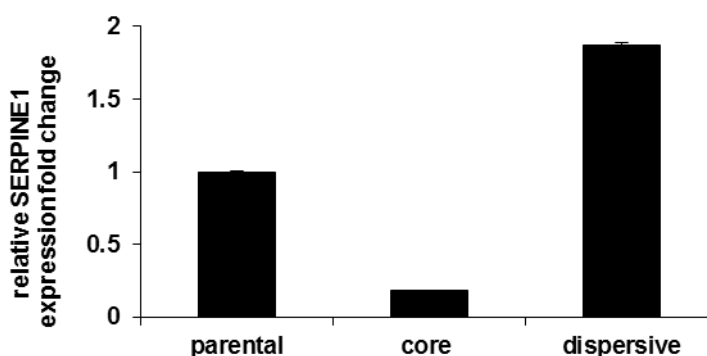
Figure 3.17. *SERPINE1* **expression in cells under normal confluency, core and dispersive rim.** Expression is normalized to parental cells which are cultured under normal confluency.

3.3.1. Endogenous *SERPINE1* Expression is Different for the Cell Lines and a Primary Cell Line Used in the Experiments

Before functional experiments related to SERPINE1, we assessed the endogenous SERPINE1 expression in the cell lines (U373 and A172) and the primary cell line (GBM8).

We found that endogenous expression levels of SERPINE1 is different for the cells used (**Figure** *3.18*). Despite their overall high dispersal, GBM8 cells had the lowest SERPINE1 expression.
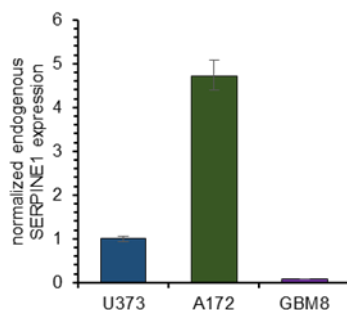
Figure 3.18. Endogenous *SERPINE1* expression for U373, A172 and GBM8 cells.

3.4.   *SERPINE1* Knock-down Reduces GBM Dispersal

To assess the effect of SERPINE1 on GBM cell dispersal, we have used multiple SERPINE1 shRNAs and were able to achieve significant SERPINE1 silencing in mRNA level in U373 cells (**Figure 3.19**).
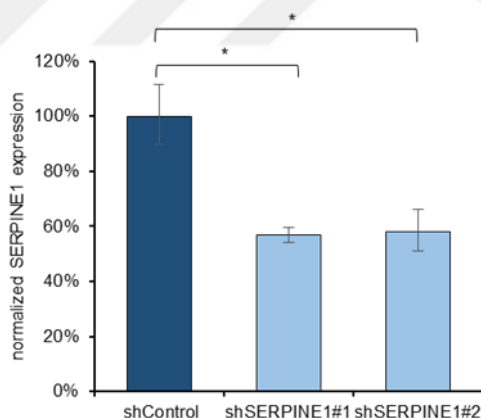
Figure 3.19. qRT-PCR analysis of *SERPINE1* expression levels after shRNA knock-down with multiple shRNAs in U373 cells. (* denotes $p < 0.05$, two-tailed Student's *t*-test).

We then selected the shRNA which gave better results, shSERPINE1#1, and used this shRNA to achieve significant SERPINE1 silencing in both cell lines, as revealed by qRT-PCR (**Figure 3.20**) and Western Blots (**Figure 3.21**).
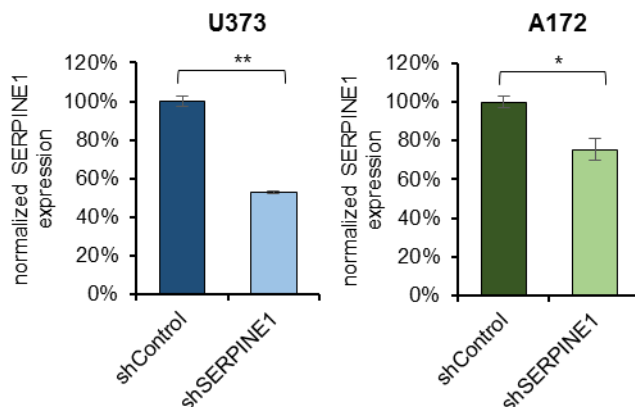
Figure 3.20. qRT-PCR analysis of *SERPINE1* expression levels after shRNA knock-down in U373 and A172 cells. (* and ** denote $p < 0.05$ and $p < 0.01$ respectively, two-tailed Student's *t*-test).
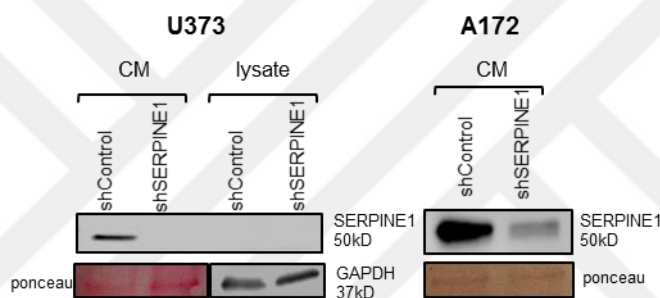
Figure 3.21. SERPINE1 protein levels after shRNA knock-down. *Western Blot experiment performed by Dr. İlknur Sur.*

Following the successful SERPINE1 knock-down, we assessed the effect of SERPINE1 inhibition on dispersal. We generated spheroids from control and SERPINE1 knock-down cells and compared their dispersal. We were able to show that SERPINE1 knock-down spheroids show a reduced dispersal phenotype for both of the cell lines, dispersal was reduced down to 63% for U373 and 74% for A172 spheroids (**Figure 3.22**).
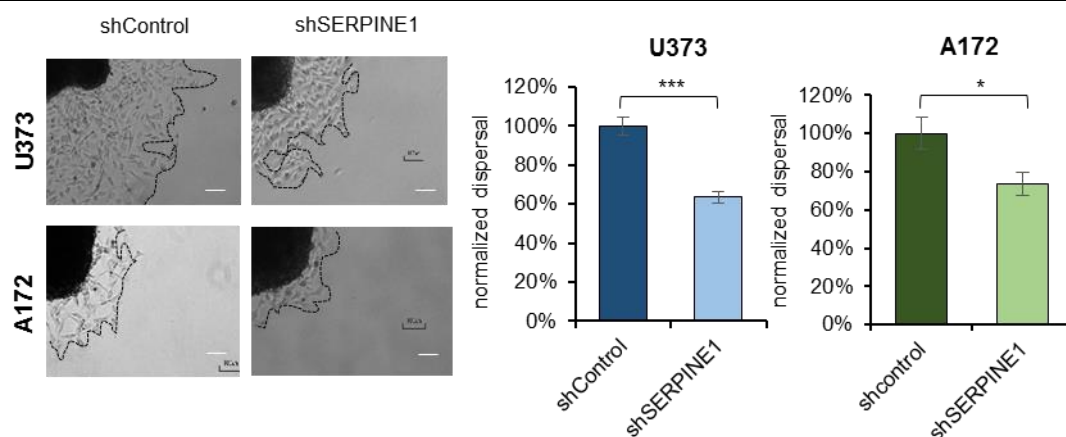
Figure 3.22. Dispersal assay with SERPINE1 knock-down. Dispersal assay showing *SERPINE1* knock-down reduces dispersal of U373 and A172 spheroids significantly. (n = 24 spheroids for each condition, scale bar: 200 μm). (* and *** denote p < 0.05 and p < 0.001 respectively, two-tailed Student's t-test).

We also validated this phenotype by conducting a migration assay. For wound healing assay, we first cultured cells to confluence and then induced cells to migrate by forming a scratch in the monolayer. In accordance with previous findings, we showed that SERPINE1 knock-down reduces the migration of the cells. For U373 cells, while the control cells can close the wound to 69%, SERPINE1 knock-down cells can close the wound to 45%. In accordance, for A172 cells, control cells can close the wound to 67%, SERPINE1 knock-down cells can close the wound to 58% (**Figure 3.23**).
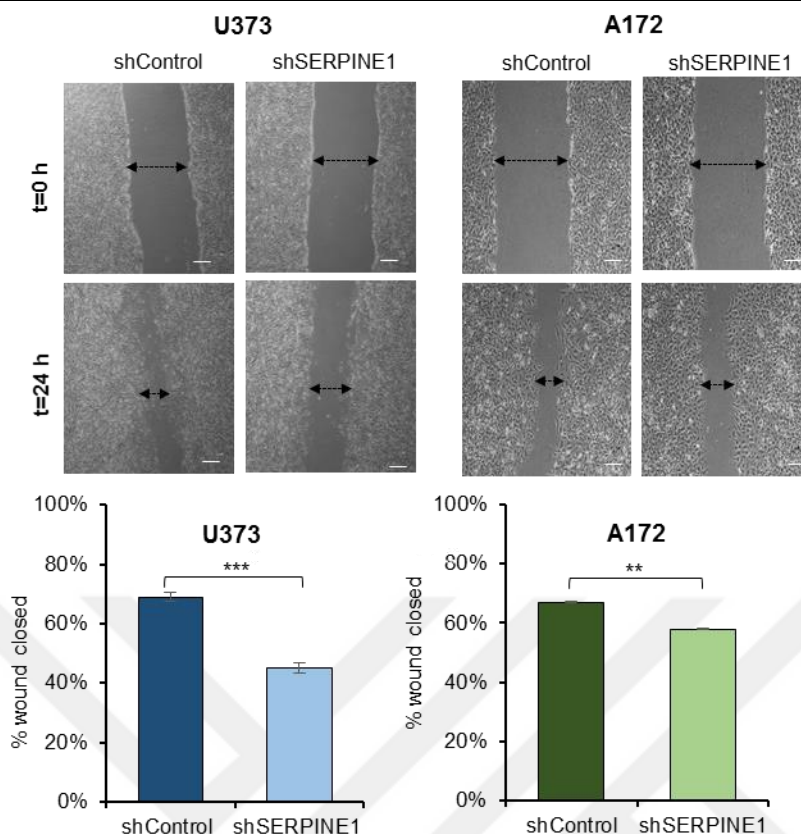
Figure 3.23. Wound healing analysis with *SERPINE1* knock-down. SERPINE1 knock-down reduces migration of *left:* U373 and *right:* A172 cells. (*n* = 35 areas for each condition, scale bar: 200 μm). (** and *** denote $p < 0.01$ and $p < 0.001$ respectively, two-tailed Student's *t*-test).

3.5. Pharmacological Inhibition of SERPINE1 Reduces GBM Cell Dispersal

In parallel to genetic inhibition of SERPINE1, we also assessed the effect of pharmacologic inhibition of SERPINE1 with a chemical inhibitor, Tiplaxtinin. We generated spheroids and applied Tiplaxtinin or DMSO to media of spheroids during dispersal.Tiplaxtinin led to a significant decrease down to 29% in dispersal of U373 cells in accordance with the observed effects of genetic manipulation (**Figure 3.24**).
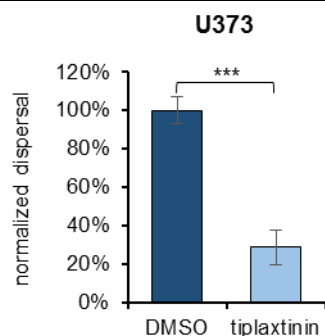
Figure 3.24. Dispersal analysis with Tiplaxtinin. Dispersal analysis showing that chemical inhibitor of SERPINE1, tiplaxtinin, reduces dispersal of U373 spheroids. ($n = 12$ spheroids for each condition, scale bar: 200 µm). (*** denotes $p < 0.001$, two-tailed Student's *t*-test).

3.6.   SERPINE1 Inhibiton has no marked effect in cell Viability

To test whether the reduced dispersal or migration is due to a decrease in cell proliferation, we analyzed the effect of SERPINE1 knock-down on cell viability and observed comparable proliferative capacities of cells over seven days. Accordingly, the U373 shControl cells grew to 9.56 fold of initial population and shSERPINE1 cells grew to 11.23 fold of initial population. A172 shControl and shSERPINE1 cell grew to 6.54 and 7.48 fold of initial population respectively (**Figure 3.25**).
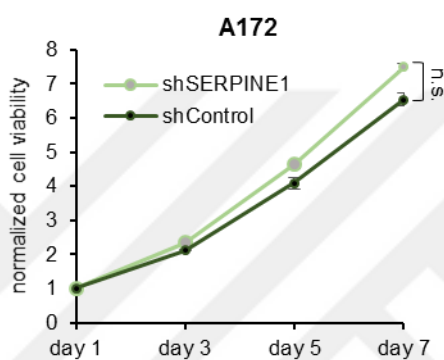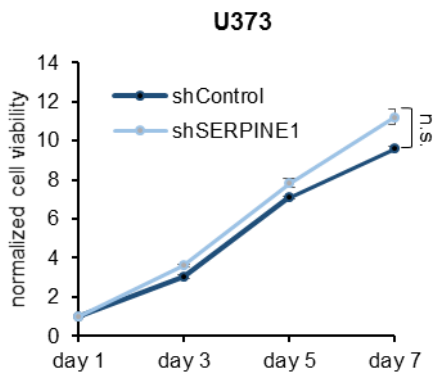
Figure 3.25. Cell viability analysis of *SERPINE1* knock-down. *SERPINE1* knock-down does not change U373 or A172 cell growth.

In accordance with genetic inhibition, chemical inhibiton of SERPINE1 with tiplaxtinin did not affect the viability of the cells in the doses used for the dispersal experiments (**Figure 3.26**).
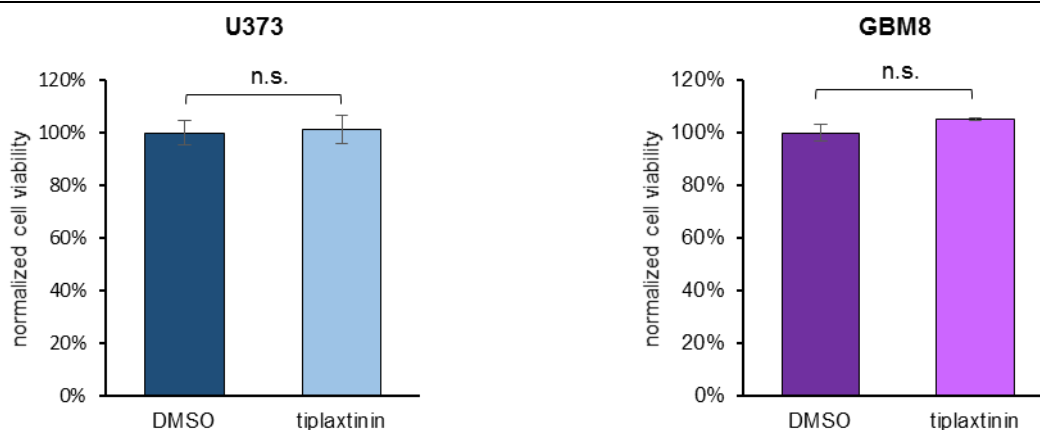
Figure 3.26. Effect of tiplaxtinin on cell viability. For U373 cells (Tiplaxtinin: 300 µM) and for GBM8 cells (Tiplaxtinin: 25 µM).

On the other hand, we assessed the viability of cells with reduced expression of cell cycle regulators, *CDC45*, and *MCM3*. These two genes were enriched in the dispersive cells as part of the "G2M checkpoint" and "E2F targets" gene set in RNA seq experiments. We also validated their increase by qRT-PCR (**Figure 3.27**).
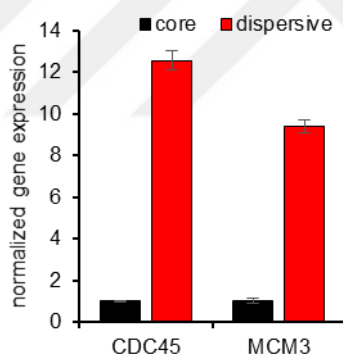
Figure 3.27. Expression of *CDC45* and *MCM3* genes in core and dispersive cells. Data is normalized to fold of core expression.

To then assess their effects on viability, we knocked-down CDC45 or MCM3 genes in U373 cells by shRNA. Significant knockdown was achieved for CDC45 and MCM3 genes down to 19% and 7% respectively (**Figure 3.28**).
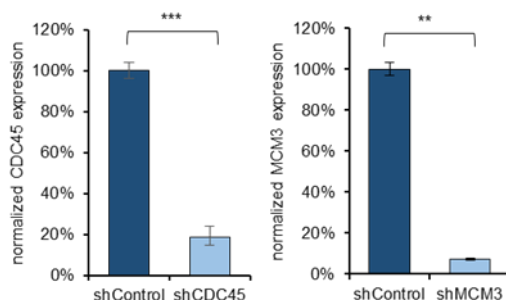
Figure 3.28. mRNA levels of CDC45 and MCM3 after shRNA knock-down. (** and *** denote $p < 0.01$ and $p < 0.001$ respectively, two-tailed Student's *t*-test).

After shRNA knock-down, we assessed the viability of the cells and showed that CDC45 or MCM3 knock-down resulted in reduced viability. While the shControl cells grew up to 9.56 fold of initial seeding day, shCDC45 and shMCM3 cells grew up to 2.80 and 5.72 fold respectively (**Figure 3.29**).
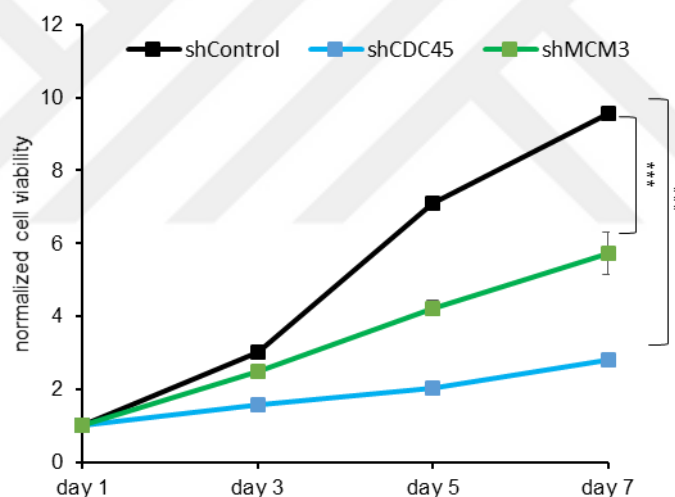
Figure 3.29. Effect of *CDC45* or *MCM3* knock-down on viability. Knock-down of *CDC45* or *MCM3* genes reduces viability of U373 cells. (*** denotes $p < 0.001$, two-tailed Student's *t*-test).

We also analyzed the dispersal of CDC45 or MCM3 knock-down cell spheroids and showed that these spheroids have reduced dispersal (**Figure 3.30**).
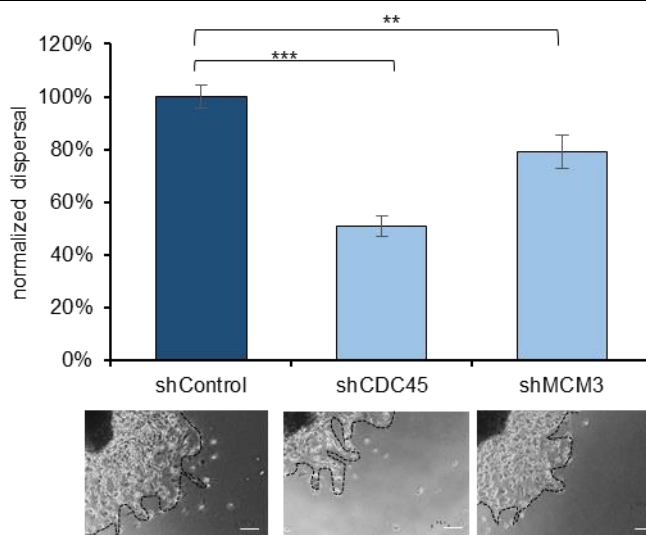
Figure 3.30. Effect of knock-down of *CDC45* or *MCM3* genes on dispersal. Knock-down of *CDC45* or *MCM3* reduces dispersal of U373 spheroids significantly. ($n = 24$ spheroids for each condition, scale bar: 200 µm). (** and *** denote $p < 0.01$ and $p < 0.001$ respectively, two-tailed Student's *t*-test).

The changes in cell cycle of these cells were in line with the viability results, where alterations in cell cycle were observed in shCDC45 and shMCM3 cells more prominent compared to shSERPINE1 or shControl cells (**Figure 3.31**).
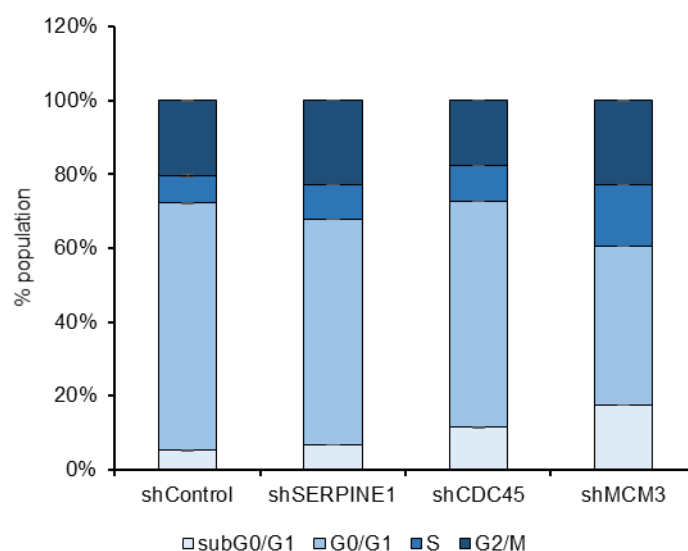
Figure 3.31. Cell cycle analysis for *CDC45*, *MCM3* and *SERPINE1* knock-down. *Cell cycle analysis carried out with Alişan Kayabölen.*

Together, these results suggest that the effects of *SERPINE1* knockdown on the dispersal of U373 or A172 cells were independent of cell viability changes.

3.7. *SERPINE1* Silencing does not Change Overall Mesenchymal State of the Cells

Since SERPINE1 silencing reduces the dispersal of the cells, we also assessed the changes in epithelial and mesencymal state upon SERPINE1 silencing (**Figure 3.32**). Silencing of SERPINE1 did not markedly change the expression of selected mesenchymal genes, including TWIST, SNAIL, N-CADHERIN, and SLUG. However, there was a slight decrease in WNT5A expression upon SERPINE1 silencing.
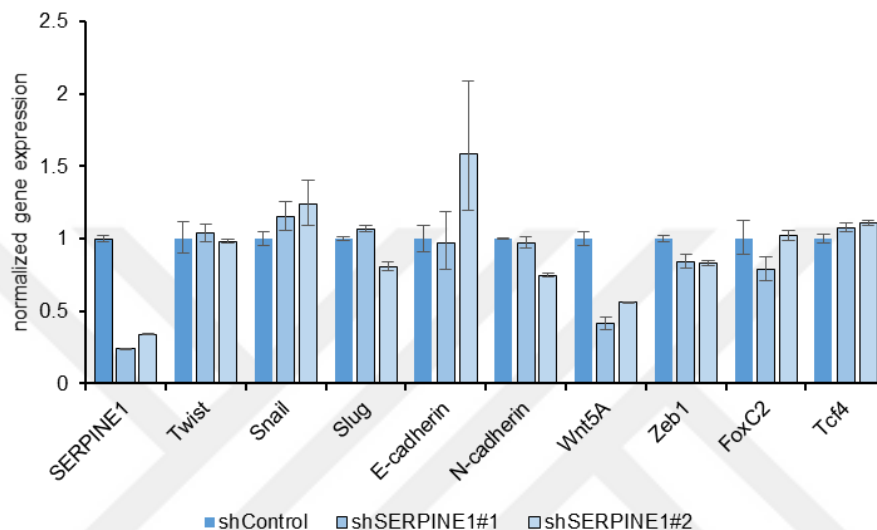
Figure 3.32. *SERPINE1* knock-down does not affect the expression levels of EMT genes markedly. Data is normalized to fold of expression of shControl.

3.8. *SERPINE1* Knock-Down Reduces GBM Cell Adhesion

Cell migration and dispersal are governed by the dynamic changes that occur at the contact points of cells with their extracellular environment, called focal adhesions. Indeed, motile cells display constant turnover of focal adhesions at their leading and trailing edges[107]. To investigate the mechanism by which SERPINE1 regulates dispersal, we examined focal adhesions using immunofluorescent staining for Vinculin, a known marker of focal adhesions. Accordingly, there was a remarkable reduction in the number of focal adhesions in *SERPINE1* knock-down cells compared to controls (**Figure 3.33** and **Figure 3.34**).
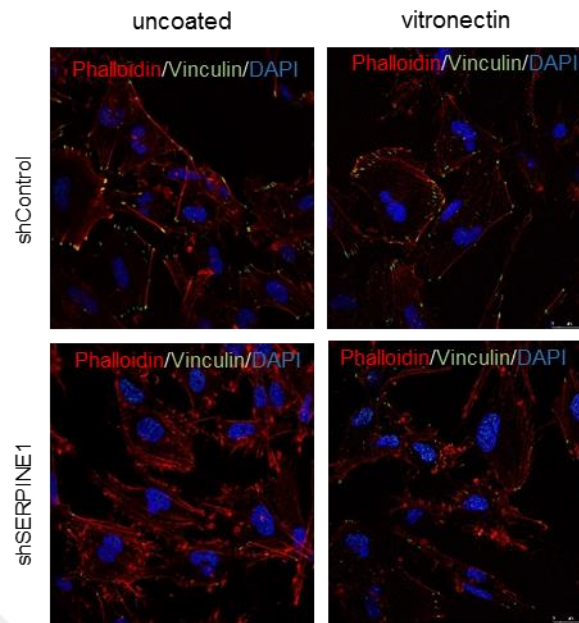
Figure 3.33. Immunofluorescence staining for shControl and sh*SERPINE1* U373 cells.
(red: phalloidin, green: vinculin, blue: DAPI, scale bar: 200 µm) with/without vitronectin
coating.
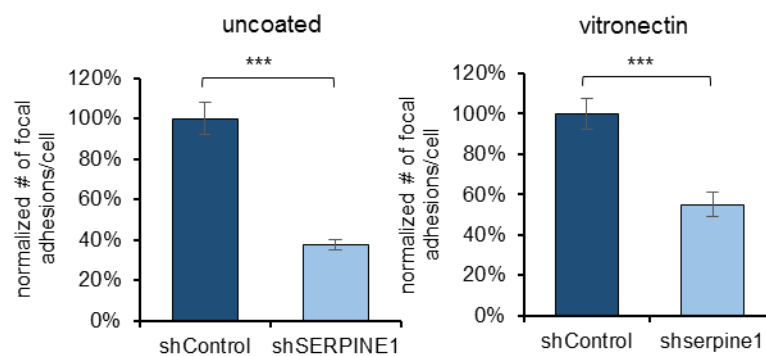
Figure 3.34. Analysis of focal adhesion number with *SERPINE1* knock-down. Analysis
showing that the number of focal adhesions per cell is significantly reduced with *SERPINE1*
knock-down. ($n = 20$ cells analyzed for each condition). (*** denotes $p < 0.001$, two-tailed
Student's *t*-test).

We hypothesized that the reduction in the number of focal adhesions could also affect
the adhesion properties of the cells. By conducting adhesion experiments to directly plastic or

to vitronectin coating, we found that there is a marked difference in the overall adhesion ability of cells, where the cells with *SERPINE1* knock-down were less adherent (**Figure 3.35**).
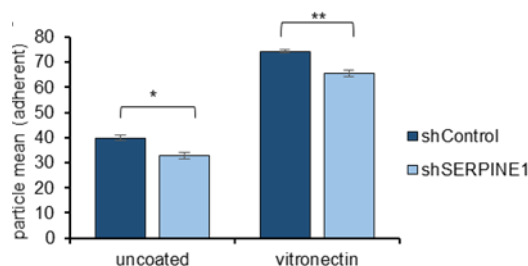
Figure 3.35. Adhesion analysis for shControl and shSERPINE1 U373 cells. (three wells/condition were analyzed, adherent particles were measured two hours after cell seeding). (* and ** denote $p < 0.05$ and $p < 0.01$ respectively, two-tailed Student's *t*-test).

When the cells were subjected to vitronectin, an extracellular matrix protein and a co-factor for SERPINE1[267], the reduction in the number of focal adhesions and cell adhesiveness were still evident, noting that the number of focal adhesions per cell and overall adhesive nature was more prominent on vitronectin coating (**Figure 3.34** and **Figure 3.35**).

3.9. Effects of Vitronectin on Dispersal of GBM Spheroids was Examined

We wanted to assess the effects of vitronectin on dispersal, which is an extracellular matrix protein and a co-factor for SERPINE1[267]. We first tested the effects of vitronectin alone on dispersal and showed that vitronectin alone increased dispersal of U373 and A172 spheroids (**Figure 3.36**).
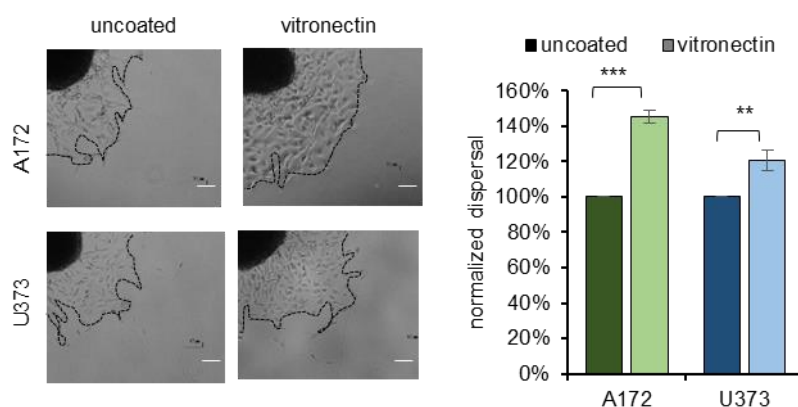
Figure 3.36. Dispersal analysis on vitronectin coating. Analysis showing that vitronectin coating induces dispersal of A172 and U373 spheroids ($n = 24$ spheroids for each condition,

scale bar: 200 µm). (** and *** denote $p < 0.01$ and $p < 0.001$ respectively, two-tailed Student's *t*-test).

We then assessed the effects of *SERPINE1* knock-down in the presence of Vitronectin coating. We showed that while U373 spheroid dispersal is reduced with SERPINE1 knock-down on vitronectin (**Figure 3.37**) as we have shown in uncoated conditions, SERPINE1 knock-down does not affect the dispersal of A172 spheroid on vitronectin (**Figure 3.38**).
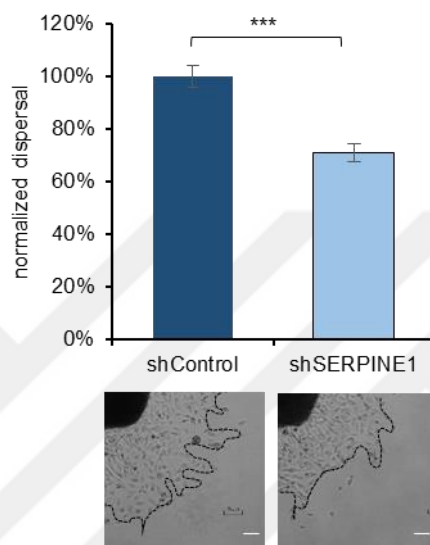
Figure 3.37. *SERPINE1* knockdown reduces dispersal of U373 spheroids on vitronectin. ($n = 24$ spheroids for each condition, scale bar: 200 µm). (*** denotes $p < 0.001$, two-tailed Student's *t*-test).
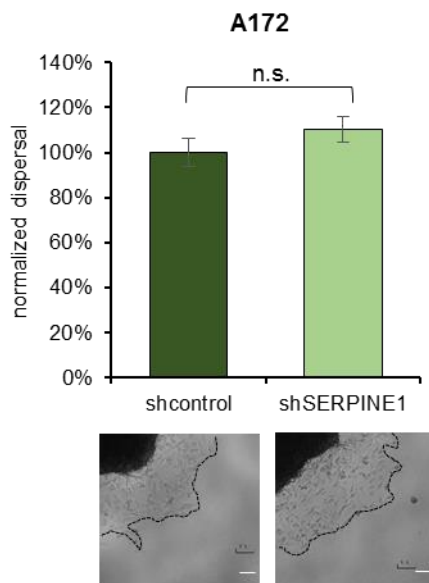
Figure 3.38. *SERPINE1* **knockdown does not affect the dispersal of A172 spheroids on vitronectin.** (*n* = 24 spheroids for each condition, scale bar: 200 um).

We wanted to understand whether the effect of vitronectin is derived from the changes in SERPINE1 expression. When we compared the basal expression of *SERPINE1* in the cells seeded on vitronectin or on plastic, we found that expression was not affected by vitronectin coating (**Figure 3.39**).
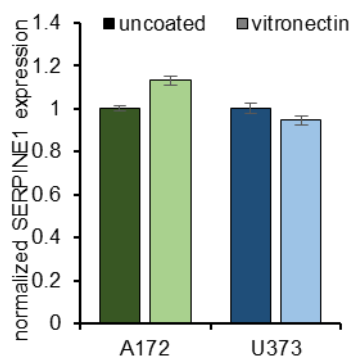
Figure 3.39. Comparison of *SERPINE1* expression with or without vitronectin coating for A172 and U373 cells.

3.10. *SERPINE1* Knock-Down Limits the Movement of Individual Cells and Reduces Persistance and Distance of Movement in GBM Cells

To further dissect the effects of SERPINE1 on GBM cell motility, we tracked the movement of individual control and *SERPINE1* knock-down cells using live cell imaging.

Consistent with our previous findings described previously, *SERPINE1* knock-down limited the movement of individual cells (**Figure 3.40**).
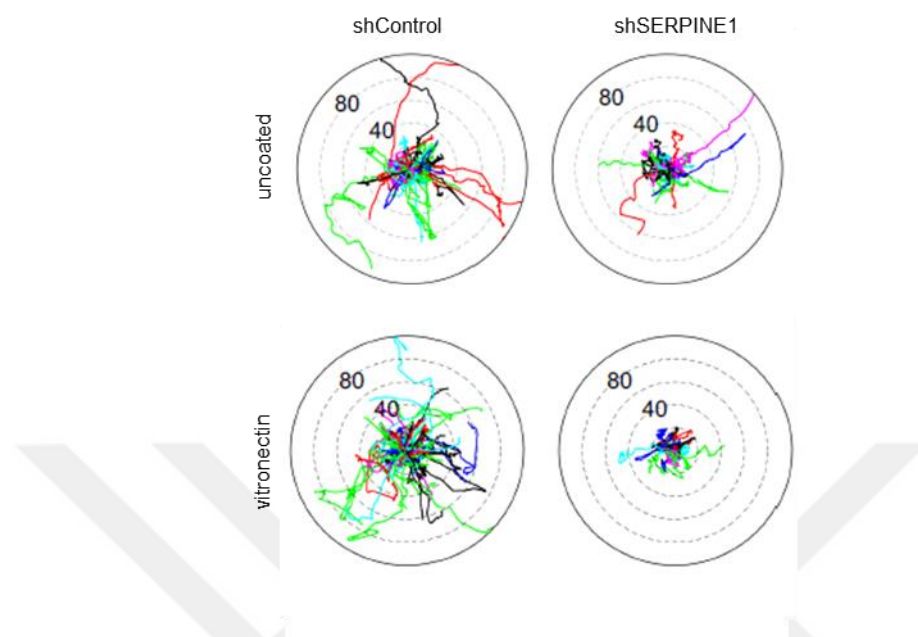
Figure 3.40. Single-cell tracking of *SERPINE1* knock-down cells. Polar plot obtained by tracking movement of individual shControl or shSERPINE1 cells with no coating or on vitronectin coating. (*n*>200 cells per condition tracked). *Single cell tracking analysis performed by Dr. Halil Bayraktar.*

We also analyzed the persistence and distance of cell movement and found that SERPINE1 knock-down reduced these features which are directly related to cell movement (**Figure 3.41**).
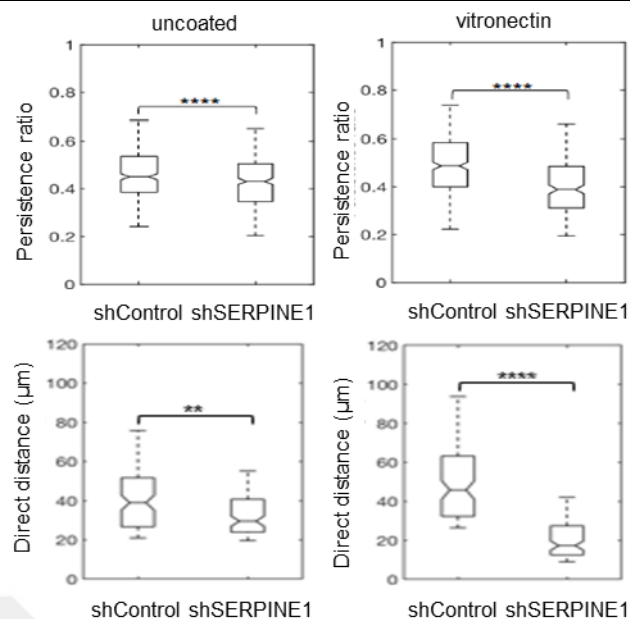
Figure 3.41. Persistence ratio and direct distance analysis. Graphs for shControl and shSERPINE1 cells with no coating or on vitronectin coating plotted for: *top:* persistence ratio, *bottom:* direct distance (*n*>200 cells per condition tracked). (** and **** denote $p < 0.01$ and $p < 0.0001$ respectively, two-tailed Student's t-test). *Single cell tracking analysis performed by Dr. Halil Bayraktar.*

3.11. TGFβ Is an Upstream Regulator of SERPINE1

Given the remarkable induction of *SERPINE1* during dispersal, we wanted to examine the possible upstream regulators of *SERPINE1* expression. Based on the GSEA analysis, TGFβ signaling was activated in the dispersive population as given in **Figure** *3.42*.
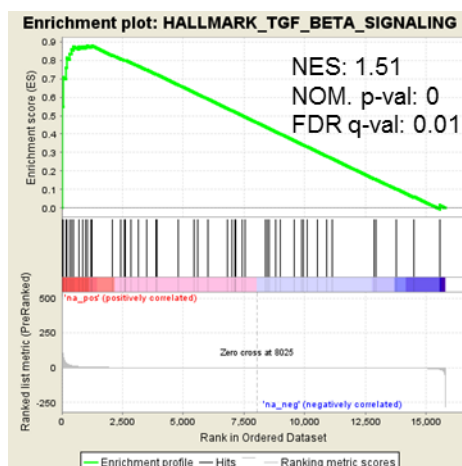
Figure 3.42. GSEA enrichment plot for TGFβ signaling in dispersive cells. *GSEA analysis performed with Alişan Kayabölen.*

Using ingenuity pathway analysis tool, we generated a list of upstream regulators activated or inhibited in dispersive cells. In this list, we have found that both SMAD2 and SMAD3 were activated in dispersive cells (**Figure *3.43***).

Upstream Regulator	Predicted Activation State	Activation z-score
MYC	Activated	7,37
ESR1	Activated	5,59
E2F3	Activated	5,38
MITF	Activated	4,73
E2F1	Activated	4,23
CTNNB1	Activated	4,12
JUN	Activated	3,71
TP63	Activated	3,70
SP1	Activated	3,36
ETS1	Activated	3,11
NOTCH1	Activated	2,97
E2F2	Activated	2,84
SMAD2	Activated	2,71
HOXD3	Activated	2,59
FOSB	Activated	2,41
EGR1	Activated	2,40
HDAC6	Activated	2,38
AR	Activated	2,16
FOSL1	Activated	2,15
SMAD3	Activated	2,05
PPARG	Inhibited	-2,03
NR3C1	Inhibited	-2,32
GLIS2	Inhibited	-2,45
SPDEF	Inhibited	-2,53
HNF4A	Inhibited	-2,70
E2F6	Inhibited	-3,00
HDAC1	Inhibited	-3,10
TP53	Inhibited	-3,12
THRB	Inhibited	-3,16
KLF2	Inhibited	-3,43
RB1	Inhibited	-3,61
NUPR1	Inhibited	-4,75
CDKN2A	Inhibited	-6,26

Figure 3.43. List of upstream regulators activated or inhibited in dispersive cells.

In the light of this information and since TGFβ is also a known regulator of EMT, we addressed whether it would change *SERPINE1* expression and ultimately cell dispersal. To this end, we treated U373 or A172 cells with TGFβ and compared the expression of SERPINE1. We showed that TGFβ induced *SERPINE1* expression in both cell lines (**Figure *3.44***).
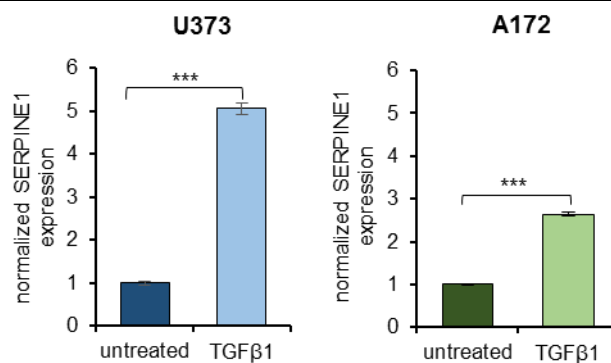
Figure 3.44. qRT-PCR analysis of SERPINE1 expression upon TGFβ treatment. *left:* U373 and *right:* A172 cells. (*** denotes $p < 0.001$, two-tailed Student's *t*-test).

On the contrary, inhibition of TGFβ signaling with two independent chemical inhibitors, Repsox or SB431542, decreased *SERPINE1* expression in these cells (**Figure *3.45***).
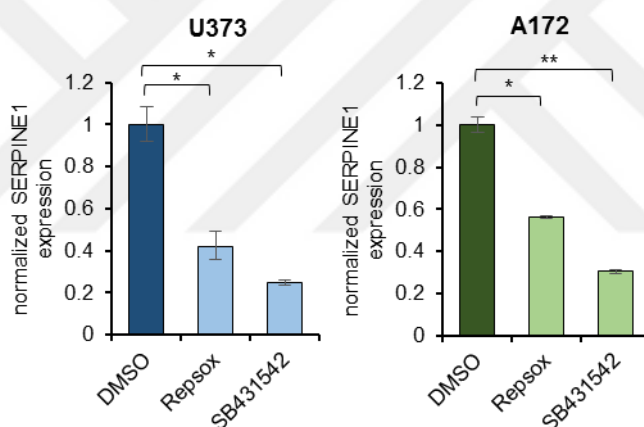
Figure 3.45. qRT-PCR analysis of SERPINE1 expression upon TGFβ inhibitor treatment. Inhibitors are Repsox and SB431542, *left:* U373 and *right:* A172 cells. (* and ** denote $p < 0.05$ and $p < 0.01$ respectively, two-tailed Student's *t*-test).

In parallel with the changes in *SERPINE1* expression levels, dispersal of the spheroids was increased with TGFβ (**Figure *3.46***) and decreased with TGFβ inhibitors (**Figure *3.47***).
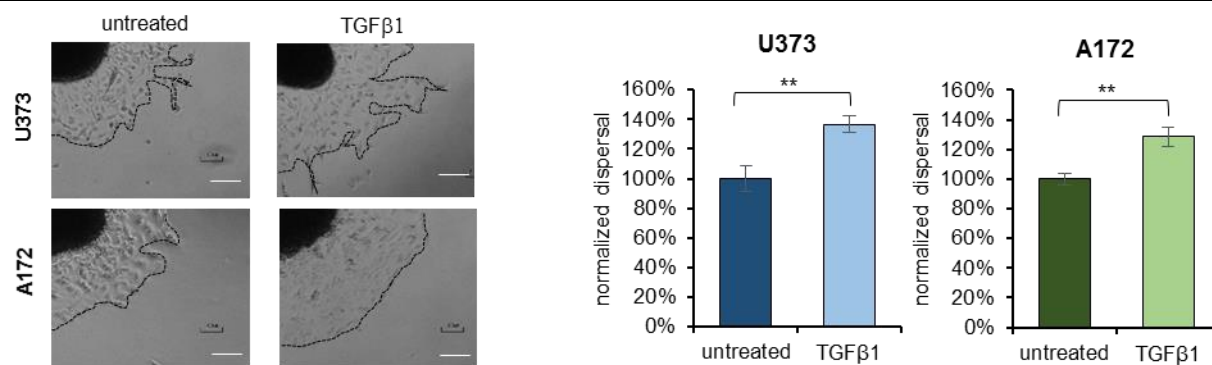
Figure 3.46. Dispersal assay in the presence of TGFβ1. Dispersal assay shows TGFβ induces dispersal of U373 and A172 ($n = 12$ spheroids for each condition, scale bar: 300 μm). (** denotes $p < 0.01$, two-tailed Student's t-test).
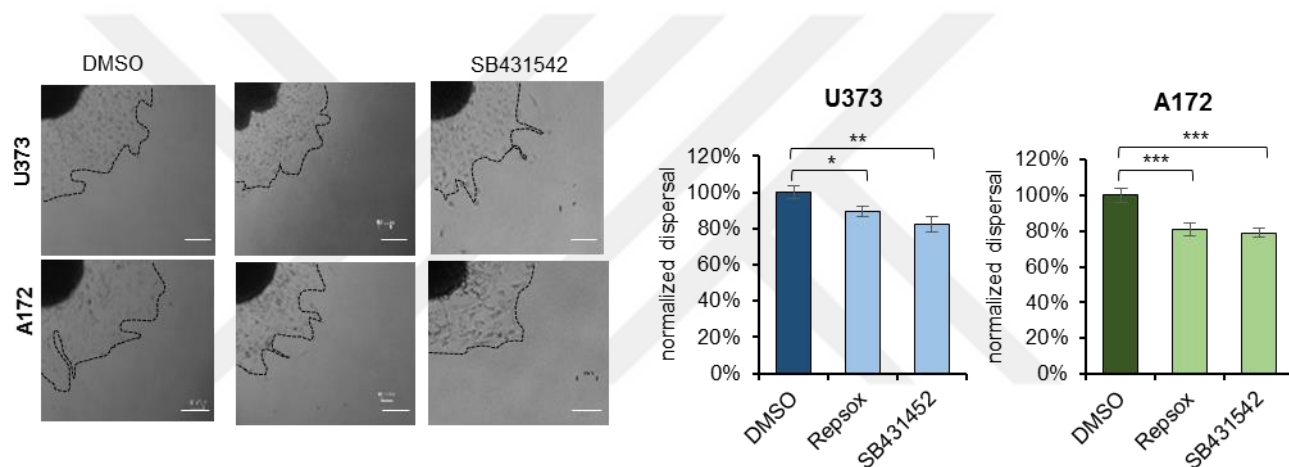
Figure 3.47. Dispersal assay in the presence of TGFβ inhibitors. Dispersal assay that shows Repsox or SB431542 reduce dispersal of U373 and A172 spheroids ($n = 24$ spheroids for each condition, scale bar: 300 μm). (*, ** and *** denote $p < 0.05$, $p < 0.01$ and $p < 0.001$ respectively, two-tailed Student's t-test).

To test whether the dynamic induction of *SERPINE1* is dependent on TGFβ signaling, we added TGFβ inhibitor Repsox on spheroids and assessed *SERPINE1* expression between core and dispersive cells. Accordingly, upregulation of *SERPINE1* in dispersive population was partly inhibited by Repsox, demonstrating a regulatory role of TGFβ signaling in *SERPINE1* induction (**Figure** *3.48*).
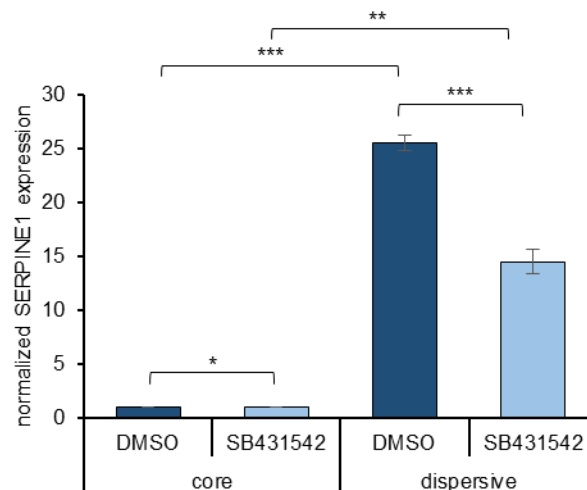
Figure 3.48. *SERPINE1* expression in core and dispersive cells with TGFβ inhibitors.
SERPINE1 upregulation in dispersive cells in the presence of TGFβ inhibitor Repsox for U373 and A172 cells. (*, ** and *** denote $p < 0.05$, $p < 0.01$ and $p < 0.001$ respectively, two-tailed Student's *t*-test).

3.12. *SERPINE1* Expression is Correlated with Increasing Glioma Grade and Associated with Poor Patient Survival

To examine the clinical relevance of SERPINE1, we examined the relation of *SERPINE1* expression with patient survival in the TCGA datasets. Accordingly, in a total of 663 patient samples composed of low-grade glioma and GBM, Kaplan–Meier survival curves of the "*SERPINE1* high" and "*SERPINE1* low" groups revealed inverse correlation of *SERPINE1* with patient survival *(p = 0.000014)* (**Figure *3.49***).
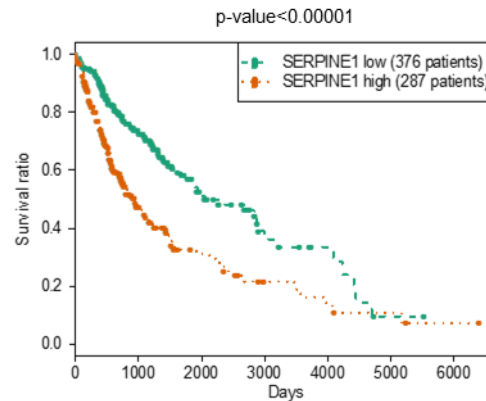
Figure 3.49. Correlation of *SERPINE1* expression with glioma patient survival. TCGA survival data plotted for high/low *SERPINE1* expressing glioma patients. *Analysis performed by Dr. Mehmet Gönen.*

In addition, we analyzed the distribution of *SERPINE1* expression among different glioma grades and found that SERPINE1 expression was correlated with increasing glioma grade and therefore the highest in GBM (**Figure *3.50***).
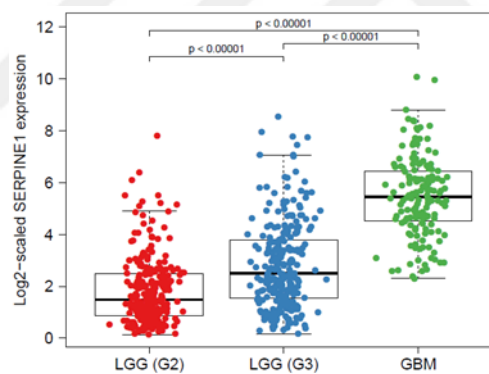
Figure 3.50. Correlation of *SERPINE1* expression with glioma grade. *SERPINE1* expression increases with higher glioma grade. *Analysis performed by Dr. Mehmet Gönen.*

Moreover, *SERPINE1* expression was mostly enriched in the mesenchymal subtype GBM (**Figure *3.51***), which corresponds to poor survival, invasiveness, and therapy resistance in GBM[26].
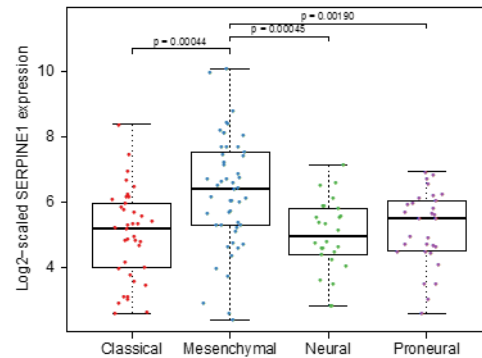
Figure 3.51. Correlation of *SERPINE1* expression with GBM subtypes. *Analysis performed by Dr. Mehmet Gönen.*

3.13. SERPINE1 Silencing Reduces Dispersal in A Clinically-Relevant Model

To further examine the effects of SERPINE1 in a clinically-relevant model, we chose a patient-derived primary cell line, GBM8, which is stem-cell like population coming from a patient specimen[6]. These cells carry the characteristics of GSC cells and models very aggressive and invasive GBM. in this primary cell line, we knocked-down SERPINE1 (**Figure *3.52***).
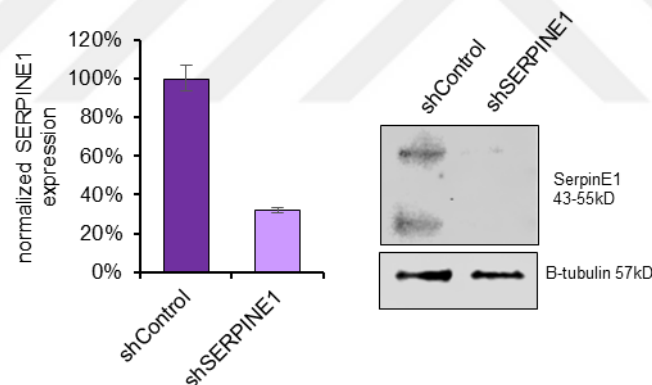
Figure 3.52. SERPINE1 mRNA and protein levels after shRNA knock-down in GBM8 cells. *Western Blot experiment performed by Dr. İlknur Sur.*

We assessed the effect of *SERPINE1* silencing on GBM8 cells and observed that *SERPINE1* silencing had a growth-slowing effect on GBM8 cells. Accordingly, while control cells grew up to 16.97 fold of initial seeding day, SERPINE1 knock-down cells grew up to 11.01 fold (**Figure *3.53***).
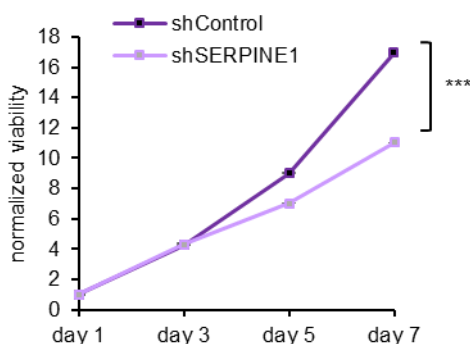
Figure 3.53. Cell viability assay with *SERPINE1* knock-down. Cell viability assays that show *SERPINE1* knock-down slows down GBM8 cell proliferation. (*** denotes $p < 0.001$, two-tailed Student's *t*-test).

Using live-cell imaging to track motility of cells dispersing out of tumor spheres, we observed that *SERPINE1* knock-down reduced dispersal significantly in these cells in a short time window of five hours due to the highly invasive nature of this primary cell line (**Figure 3.54**).
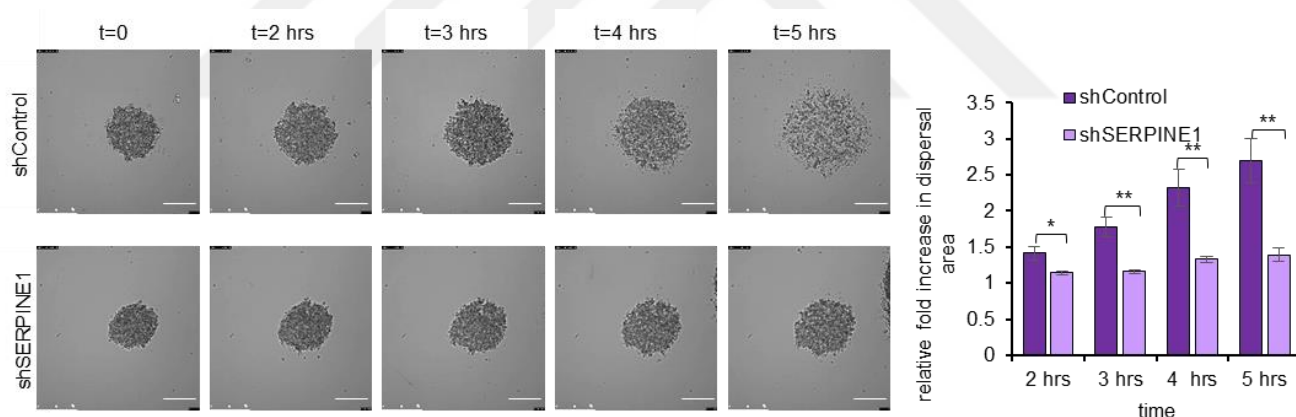
Figure 3.54. Live cell imaging analysis of GBM8 spheroids with *SERPINE1* knockdown. Live cell imaging and analysis of shControl and shSERPINE1 spheroids. *SERPINE1* knockdown reduces dispersal of GBM8 spheroids (video for five hours of dispersal, images taken every 5 minutes, scale bar: 200 µm, $n = 10$ spheroids for each condition). (* and ** denote $p < 0.05$ and $p < 0.01$ respectively, two-tailed Student's *t*-test).

Concomitantly, chemical inhibition of SERPINE1 with Tiplaxtinin reduced dispersal markedly in GBM8 cells (**Figure 3.55**).
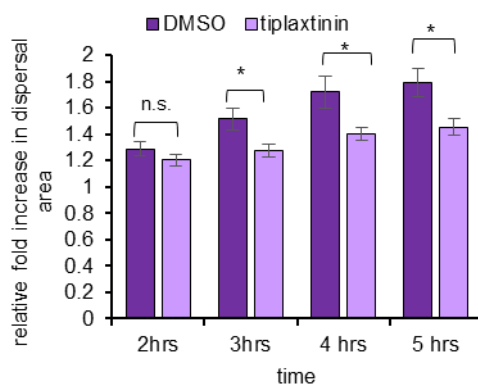
Figure 3.55. Live cell imaging analysis of GBM8 spheroids with Tiplaxtinin. Live cell imaging analysis of DMSO- or Tiplaxtinin-treated GBM8 spheroids. (video for five hours of dispersal, images taken in every 60 minutes, magnification is 10×, $n = 12$ spheroids for each condition). (* denotes $p < 0.05$, two-tailed Student's *t*-test).

Given the heterogeneity of primary GBM cell lines, we analyzed the effect of tiplaxtinin in two other primary cell lines that exhibit different characteristics, GBM4 and MGG119. We were able to show that SERPINE1 inhibition also reduces the dispersal of these primary cell line spheroids (**Figure *3.56***).
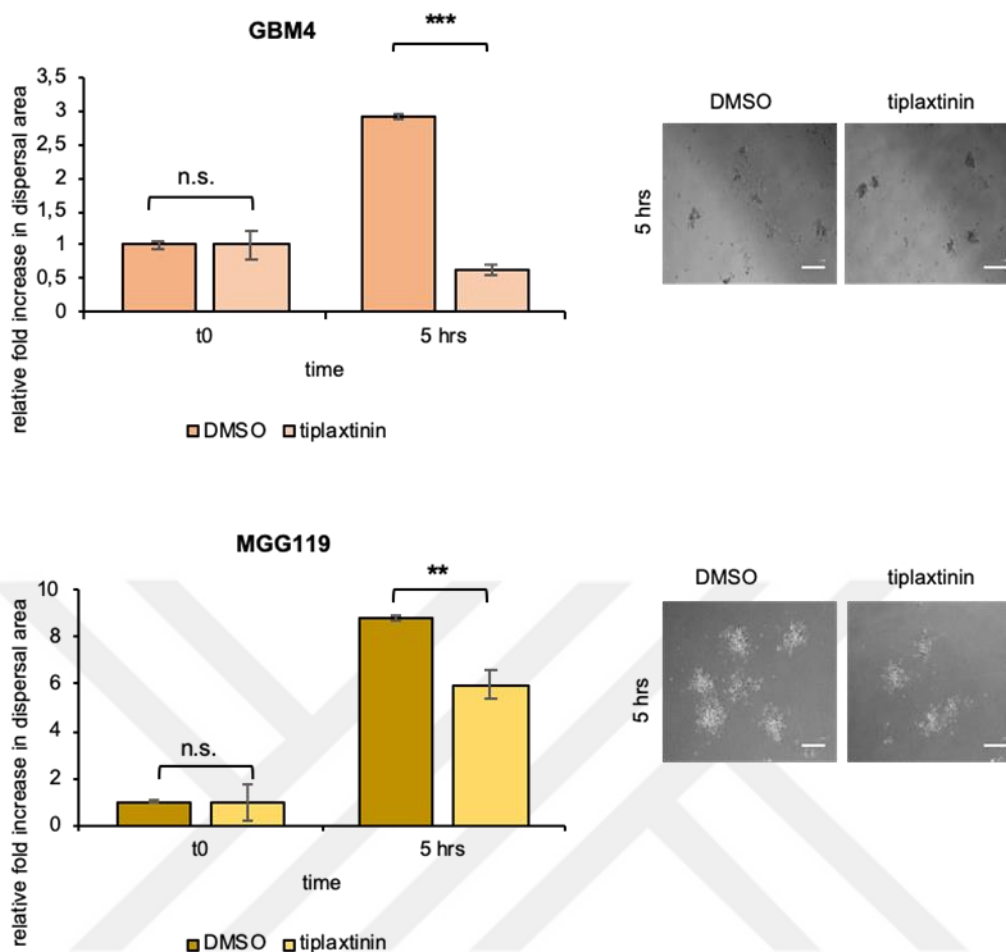
Figure 3.56. Dispersal analysis of GBM4 and MGG119 spheroids with Tiplaxtinin. Tiplaxtinin reduces dispersal of GBM4 spheroids (n= 140 spheroids analyzed per condition, scale bar: 140 μm) or MGG119 spheroids (n = 55 spheroids analyzed per condition, scale bar: 140 μm). (** and *** denote $p < 0.01$ and $p < 0.001$ respectively, two-tailed Student's *t*-test).

Consistent with our previous results in GBM cell lines, *SERPINE1* knock-down cells were less adherent than control cells also in primary cell line GBM8 (**Figure 3.57**).
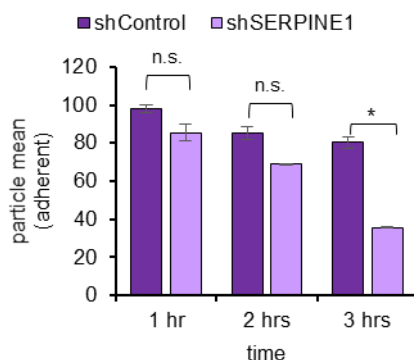
Figure 3.57. Adhesion analysis of GBM8 cells with *SERPINE1* knock-down. *SERPINE1* knock-down reduces the number of attached cells in different time points (three wells analyzed for each condition and each time point). (* denotes $p < 0.05$, two-tailed Student's *t*-test).

Overall, we were able to validate the effects of SERPINE1 on dispersal in a clinically relevant model.

3.14.   SERPINE1 Knock-Down Reduces Tumor Progression *in vivo*

To test the effect of *SERPINE1* knock-down on tumor growth, we used an orthotopic xenograft model of GBM8 cells transduced with shControl or shSERPINE1. To noninvasively monitor tumor growth, we transduced these cells with a vector encoding firefly luciferase (Fluc) and mCherry. We implanted these cells intracranially and let the tumors grow for a month regularly monitoring tumor growth (**Figure** *3.58*).
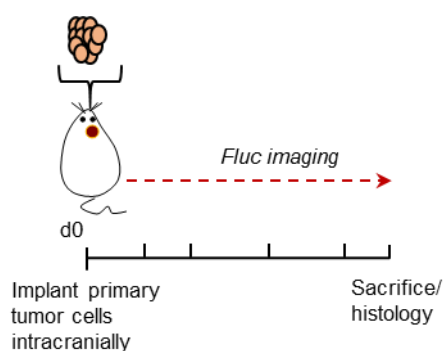
Figure 3.58. Strategy of the in vivo experiment.

Repeated bioluminescence imaging measurements revealed that the rate of growth of SERPINE1 knock-down tumors was significantly lower than that of control tumors (**Figure** *3.59*, **Figure** *3.60* and **Figure** *3.61*).
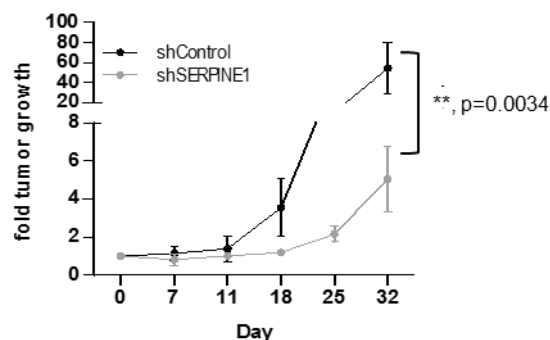
Figure 3.59. Tumor growth data of control and *SERPINE1* knock-down tumors. Graph showing tumor growth as measured by bioluminescence radiance for 32 days after tumor cell injection. Data were normalized to day 0 signal of each group ($n = 7$ mice for shControl, $n = 5$ mice for shSERPINE1). *In vivo experiments were performed with Dr. Ahmet Cingöz.*
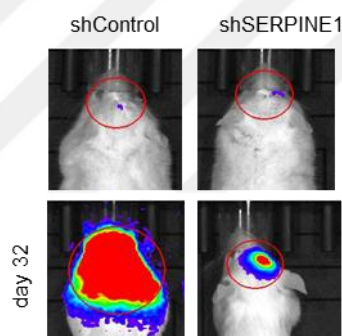
Figure 3.60. Representative bioluminescence images of tumors from day 0 and 32. Images displaying normalized bioluminescent efficiencies acquired (blue to red indicates lower to higher radiance as photons/s/cm^2/steradian). *In vivo experiments were performed with Dr. Ahmet Cingöz.*
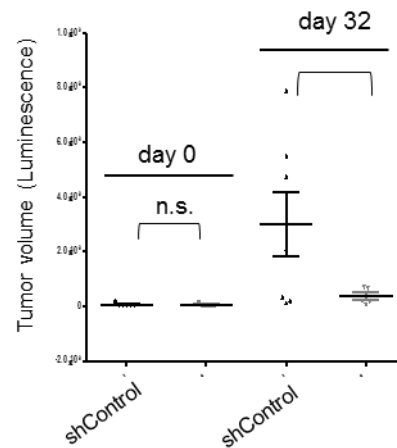
Figure 3.61. Tumor volume data for day 0 and day 32. Plot depicting individual tumor volumes on day 0 and day 32. *In vivo experiments were performed with Dr. Ahmet Cingöz.*

End-point histological examination of brain tumor sections showed that the overall sizes of shControl tumors were markedly larger than shSERPINE1 tumors and that individual shControl tumor cells invaded into distant sites in the brain parenchyma. In contrast, shSERPINE1 tumors remained small and appeared to have less distal invasion (**Figure 3.62**).
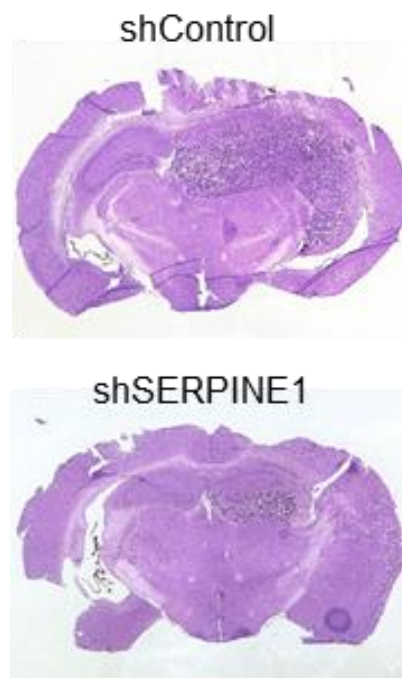
Figure 3.62. Representative H&E images of tumors. H&E staining of shControl and shSERPINE1 tumors (magnification is 13.5×).

Chapter 3: Results

Taken together, these findings showed that *SERPINE1* silencing attenuated GBM growth and invasion in the brain in a clinically relevant in vivo model.

4.   DISCUSSION

GBM is the most common and malignant primary brain tumor[3]. Despite the advances in diagnosis and treatment, GBM is still one of the deadliest human cancers. In case of highly aggressive tumors as GBM, tumor cells infiltrate and invade to normal neural tissue. Despite tumor removal, invasive GBM cells remain embedded into CNS which is resistant to chemo-radiotherapy and responsible from recurrence of the disease. Dissemination of invasive GBM cells results in failure of the current therapeutic strategies in long term. High mortality rates of GBM patients are partly attributed to the invasive behavior of tumor cells, which show extensive infiltration into adjacent brain tissue leading to rapid and almost inevitable recurrence. Given the additional chemo- and radio-resistant characteristics of these invasive cells "left behind" after surgical resection, conventional therapies remain ineffective. Therefore, understanding the mechanisms of GBM cell invasiveness is of utmost priority to develop successful therapeutic approaches.

In this study, we analyzed the dynamic changes in transcriptome of motile (dispersive) and non-motile (core) GBM cells and identified *SERPINE1* as a dramatically induced gene in the dispersive cell populations. We showed that genetic or pharmacological inhibition of SERPINE1 led to reduction of dispersal, attributing a functional role for SERPINE1 in dispersal. Furthermore, we demonstrated that SERPINE1 regulates cell-substrate adhesion and directional movement of GBM cells, and that its expression is regulated by TGFβ signaling (model in **Figure 4.1**). Together, our results suggest that SERPINE1 is a key player in GBM dispersal providing insight into the future design of anti-invasive therapies.
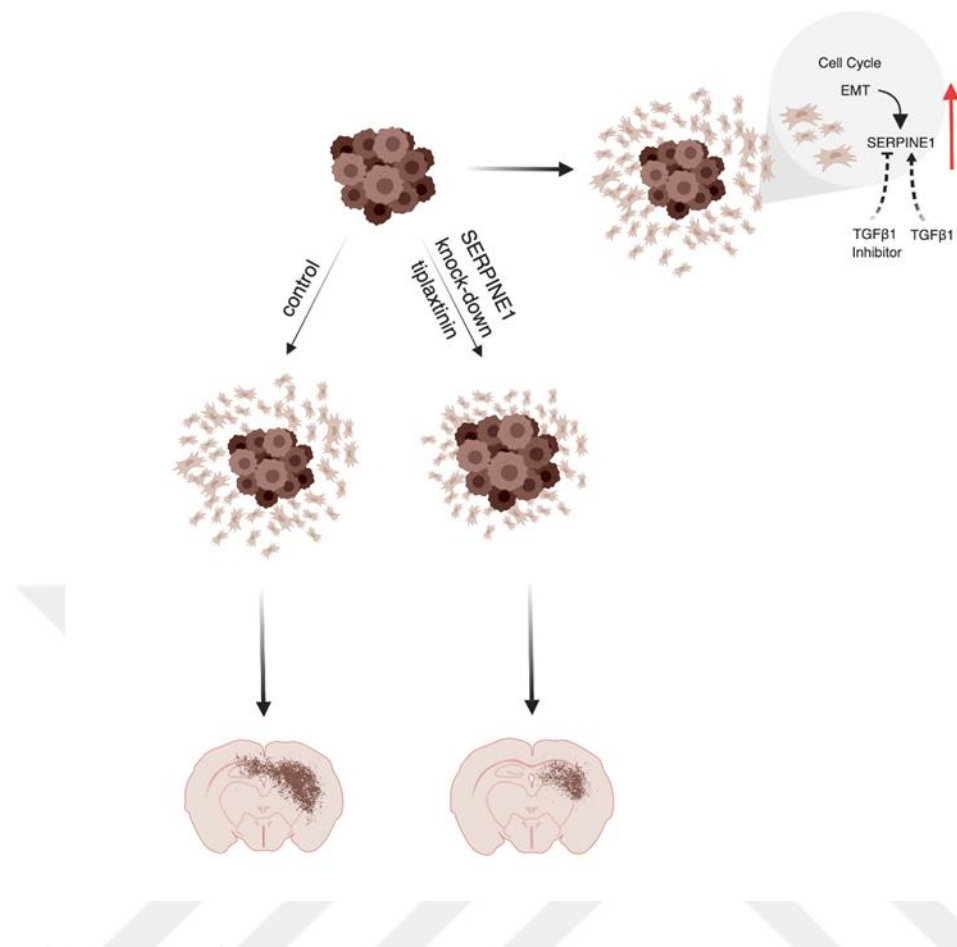
Figure 4.1. Model of the study. Model describing dynamic regulation of SERPINE1 and mechanism of SERPINE1 knock-down acting on dispersal. *Figure generated with Nareg Pınarbaşı.*

The approach we employed in this study was transcriptome profiling of dispersive cells in a spheroid model, which mimics the three-dimensional tumor environment and outward cell migration. This model is applicable and useful for in vitro assays for analyzing the invasive capacities[64]. Since analysis of the protein and gene expression profiles using spheroids have been shown to recapitulate clinical and in vivo gene expression profiles, we have decided to use this model for transcriptome profiling[58,268]. First, we assessed the fitness of GBM cell lines to hanging drops spheroid model, we formed tumor spheroids from six different cell lines and compared their sphere forming ability. To generate an in vitro model that better mimics the dynamics that operate between the tumor core and tumor rim, we also tested dispersal capacities of spheroids. In the light of these experiments, we chose U373 cell line for transcriptome analysis, since this cell line can generate compact spheroids and these spheroids have the highest dispersal capacity among cell lines tested. After that, we generated U373 cell spheroids, let them disperse for 24 hours and collected core cells, which remained in spheroid after 24

hours, and dispersive cells, which moved out of the core in 24 hours separately. Using these samples, we analyzed the transcriptome of GBM cells during dispersal. With this approach, we provided a motility signature of GBM cells. Comparative studies that utilized laser capture microdissection followed by microarray analysis identified signature differences in tumor cores vs. infiltrating cells[157,158]. In addition to comparative studies, functional studies with genetic or proteomic approaches were conducted to discover regulators of tumor cell movement. Accordingly, expression screens[160,161], RNAi-based loss-of-function screens[162,164], and proteomic screens[165] have already identified several novel regulators of tumor cell migration. Consistent with these studies, our study identified a larger number of differentially expressed genes, most of which were upregulated during dispersal, revealing dynamic and adaptable transcriptome of moving cells. With transcriptome analysis, we have seen that while the transcriptome of core population is more stable, transcriptome of dispersive cells is more dynamic. The cells may change their transcriptome in order to move, or moving cells already had upregulation of the genes that pushes them to move out. Our approach does not directly test the causality or functionality of the altered genes; however, it provides a groundwork and several candidate networks to examine in detail. Indeed, our study identified several markedly upregulated genes, some of which were previously shown, supporting the validity and strength of our approach. Notably, *CTGF* and *CYR61* genes were defined as part of "migratory signature"[159], with expression changes and functionality validated in our model. We have found that these genes are upregulated in dispersive cells and their knock-down reduces dispersal of spheroids.

Notably, with transcriptome analysis, we also demonstrated that cell proliferation and migration programs were coupled in dispersal. Our approach was in accordance with previous reports. Demuth et. al. have conducted a comparative analysis for migratory and stationary populations of human glioma cells and provided gene signatures defining cell migration[159]. In addition, we identified many altered cell cycle related gene sets as "E2F targets", "G2M checkpoint" and "MYC targets" were upregulated in dispersive cell transcriptome. Upregulation of most cell division and proliferation related genes in dispersive cells suggested that cells that disperse out of spheres can also alter their gene expression in favor of growth. This finding is in contrast with the model of dichotomy between migration and proliferation[269], which suggests that proliferation and migration are mutually exclusive. Dissecting the interplay between dispersal and proliferation with single-cell based assays will be crucial to address these questions that remain to be resolved.

Chapter 4: Discussion

We analyzed the function of the genes which are upregulated in dispersive cell transcriptome to better understand their roles using Ingenuity Pathway Analysis (IPA) tool and we showed that "cell movement" was a majorly activated pathway in dispersive cell transcriptome as it was statistically significant in multiple disease and pathway sets. When we further dissected the pathways enriched in dispersive cell transcriptome using Gene Set Enrichment Analysis (GSEA), we found that EMT gene set was significantly upregulated in dispersive cells. While EMT and distant metastasis is not readily observed in GBMs, invasive GBMs share common molecular features with metastatic cancers[148]. Indeed, GBMs that undergo mesenchymal transition are associated with a more aggressive and treatment-resistant phenotype[26]. We analyzed the mesenchymal characteristics of GBM cell lines (U373 and A172) and primary cell line (GBM8) used in the experiments by assessing the expression of select epithelial and mesenchymal genes. For comparison, we used an epithelial cancer cell line, SUM149 and found that GBM cell lines and primary GBM cell line display mesenchymal characteristics as shown by the expression of the genes assessed compared to an epithelial cancer cell line.

Within EMT genes that were upregulated in dispersive cells, *SERPINE1* had the highest levels reaching up to 36-fold of core cells at 24 hours. Furthermore, the induction of *SERPINE1* expression was persistent suggesting a critical role for it in GBM cells dispersal. To verify the dynamic induction of SERPINE1 expression in dispersive cells, we assessed how the SERPINE1 expression changes in cells cultured with normal confluency, cells in core and dispersive populations. We showed that endogenous *SERPINE1* expression in cells cultured in normal confluency is dynamically regulated in core and dispersive cells. Before functional experiments related to SERPINE1, we assessed the endogenous *SERPINE1* expression in the cell lines (U373 and A172) and the primary cell line (GBM8). We found that endogenous expression levels of *SERPINE1* is different for the cells used.

SERPINE1 is a member of the serine proteinase inhibitor (serpin) superfamily and also known as a plasminogen activator inhibitor (PAI-1)[173]. Being a regulator of plasminogen activator system, SERPINE1 has a central role in ECM degradation and remodeling[173] as well as cell migration in different physiological conditions[270]. SERPINE1 carries out its central roles by interacting with ECM proteins and vitronectin, regulating cellular adhesion and migration[173]. Indeed, high levels of SERPINE1/PAI-1 have been correlated with poor prognosis and increased invasiveness in several cancer types[172,271]. Plasminogen activator (PA) system molecules uPA, uPAR and SERPINE1 together with ECM proteins, integrins, endocytosis

receptors and growth factors generate molecular and functional interactions that degrade and re-organize ECM proteins and facilitate cell invasion. As a result, differential expression of these components in cancer cells becomes a determinant for poor prognosis. SERPINE1 has been shown to be a prognostic marker for squamous cell carcinoma, breast cancer, gastric cancer, lung adenocarcinoma, advanced ovarian cancer and many other cancer types[172]. Recent studies showed that *SERPINE1* expression is correlated with glioma grade[272] and that SERPINE1 is found in the unique proteomic signature of mesenchymal subtype of GBMs[273]. These reports are in line with our demonstration that high levels of *SERPINE1* expression strongly correlate with poor survival in glioma patients in the TCGA cohort. In addition, we show that *SERPINE1* is highly enriched in mesenchymal subtype of GBM, in which recurrent and therapy resistant tumors are enriched and corresponds to poor survival[4,27,28]. Overall, SERPINE1 is a strong prognostic indicator for GBM and might play a critical role in its progression through mechanisms that are largely unresolved.

The role of SERPINE1 in cell migration has been explored in non-malignant contexts, especially in epithelial cells[122,274–276]. It has been shown that SERPINE1 expression is induced with wounding of epithelial cells and SERPINE1 is required for injury repair. In this case, SERPINE1 is upregulated in the cells surrounding the wound or the cells actively migrating for repair, it has an integral role in regulating directional migration and wound closure. SERPINE1 expression is induced until the wound is closed and SERPINE1 loss results in impaired wound closure[274]. In addition, it was shown that elevated SERPINE1 levels have a center role in transition of epithelial cells to more migratory phenotype through its interactions with ECM and cell surface constituents. Increased SERPINE1 levels have been associated with several diseases typified with fibrosis and cellular infiltration[277,278], inflammation, hypertrophic scarring, atherosclerosis, thrombosis, myocardial infarction, diabetes and obesity[122].

While SERPINE1 has been studied in non-malignant contexts and several cancer types, its specific role in GBM cells has been elusive. There have been few reports indirectly linking SERPINE1 expression to GBM progression. For example, a recent study showed that *SERPINE1* is a target of a microRNA (miR-1275) that regulates proliferation and invasion of glioma cells[279]. Another report suggested that GBM cell *SERPINE1* expression is controlled by GDF-15 and SERPINE1 silencing itself does not have an effect on glioma cell migration and invasion[280]. To our knowledge, our study provides the first functional demonstration of a direct role of SERPINE1 in GBM cell motility as well as a pro-tumorigenic role in in vivo GBM models.

Chapter 4: Discussion

To assess the effect of SERPINE1 on GBM cell dispersal, we have used SERPINE1 shRNAs to knock-down this gene. After validating SERPINE1 silencing in mRNA and protein levels, we assessed the effect of SERPINE1 inhibition on dispersal. When we anayzed and compared the dispersal of spheroids generated from control and SERPINE1 knock-down cells, we showed that SERPINE1 knock-down spheroids show a reduced dispersal phenotype. Similarly, we showed this phenotype in wound healing migration assay. In accordance with previous findings, we showed that SERPINE1 knock-down reduces the migration of the cells. In parallel to genetic inhibition of SERPINE1, we also assessed the effect of pharmacologic inhibition of SERPINE1 with chemical inhibitor Tiplaxtinin. Tiplaxtinin led to a significant decrease in dispersal of spheroids in accordance with the observed effects of genetic manipulation.

To test whether the reduced dispersal or migration is due to a decrease in cell proliferation, we analyzed the effect of SERPINE1 knock-down on cell viability and observed comparable proliferative capacities of cells. In accordance with genetic inhibition, chemical inhibition of SERPINE1 with tiplaxtinin does not affect the viability of the cells in the doses used for the dispersal experiments.

Since SERPINE1 silencing reduces the dispersal of the cells, we also assessed the changes in mesencymal state. Silencing of SERPINE1 did not markedly change the expression of selected mesenchymal genes, so we concluded that SERPINE1 silencing has a different mechanism acting on cells and eventually decreasing dispersive properties of the cells.

Regulation of cell adhesion to extracellular matrix is an important component of tumor cell invasion, where the cells generate or breakdown receptor-mediated focal adhesion points in the direction of cell movement. These focal adhesions are the protein complexes that connect the cytoskeleton of cells to ECM via integrins. Turn-over of focal adhesion proteins are crucial for cell movement since the cell needs to de-attach and re-attach to the surface in order to move[281]. We demonstrate that SERPINE1 is a critical regulator of the adhesion process, as the number of focal adhesions was greatly affected by SERPINE1 silencing in our models. We support this hypothesis by adhesion experiments, where we found that there is a marked difference in the overall adhesion ability of cells and the cells with *SERPINE1* knock-down were less adherent. This is in accordance with previous findings that showed that SERPINE1 regulated adhesive behavior of smooth muscle cells[282], or fibrosarcoma cells[283]. Since adhesion complexes are generated by vinculin, integrin clusters and focal adhesion kinase[121], it will be

very interesting to analyze the changes in other components of adhesion complex with SERPINE1 silencing to better dissect the mechanism in the future.

We analyzed the effects of vitronectin on dispersal, since it is an extracellular matrix protein and a co-factor for SERPINE1[267]. We first tested the effects of vitronectin alone on dispersal and showed that presence of vitronectin induced dispersal. This result is in accordance with previous finding showing vitronectin expression is correlated with increased invasiveness [105]. We then assessed the effects of *SERPINE1* knock-down in the presence of Vitronectin coating. We showed that while U373 spheroids dispersal is reduced with SERPINE1 knock-down on vitronectin as we have shown in uncoated conditions, but SERPINE1 knock-down loses its effect on dispersal of A172 spheroids on vitronectin.

We further dissected the effects of SERPINE1 on GBM cell motility and tracked the movement of individual control and *SERPINE1* knock-down cells using live cell imaging. Consistent with our previous findings described previously, *SERPINE1* knock-down limited the movement of individual cells. We also analyzed the persistence and distance of cell movement and found that SERPINE1 knock-down reduced these features which are directly related to cell movement.

How *SERPINE1* gene expression is regulated is an interesting question, given its marked elevation during GBM dispersal. Assessing upstream molecular events might be crucial to find novel anti-invasive approaches. To this end, our study demonstrated that TGFβ signaling is a critical regulator of *SERPINE1* expression in GBM cells. Indeed, treatment with TGFβ or TGFβ inhibitors markedly regulated *SERPINE1* expression. In parallel with the changes in *SERPINE1* expression levels, dispersal of the spheroids was increased with TGFβ and decreased with TGFβ inhibitors. This is in consistence with previous findings on regulation of *SERPINE1* expression[284,285] and is also supported by our IPA analysis that identified Smad2 and Smad3 as potential upstream regulators of *SERPINE1* expression in dispersive cells. To test whether the dynamic induction of *SERPINE1* is dependent on TGFβ signaling, we added TGFβ inhibitor Repsox on spheroids and assessed *SERPINE1* expression between core and dispersive cells. Accordingly, upregulation of *SERPINE1* in dispersive population was partly inhibited by Repsox, demonstrating a regulatory role of TGFβ signaling in *SERPINE1* induction.

We examined the effects of SERPINE1 in a clinically-relevant model and conducted our experiments also using a patient-derived primary cell line, GBM8. These primary cells are the stem-cell like population derived from a patient specimen[6]. These cells carry the

characteristics of GSC cells and models very aggressive and invasive GBM. We first assessed the effect of *SERPINE1* silencing on GBM8 cells and observed that *SERPINE1* silencing had a growth-slowing effect on GBM8 cells. We tracked motility of control and SERPINE1 knock-down GBM spheres using live cell imaging and confirmed that *SERPINE1* knock-down reduced dispersal significantly in these cells in a short time window of five hours due to the highly invasive nature of this primary cell line. Concomitantly, chemical inhibition of SERPINE1 with Tiplaxtinin reduced dispersal markedly also in GBM8 cells. Consistent with our previous results in GBM cell lines, *SERPINE1* knock-down cells were less adherent than control cells also in primary cell line GBM8. Given the heterogeneity of primary GBM cell lines, we added two other primary cell lines that exhibit different characteristics, GBM4 and MGG119. Using these primary cells, we confirmed the effect of tiplaxtinin on dispersal. Overall, we were able to validate the effects of SERPINE1 on dispersal in a clinically relevant model and primary cell lines. This validation has encouraged us to hypothesize that SERPINE1 may be an effective clinical target since silencing phenotype is consistent over heterogeneous primary cells.

Finally, we tested the effect of *SERPINE1* knock-down on tumor growth. We used an orthotopic xenograft model of GBM8 cells transduced with shControl or shSERPINE1. We showed that the growth rate of SERPINE1 knock-down tumors was significantly lower than that of control tumors. We confirmed our findings with end-point histological examination of brain tumor sections. While the control tumors were markedly larger and tumor cells have invaded into distant sites in the brain parenchyma, SERPINE1 knock-down tumors remained small and appeared to have less distal invasion. Taken together, we showed that *SERPINE1* silencing attenuated GBM growth and invasion in the brain in a clinically relevant in vivo model.

Invasion ability toward surrounding tissue is a determinant for the malignant tumor progression[150]. In the case of GBM, high mortality of patients is mostly caused by the invasive behavior of GBM cancer cells, which show extensive infiltration into healthy adjacent tissue and result in inevitable recurrence. Despite the accumulating knowledge on the biology of invasive cells in GBMs, there is no therapy directed against these populations[49]. Even worse, current therapeutic strategies further increase invasiveness of the cells[152]. As anti-invasive strategies in GBM, there are several druggable targets. There are available inhibitors for TGFβR1, ephrin receptors, FAK, ROCK, CK2, AKT, JAK, NF-κB and STAT3. Among these targets, inhibitors against TGFβR1, ephrin receptors, FAK, ROCK and CK2 are more specific to target GBM invasion[82]. In addition, inhibiting MMPs can be a good approach; however,

application of MMP inhibitors in clinical trials did not improve patient survival when combined with temozolomide[155]. Other trials targeting integrins failed to show significant survival benefit in Phase III[286]. Currently, various TGFβ inhibitors, including Galunisertib in combination with standard therapy are being tested in glioma patients[82]. Our identification of SERPINE1 as a mediator of GBM progression provides another member to the growing list of therapy targets. Silencing of SERPINE1 or its pharmacological inhibition reduced the migration and dispersal of GBM cells in vitro, as well as tumor growth in a primary GBM model in vivo. Given its well-established clinical relevance, and, in light of our findings, inhibition of SERPINE1 may be a promising anti-invasive strategy for GBM.

Since SERPINE1 has three forms as active, cleaved and latent, which are activated by binding of different factors and induces several signaling hubs[169–171], it would be a good approach to dissect the role of each form in the context of GBM dispersal. Targeting a specific SERPINE1 form would be a more specific treatment option and reduce the complexity of the feedback mechanisms in the signaling cascades to which SERPINE1 contributes. On the other hand, all three forms of SERPINE1 can induce cell motility in LRP1 dependent manner; however, while the active form has a routine turn-over, latent and inactive forms remain embedded in matrix to act as a reservoir for motility induction[176]. To this end, another strategy may be targeting LRP1 or inhibiting the activation of Jak/Stat pathway by LRP1 pathway[205] specifically in tumor cells.

All in all, with the work described in this thesis, we suggest a potent anti-invasive therapy target. Considering that highly invasive cells have already disseminated to other locations than the primary tumor area and formed tumor seeds in secondary locations, preventing only the invasion may not eradicate these cells and may not change the patient survival considerably. To this end, anti-invasive therapies should be combined with other treatments. Considering that TMZ is the frontline drug in clinic for GBM therapy, combining SERPINE1 inhibitors with TMZ may have the potential to result in more effective results since therapy will be directed against both proliferative and invasive cells. Similarly, SERPINE1 inhibitor and radiation combination should also be examined in detail for future clinical applications. However, biggest challenge for SERPINE1 anti-invasive therapy is based on the limitations of SERPINE1 chemical inhibitors. SERPINE1 inhibitors do not show activity against vitronectin-bound stable form of PAI-1, they have a very short half-life and they are needed at high concentrations as a single agent[287]. Developing better inhibitors compatible with *in vivo* and clinical testing would be the rate-limiting, but very high priority for anti-SERPINE1

therapies. Combining improved inhibitors with golden standards of GBM therapy would be more effective. Therefore, our findings offer a groundwork for future anti-invasive therapy design. Given its well-established clinical relevance and in the light of our findings, inhibition of SERPINE1 may be a promising anti-invasive strategy for GBM.

5.   BIBLIOGRAPHY

1.   Gupta, M. K., Jayaram, S., Reddy, D. N., Polisetty, R. V. & Sirdeshmukh, R. Transcriptomic and Proteomic Data Integration and Two-Dimensional Molecular Maps with Regulatory and Functional Linkages: Application to Cell Proliferation and Invasion Networks in Glioblastoma. *J. Proteome Res.* **14**, 5017–5027 (2015).

2.   Fortin Ensign, S. P., Mathews, I. T., Symons, M. H., Berens, M. E. & Tran, N. L. Implications of Rho GTPase Signaling in Glioma Cell Invasion and Tumor Progression. *Front. Oncol.* **3**, 1–11 (2013).

3.   Ramirez, Y. P., Weatherbee, J. L., Wheelhouse, R. T. & Ross, A. H. Glioblastoma multiforme therapy and mechanisms of resistance. *Pharmaceuticals* **6**, 1475–1506 (2013).

4.   Verhaak, R. G. W. *et al.* Integrated Genomic Analysis Identifies Clinically Relevant Subtypes of Glioblastoma Characterized by Abnormalities in PDGFRA, IDH1, EGFR, and NF1. *Cancer Cell* **17**, 98–110 (2010).

5.   Nakada, M. *et al.* Molecular targets of glioma invasion. *Cell. Mol. Life Sci.* **64**, 458–478 (2007).

6.   Wakimoto, H. *et al.* Human glioblastoma-derived cancer stem cells: establishment of invasive glioma models and treatment with oncolytic herpes simplex virus vectors. *Cancer Res.* **69**, 3472–81 (2009).

7.   Dunn, G. P. *et al.* Emerging insights into the molecular and cellular basis of glioblastoma. 756–784 (2012). doi:10.1101/gad.187922.112.and

8.   Stupp, R. *et al.* Effects of radiotherapy with concomitant and adjuvant temozolomide versus radiotherapy alone on survival in glioblastoma in a randomised phase III study: 5-year analysis of the EORTC-NCIC trial. *Lancet Oncol.* **10**, 459–466 (2009).

9.   Silber, J. R., Bobola, M. S., Blank, A. & Chamberlain, M. C. O6-Methylguanine-DNA methyltransferase in glioma therapy: Promise and problems. *Biochim. Biophys. Acta - Rev. Cancer* **1826**, 71–82 (2012).

10. Vinagre, J. *et al.* Frequency of TERT promoter mutations in human cancers. *Nat.*

Commun. **4**, (2013).

11.   Brennan, C. W. *et al.* The Somatic Genomic Landscape of Glioblastoma. *Cell* **157**, 753 (2014).

12.   Herting, C. J. *et al.* Genetic driver mutations define the expression signature and microenvironmental composition of high-grade gliomas. *Glia* **65**, 1914–1926 (2017).

13.   Ozawa, T. *et al.* Most human non-GCIMP glioblastoma subtypes evolve from a common proneural-like precursor glioma. *Cancer Cell* **26**, 288–300 (2014).

14.   Li, Q. J., Cai, J. Q. & Liu, C. Y. Evolving molecular genetics of glioblastoma. *Chin. Med. J. (Engl).* **129**, 464–471 (2016).

15.   Phillips, J. J. *et al.* PDGFRA Amplification is Common in Pediatric and Adult High-Grade Astrocytomas and Identifies a Poor Prognostic Group in IDH1 Mutant Glioblastoma. *Brain Pathol.* **23**, 565–573 (2013).

16.   Losman, J. A. & Kaelin, W. G. What a difference a hydroxyl makes: Mutant IDH, (R)-2-hydroxyglutarate, and cancer. *Genes Dev.* **27**, 836–852 (2013).

17.   Ye, D., Xiong, Y. & Guan, K. L. The mechanisms of IDH mutations in tumorigenesis. *Cell Res.* **22**, 1102–1104 (2012).

18.   Gravendeel, L. A. M. *et al.* Intrinsic gene expression profiles of gliomas are a better predictor of survival than histology. *Cancer Res.* **69**, 9065–9072 (2009).

19.   Snuderl, M. *et al.* Mosaic amplification of multiple receptor tyrosine kinase genes in glioblastoma. *Cancer Cell* **20**, 810–817 (2011).

20.   Koschmann, C., Lowenstein, P. R. & Castro, M. G. ATRX mutations and glioblastoma: Impaired DNA damage repair, alternative lengthening of telomeres, and genetic instability. *Mol. Cell. Oncol.* **3**, 1–3 (2016).

21.   Amorim, J. P., Santos, G., Vinagre, J. & Soares, P. The role of ATRX in the alternative lengthening of telomeres (ALT) phenotype. *Genes (Basel).* **7**, (2016).

22.   Lovejoy, C. A. *et al.* Loss of ATRX, genome instability, and an altered DNA damage response are hallmarks of the alternative lengthening of Telomeres pathway. *PLoS Genet.* **8**, 12–15 (2012).

Bibliography

23. Guan, X. *et al.* Molecular subtypes of glioblastoma are relevant to lower grade glioma. *PLoS One* **9**, (2014).

24. Zhang, Y. *et al.* The p53 Pathway in Glioblastoma. doi:10.3390/cancers10090297

25. Biernat, W., Tohma, Y., Yonekawa, Y., Kleihues, P. & Ohgaki, H. Alterations of cell cycle regulatory genes in primary (de novo) and secondary glioblastomas. *Acta Neuropathol.* **94**, 303–309 (1997).

26. Verhaak, R. G. W. *et al.* Integrated Genomic Analysis Identifies Clinically Relevant Subtypes of Glioblastoma Characterized by Abnormalities in PDGFRA, IDH1, EGFR, and NF1. *Cancer Cell* **17**, 98–110 (2010).

27. Phillips, H. S. *et al.* Molecular subclasses of high-grade glioma predict prognosis, delineate a pattern of disease progression, and resemble stages in neurogenesis. *Cancer Cell* **9**, 157–173 (2006).

28. Segerman, A. *et al.* Clonal Variation in Drug and Radiation Response among Glioma-Initiating Cells Is Linked to Proneural-Mesenchymal Transition. *Cell Rep.* **17**, 2994–3009 (2016).

29. Bjerkvig, R., Laerum, O. D. & Rucklidge, G. J. Immunocytochemical characterization of extracellular matrix proteins expressed by cultured glioma cells. *Cancer Res.* **49**, 5424–8 (1989).

30. Savaraj, N. *et al.* Procollagen alpha 1 type I: A potential aide in histopathological grading of glioma. *Cancer Invest.* **23**, 577–581 (2005).

31. Zhang, J., F.G. Stevens, M. & D. Bradshaw, T. Temozolomide: Mechanisms of Action, Repair and Resistance. *Curr. Mol. Pharmacol.* **5**, 102–114 (2011).

32. Messaoudi, K., Clavreul, A. & Lagarce, F. Toward an effective strategy in glioblastoma treatment. Part I: resistance mechanisms and strategies to overcome resistance of glioblastoma to temozolomide. *Drug Discov. Today* **20**, 899–905 (2015).

33. Shen, W., Hu, J. A. & Zheng, J. S. Mechanism of temozolomide-induced antitumour effects on glioma cells. *J. Int. Med. Res.* **42**, 164–172 (2014).

34. Arora, A. & Somasundaram, K. Glioblastoma vs temozolomide: can the red queen race be won? *Cancer Biol. Ther.* **20**, 1083–1090 (2019).

Bibliography

35.   Hegi, M. E. *et al. MGMT* Gene Silencing and Benefit from Temozolomide in Glioblastoma. *N. Engl. J. Med.* **352**, 997–1003 (2005).

36.   Xie, Q., Mittal, S. & Berens, M. E. Targeting adaptive glioblastoma: An overview of proliferation and invasion. *Neuro. Oncol.* **16**, 1575–1584 (2014).

37.   Mooney, J. *et al.* Current Approaches and Challenges in the Molecular Therapeutic Targeting of Glioblastoma. *World Neurosurg.* **129**, 90–100 (2019).

38.   Schijns, V. E. J. C. *et al.* First clinical results of a personalized immunotherapeutic vaccine against recurrent, incompletely resected, treatment-resistant glioblastoma multiforme (GBM) tumors, based on combined allo- and auto-immune tumor reactivity. *Vaccine* **33**, 2690–2696 (2015).

39.   Martikainen, M. & Essand, M. Virus-based immunotherapy of glioblastoma. *Cancers (Basel).* **11**, (2019).

40.   Zanders, E. D., Svensson, F. & Bailey, D. S. Therapy for glioblastoma: is it working? *Drug Discov. Today* **24**, 1193–1201 (2019).

41.   Ganipineni, L. P., Danhier, F. & Préat, V. Drug delivery challenges and future of chemotherapeutic nanomedicine for glioblastoma treatment. *J. Control. Release* **281**, 42–57 (2018).

42.   Lu, C. & Shervington, A. Chemoresistance in gliomas. *Mol. Cell. Biochem.* **312**, 71–80 (2008).

43.   Ghia, A. J. Fractionated Radiotherapy of Intracranial Gliomas. *Prog. Neurol. Surg.* **31**, 38–47 (2018).

44.   Larson, E. W. *et al.* Clinical outcomes following salvage Gamma Knife radiosurgery for recurrent glioblastoma. *World J. Clin. Oncol.* **5**, 142–148 (2014).

45.   Moghaddasi, L. & Bezak, E. Development of an integrated Monte Carlo model for glioblastoma multiforme treated with boron neutron capture therapy. *Sci. Rep.* **7**, 1–14 (2017).

46.   PI, D. Tretichnye flory zapadnoi {Sibiri} ({The} {Tertiary} floras of western {Siberia}). *Moscow Izd. Akad. Nauk SSSR* **125**, 4269–4280 (1963).

47.   Brown, C. E. *et al.* Regression of Glioblastoma after Chimeric Antigen Receptor T-Cell

Therapy. *N. Engl. J. Med.* **375**, 2561–2569 (2016).

48.   Jain, K. K. A critical overview of targeted therapies for glioblastoma. *Front. Oncol.* **8**, 1–19 (2018).

49.   Cha, J., Kang, S. G. & Kim, P. Strategies of Mesenchymal Invasion of Patient-derived Brain Tumors: Microenvironmental Adaptation. *Sci. Rep.* **6**, 1–12 (2016).

50.   Valster, A. *et al.* Cell migration and invasion assays. *Methods* **37**, 208–215 (2005).

51.   Justus, C. R., Leffler, N., Ruiz-Echevarria, M. & Yang, L. V. In vitro cell migration and invasion assays. *J. Vis. Exp.* 1–8 (2014). doi:10.3791/51046

52.   Gritsenko, P. G., Ilina, O. & Friedl, P. Interstitial guidance of cancer invasion. *J. Pathol.* **226**, 185–199 (2012).

53.   Rao, S. S., Lannutti, J. J., Viapiano, M. S., Sarkar, A. & Winter, J. O. Toward 3D biomimetic models to understand the behavior of glioblastoma multiforme cells. *Tissue Eng. - Part B Rev.* **20**, 314–327 (2014).

54.   Wang, C. *et al.* Three-dimensional in vitro cancer models: A short review. *Biofabrication* **6**, (2014).

55.   Friedl, P., Sahai, E., Weiss, S. & Yamada, K. M. New dimensions in cell migration. *Nat. Rev. Mol. Cell Biol.* **13**, 743–747 (2012).

56.   Underwood, T. J. *et al.* Cancer-associated fibroblasts predict poor outcome and promote periostin-dependent invasion in oesophageal adenocarcinoma. *J. Pathol.* **235**, 466–477 (2015).

57.   Carter, J. C. & Church, F. C. Mature breast adipocytes promote breast cancer cell motility. *Exp. Mol. Pathol.* **92**, 312–317 (2012).

58.   Friedrich, J., Seidel, C., Ebner, R. & Kunz-Schughart, L. A. Spheroid-based drug screen: Considerations and practical approach. *Nat. Protoc.* **4**, 309–324 (2009).

59.   Koide, N. *et al.* Formation of multicellular spheroids composed of adult rat hepatocytes in dishes with positively charged surfaces and under other nonadherent environments. *Exp. Cell Res.* **186**, 227–235 (1990).

60.   Underhill, G. H., Chen, A. A., Albrecht, D. R. & Bhatia, S. N. Assessment of

Bibliography

hepatocellular function within PEG hydrogels. *Biomaterials* **28**, 256–270 (2007).

61. Hirschhaeuser, F. *et al.* Multicellular tumor spheroids: An underestimated tool is catching up again. *J. Biotechnol.* **148**, 3–15 (2010).

62. Mehta, G., Hsiao, A. Y., Ingram, M., Luker, G. D. & Takayama, S. Opportunities and challenges for use of tumor spheroids as models to test drug delivery and efficacy. *J. Control. Release* **164**, 192–204 (2012).

63. Fennema, E., Rivron, N., Rouwkema, J., van Blitterswijk, C. & De Boer, J. Spheroid culture as a tool for creating 3D complex tissues. *Trends Biotechnol.* **31**, 108–115 (2013).

64. Del Duca, D., Werbowetski, T. & Del Maestro, R. F. Spheroid preparation from hanging drops: Characterization of a model of brain tumor invasion. *J. Neurooncol.* **67**, 295–303 (2004).

65. Wang, L. *et al.* Astrocytes directly influence tumor cell invasion and metastasis in vivo. *PLoS One* **8**, (2013).

66. Coniglio, S. J. & Segall, J. E. Review: Molecular mechanism of microglia stimulated glioblastoma invasion. *Matrix Biol.* **32**, 372–380 (2013).

67. Chonan, Y., Taki, S., Sampetrean, O., Saya, H. & Sudo, R. Endothelium-induced three-dimensional invasion of heterogeneous glioma initiating cells in a microfluidic coculture platform. *Integr. Biol. (United Kingdom)* **9**, 762–773 (2017).

68. Gao, Y. *et al.* A versatile valve-enabled microfluidic cell co-culture platform and demonstration of its applications to neurobiology and cancer biology. *Biomed. Microdevices* **13**, 539–548 (2011).

69. Guan, P. P. *et al.* By activating matrix metalloproteinase-7, shear stress promotes chondrosarcoma cell motility, invasion and lung colonization. *Oncotarget* **6**, 9140–9159 (2015).

70. Ogawa, J., Pao, G. M., Shokhirev, M. N. & Verma, I. M. Glioblastoma Model Using Human Cerebral Organoids. *Cell Rep.* **23**, 1220–1229 (2018).

71. Nakada, M., Niska, J. A., Tran, N. L., McDonough, W. S. & Berens, M. E. EphB2/R-ras signaling regulates glioma cell adhesion, growth, and invasion. *Am. J. Pathol.* **167**, 565–576 (2005).

Bibliography

72. Jung, S. *et al.* Brain tumor invasion model system using organotypic brain-slice culture as an alternative to in vivo model. *J. Cancer Res. Clin. Oncol.* **128**, 469–476 (2002).

73. Yamada, K. M. & Cukierman, E. Modeling Tissue Morphogenesis and Cancer in 3D. *Cell* **130**, 601–610 (2007).

74. Krusche, B. *et al.* EphrinB2 drives perivascular invasion and proliferation of glioblastoma stem-like cells. *Elife* **5**, 1–32 (2016).

75. Invasiveness, G. *et al.* Identification of a Druggable Pathway Controlling Article Identification of a Druggable Pathway Controlling Glioblastoma Invasiveness. 48–60 (2017). doi:10.1016/j.celrep.2017.06.036

76. Guillamo, J. S. *et al.* Migration pathways of human glioblastoma cells xenografted into the immunosuppressed rat brain. *J. Neurooncol.* **52**, 205–215 (2001).

77. Yoshida, D. *et al.* Inhibition of Glioma Angiogenesis and Invasion by SI-27, an Anti-matrix Metalloproteinase Agent in a Rat Brain Tumor Model. *Neurosurgery* **54**, 1213–1221 (2004).

78. Jensen, S. S. *et al.* Establishment and characterization of a tumor stem cell-based glioblastoma invasion model. *PLoS One* **11**, (2016).

79. Zhang, F. *et al.* In vivo MRI tracking of cell invasion and migration in a rat glioma model. *Mol. Imaging Biol.* **13**, 695–701 (2011).

80. Ricard, C. & Debarbieux, F. C. Six-color intravital two-photon imaging of brain tumors and their dynamic microenvironment. *Front. Cell. Neurosci.* **8**, 1–9 (2014).

81. Joo, K. M. *et al.* Patient-Specific Orthotopic Glioblastoma Xenograft Models Recapitulate the Histopathology and Biology of Human Glioblastomas In Situ. *Cell Rep.* **3**, 260–273 (2013).

82. de Gooijer, M. C., Guillén Navarro, M., Bernards, R., Wurdinger, T. & van Tellingen, O. An Experimenter's Guide to Glioblastoma Invasion Pathways. *Trends Mol. Med.* **24**, 763–780 (2018).

83. Katt, M. E., Placone, A. L., Wong, A. D., Xu, Z. S. & Searson, P. C. In vitro tumor models: Advantages, disadvantages, variables, and selecting the right platform. *Front. Bioeng. Biotechnol.* **4**, (2016).

Bibliography

84.   Farin, A. *et al.* Transplanted glioma cells migrate and proliferate on host brain vasculature: A dynamic analysis. *Glia* **53**, 799–808 (2006).

85.   Pedersen, P. *et al.* Migratory Patterns oF Lac-Z Transfected Human Glioma Cells. **771**, 767–771 (1995).

86.   Bigner, S. H. *et al.* Gene Amplification in Malignant Human Gliomas : Clinical and Histopathologic Aspects. **47**, 191–205 (1988).

87.   Pedersen, P. H. *et al.* Leptomeningeal tissue: A barrier against brain tumor cell invasion. *J. Natl. Cancer Inst.* **86**, 1593–1599 (1994).

88.   Bjerkvig, R., Lund-Johansen, M. & Edvardsen, K. Tumor cell invasion and angiogenesis in the central nervous system. *Curr. Opin. Oncol.* **9**, 223–229 (1997).

89.   Ulrich, T. A., De Juan Pardo, E. M. & Kumar, S. The mechanical rigidity of the extracellular matrix regulates the structure, motility, and proliferation of glioma cells. *Cancer Res.* **69**, 4167–4174 (2009).

90.   Lu, P., Weaver, V. M. & Werb, Z. The extracellular matrix: A dynamic niche in cancer progression. *J. Cell Biol.* **196**, 395–406 (2012).

91.   O'Neill, G. M., Zhong, J., Paul, A. & Kellie, S. J. Mesenchymal migration as a therapeutic target in glioblastoma. *J. Oncol.* **2010**, (2010).

92.   Demuth, T. & Berens, M. E. Molecular mechanisms of glioma cell migration and invasion. *J. Neurooncol.* **70**, 217–228 (2004).

93.   Osswald, M. *et al.* Brain tumour cells interconnect to a functional and resistant network. *Nature* **528**, 93–98 (2015).

94.   Friedl, P. & Alexander, S. Cancer invasion and the microenvironment: Plasticity and reciprocity. *Cell* **147**, 992–1009 (2011).

95.   Bunge, R. Linkage Between Axonal Ensheathment and Basal Lamina Production by Schwann Cells. *Annu. Rev. Neurosci.* **9**, 305–328 (1986).

96.   Carbonetto, S. The extracellular matrix of the nervous system. 382–387 (1984).

97.   Novak, U. & Kaye, A. H. Extracellular matrix and the brain: Components and function. *J. Clin. Neurosci.* **7**, 280–290 (2000).

Bibliography

98.   Goldbrunner, R. H., Bernstein, J. J. & Tonn, J. C. Cell-extracellular matrix interaction in glioma invasion. *Acta Neurochir. (Wien).* **141**, 295–305 (1999).

99.   Tysnes, B. B. *et al.* Laminin expression by glial fibrillary acidic protein positive cells in human gliomas. *Int. J. Dev. Neurosci.* **17**, 531–9 (1999).

100.   Mahesparan, R. *et al.* Expression of extracellular matrix components in a highly infiltrative in vivo glioma model. *Acta Neuropathol.* **105**, 49–57 (2003).

101.   Baldwin, J. R., Mckeever, P. E., Booker, T. R. & Al, B. E. T. Products of Cultured Neuroglial Cells " II . The Production of Fibronectin by C6 Glioma Cells. **10**, 601–610 (1985).

102.   Paulus, W., Roggendorf, W. & Schuppan, D. Immunohistochemical investigation of collagen subtypes in human glioblastomas. *Virchows Arch. A Pathol. Anat. Histopathol.* **413**, 325–332 (1988).

103.   Han, J., Daniel, J. C. & Pappas, G. D. Invasion in Brain Tissue Cultures. **88**, 127–132 (1995).

104.   Giese, A. & Westphal, M. Glioma invasion in the central nervous system. *Neurosurgery* **39**, 235–252 (1996).

105.   Mechanism, A. Glioblastoma Expression of Vitronectin and the av / 83 Integrin . **88**, 1924–1932 (1991).

106.   Bourdon, M. A., Wikstrand, C. J., Furthmayr, H., Matthews, T. J. & Bigner, D. D. Human Glioma-Mesenchymal Extracellular Matrix Antigen Defined by Monoclonal Antibody Human Glioma-Mesenchymal Monoclonal Antibody Extracellular Matrix Antigen Defined by. **43**, 2796–2805 (1983).

107.   Friedl, P. & Alexander, S. Cancer invasion and the microenvironment: Plasticity and reciprocity. *Cell* **147**, 992–1009 (2011).

108.   Gkretsi, V. & Stylianopoulos, T. Cell Adhesion and Matrix Stiffness: Coordinating Cancer Cell Invasion and Metastasis. *Front. Oncol.* **8**, (2018).

109.   Nagano, O. & Saya, H. Mechanism and biological significance of CD44 cleavage. *Cancer Sci.* **95**, 930–935 (2004).

110.   Ranuncolo, S. M., Ladeda, V. & Specterman, S. CD44 Expression in Human Gliomas.

Bibliography

30–36 (2002). doi:10.1002/jso.10045

111. Okamoto, I. *et al.* Regulated CD44 Cleavage under the Control of Protein Kinase C , Calcium Influx , and the Rho Family of Small G Proteins *. **274**, 25525–25534 (1999).

112. Prag, S. *et al.* NCAM regulates cell motility. (2002).

113. Edvardsen, K. *et al.* Transmembrane neural cell-adhesion molecule (NCAM), but not secretion of matrix metalloproteinases. **90**, 11463–11467 (2000).

114. Cavallaro, U. & Christofori, G. Cell Adhesion and Signaling by Cadherins and IG-CAMS in Cancer. **4**, 118–132 (2004).

115. Perego, C. *et al.* Invasive behaviour of glioblastoma cell lines is associated with altered organisation of the cadherin- catenin adhesion system. **100**, (2002).

116. Inmoto, S. *et al.* Gene Expression of Neural Cell Adhesion Molecule LI in Malignant (Â ¿ liornas and Biological Significance of LI in Glioma Invasion1. **144**, 1440–1445 (1996).

117. Read, R. M. T., Kai, M. L., Skaftnesmo, O., Bjerkvig, R. & Engebraaten, O. Expression of extracellular matrix components in a highly infiltrative in vivo glioma model. 49–57 (2003). doi:10.1007/s00401-002-0610-0

118. Wenk, M. B., Midwood, K. S. & Schwarzbauer, J. E. Tenascin-C Suppresses Rho Activation. **150**, 913–919 (2000).

119. Hemler, M. E. Integrin associated proteins. 578–585 (1998).

120. Munson, J. *et al.* Identifying new small molecule anti-invasive compounds for glioma treatment. *Cell Cycle* **12**, 2200–2209 (2013).

121. Cox, E. A. & Huttenlocher, A. Regulation of Integrin-Mediated Adhesion During Cell Migration. **419**, 412–419 (1998).

122. Wilkins-port, C. E., Freytag, J., Higgins, S. P. & Higgins, P. J. Cell Communication Insights pAI-1 : A Multifunctional seRpIn with complex Roles in cell signaling and Migration. *Communication* 1–10 doi:10.4137/CCI.S5260

123. Deryugina, E. I. *et al.* MT1-MMP Initiates Activation of pro-MMP-2 and Integrin ⌴ v ᴺᴸ 3 Promotes Maturation of MMP-2 in Breast Carcinoma Cells. **223**, 209–223 (2001).

Bibliography

124. Rao, J. S. *et al.* Role of Plasminogen-Activator and of 92-Kda Type-Iv Collagenase in Glioblastoma Invasion Using an in-Vitro Matrigel Model. *J. Neurooncol.* **18**, 129–138 (1994).

125. Kesanakurti, D., Chetty, C., Dinh, D. H., Gujrati, M. & Rao, J. S. Role of MMP-2 in the regulation of IL-6/Stat3 survival signaling via interaction with α5β1 integrin in glioma. *Oncogene* **32**, 327–340 (2013).

126. Raithatha, S. A. *et al.* mRNA and protein in human gliomas. 145–150 (1996).

127. Nakada, M., Miyamori, Æ. H. & Kita, Æ. D. Human glioblastomas overexpress ADAMTS-5 that degrades brevican. **4**, 239–246 (2005).

128. Held-feindt, J. *et al.* Matrix-degrading proteases ADAMTS4 and ADAMTS5 (disintegrins and metalloproteinases with thrombospondin motifs 4 and 5) are expressed in human glioblastomas. **61**, 55–61 (2006).

129. Ford, H., Hospital, H. F. & State, W. Immunolocalization of cathepsin B in human glioma: implications for tumor invasion and angiogenesis. 285–290 (1995).

130. Gondi, C. S. *et al.* Advances in Brief Adenovirus-Mediated Expression of Antisense Urokinase Plasminogen Activator Receptor and Antisense Cathepsin B Inhibits Tumor Growth , Invasion , and Angiogenesis in Gliomas. 4069–4077 (2004).

131. Tysnes, B. B. & Mahesparan, R. Biological mechanisms of glioma invasion and potential therapeutic targets. *J. Neurooncol.* **53**, 129–147 (2001).

132. Yamaguchi, H. & Oikawa, T. Membrane lipids in invadopodia and podosomes: key structures for cancer invasion and metastasis. *Oncotarget* **1**, 320–8 (2010).

133. Oldberg, I. D. G., Estphal, M. W. & Osen, E. M. R. Scatter Factor Promotes Motility of Huma Glioma and Neuromicrovascular Endothelial Cells. **28**, 19–28 (1998).

134. Satol, K., Yonekawaj, Y., Ohgakil, H., Thomas, A. & Cedex, L. Overexpression of the EGF Receptor and p53 Mutations are Mutually Exclusive in the Evolution of Primary and Secondary Glioblastomas. **224**,

135. Multiforme, G. *et al.* Prognostic Value of Epidermal Growth Factor Receptor in Patients with. 6962–6970 (2003).

136. Lund-johansen, M. *et al.* Effect of Epidermal Growth Factor on Glioma Cell Growth ,

Bibliography

Migration , and Invasion in Vitro1. (1990).

137. Gumbiner, B. M. Regulation of Cadherin Mediated Adhesion in Morphogenesis. **6**, 622–634 (2005).

138. Burridge, K. & Chrzanowska-wodnicka, M. Focal Adhesions , Contractility and Signaling. (1996).

139. Cukierman, E., Cukierman, E., Pankov, R. & Stevens, D. R. Taking Cell-Matrix Adhesions to the Third Dimension. **1708**, (2013).

140. Rabinovitz, I. & Mercurio, A. M. The Integrin ⌣ 6 ᴺ⌊ 4 Functions in Carcinoma Cell Migration on Laminin-1 by Mediating the Formation and Stabilization of Actin-containing Motility Structures. **139**, 1873–1884 (1997).

141. Olsten, M. E. K. & Litchfield, D. W. Order or chaos ? An evaluation of the regulation of protein kinase CK2 1. **693**, 681–693 (2004).

142. Amodeo, V., Deli, A., Betts, J., Michod, D. & Brandner, S. Article A PML / Slit Axis Controls Physiological Cell Migration and Cancer Invasion in the CNS Article A PML / Slit Axis Controls Physiological Cell Migration and Cancer Invasion in the CNS. *CellReports* **20**, 411–426 (2017).

143. Scaglioni, P. P. *et al.* A CK2-Dependent Mechanism for Degradation of the PML Tumor Suppressor. 269–283 (2006). doi:10.1016/j.cell.2006.05.041

144. Friedmann-morvinski, D. *et al.* Targeting NF- k B in glioblastoma : A therapeutic approach. (2016).

145. Lee, D. W. *et al.* The NF- k B RelB Protein Is an Oncogenic Driver of Mesenchymal Glioma. **8**, (2013).

146. Senft, C., Priester, M., Polacin, M. & Weissenberger, J. Inhibition of the JAK-2 / STAT3 signaling pathway impedes the migratory and invasive potential of human glioblastoma cells. 393–403 (2011). doi:10.1007/s11060-010-0273-y

147. Hoelzinger, D. B., Demuth, T. & Berens, M. E. Autocrine factors that sustain glioma invasion and paracrine biology in the brain microenvironment. *J. Natl. Cancer Inst.* **99**, 1583–1593 (2007).

Bibliography

148. Xie, Q. *et al.* A highly invasive human glioblastoma pre-clinical model for testing therapeutics. *J. Transl. Med.* **6**, 1–13 (2008).

149. Siebzehnrubl, F. A. *et al.* The ZEB1 pathway links glioblastoma initiation , invasion and chemoresistance. 1196–1212 (2013). doi:10.1002/emmm.201302827

150. Hanahan, D. & Weinberg, R. A. Hallmarks of cancer: The next generation. *Cell* **144**, 646–674 (2011).

151. Gliemroth, J., Feyerabend, T., Gerlach, C., Arnold, H. & Terzis, A. J. A. Proliferation, migration, and invasion of human glioma cells exposed to fractionated radiotherapy in vitro. *Neurosurg. Rev.* **26**, 198–205 (2003).

152. Wild-bode, C., Weller, M., Rimner, A., Dichgans, J. & Wick, W. Sublethal Irradiation Promotes Migration and Invasiveness of Glioma Cells : Implications for Radiotherapy of Human Glioblastoma Sublethal Irradiation Promotes Migration and Invasiveness of Glioma Cells : Implications for Radiotherapy of Human Glioblastoma. 2744–2750 (2001).

153. Giannelli, G., Villa, E. & Lahn, M. Transforming Growth Factor- b as a Therapeutic Target in Hepatocellular Carcinoma. **74**, 1890–1895 (2014).

154. Lefranc, F., Le, E., Kiss, R. & Weller, M. Glioblastoma quo vadis : Will migration and invasiveness reemerge as therapeutic targets ? *Cancer Treat. Rev.* **68**, 145–154 (2018).

155. Levin, V. A. *et al.* Randomized, double-blind, placebo-controlled trial of marimastat in glioblastoma multiforme patients following surgery and irradiation. *J Neurooncol* **78**, 295–302 (2006).

156. Stupp, R. *et al.* Phase I/IIa study of cilengitide and temozolomide with concomitant radiotherapy followed by cilengitide and temozolomide maintenance therapy in patients with newly diagnosed glioblastoma. *J. Clin. Oncol.* **28**, 2712–2718 (2010).

157. Mariani, L. *et al.* Identification and validation of P311 as a glioblastoma invasion gene using laser capture microdissection. *Cancer Res.* **61**, 4190–4196 (2001).

158. Hoelzinger, D. B. *et al.* Gene Expression Profile of Glioblastoma Multiforme Invasive Phenotype Points to New Therapeutic Targets. *Neoplasia* **7**, 7–16 (2006).

159. Demuth, T. *et al.* Glioma cells on the run - The migratory transcriptome of 10 human

Bibliography

glioma cell lines. *BMC Genomics* **9**, 1–15 (2008).

160. Gumireddy, K. *et al.* 6696-Invivo-Metastasis-Gene.Full.Pdf. (2007). doi:10.1073/pnas.0701145104

161. Seo, M., Lee, W.-H. & Suk, K. Identification of novel cell migration-promoting genes by a functional genetic screen. *FASEB J.* **24**, 464–478 (2010).

162. Gobeil, S., Zhu, X., Doillon, C. J. & Green, M. R. A genome-wide shRNA screen identifies GAS1 as a novel melanoma metastasis suppressor gene. *Genes Dev.* **22**, 2932–2940 (2008).

163. Collins, C. S. *et al.* A small interfering RNA screen for modulators of tumor cell motility identifies MAP4K4 as a promigratory kinase. *Proc. Natl. Acad. Sci.* **103**, 3775–3780 (2006).

164. Van Roosmalen, W. *et al.* Tumor cell migration screen identifies SRPK1 as breast cancer metastasis determinant. *J. Clin. Invest.* **125**, 1648–1664 (2015).

165. Bagci, T., Wu, J. K., Pfannl, R., Ilag, L. L. & Jay, D. G. Autocrine semaphorin 3A signaling promotes glioblastoma dispersal. *Oncogene* **28**, 3537–3550 (2009).

166. Li, N. *et al.* Inhibition of GPR158 by microRNA-449a suppresses neural lineage of glioma stem/progenitor cells and correlates with higher glioma grades. *Oncogene* **37**, 4313–4333 (2018).

167. Dossenbach-glaninger, A. *et al.* Plasminogen Activator Inhibitor 1 4G / 5G Polymorphism and Coagulation Factor XIII Val34Leu Polymorphism∶ Impaired Fibrinolysis and Early Pregnancy Loss. **1086**, 1081–1086 (2003).

168. Wind, T., Hansen, M., Jensen, J. K. & Andreasen, P. A. The Molecular Basis for Anti-Proteolytic and Non- Proteolytic Functions of Plasminogen Activator Inhibitor Type-1∶ Roles of the Reactive Centre Loop , the Shutter Region , the Flexible Joint Region and the Small Serpin Fragment. **383**, 21–36 (2002).

169. Seiffert, D. Evidence That Type 1 Plasminogen Activator Inhibitor Binds to the Somatomedin B Domain of Vitronectin ". 2824–2830 (1991).

170. Lawrence, D. A., Berkenpasn, M. B., Palaniappann, S. & Ginsburg, D. Localization of Vitronectin Binding Domain in Plasminogen Activator Inhibitor-l *. **269**, 15223–15228

Bibliography

(1994).

171. Madsen, C. D. *et al.* uPAR-induced cell adhesion and migration: vitronectin provides the key. **177**, 927–939 (2007).

172. Andreasen, P. A., Kjoller, L., Christensen, L. & Duffy, M. J. The urokinase-type plasminogen activator system in cancer metastasis: a review. *Int J Cancer* **72**, 1–22 (1997).

173. Duffy, M. J. The urokinase plasminogen activator system: role in malignancy. *Curr. Pharm. Des.* **10**, 39–49 (2004).

174. Blasi, F. & Carmeliet, P. uPAR : A Versatile Signalling Orchestrator. **3**, 932–943 (2002).

175. Shen, L. J. *et al.* Subdivision of M category for nasopharyngeal carcinoma with synchronous metastasis : time to expand the M categorization system. *Chin. J. Cancer* 1–9 (2015). doi:10.1186/s40880-015-0031-9

176. Higgins, P. J. *et al.* PAI-1: An integrator of cell signaling and migration. *Int. J. Cell Biol.* **2011**, (2011).

177. Dellas, C. & Loskutoff, D. J. Historical analysis of PAI-1 from its discovery to its potential role in cell motility and disease. (2005). doi:10.1160/TH05

178. Mashiko, S. *et al.* Inhibition of plasminogen activator inhibitor-1 is a potential therapeutic strategy in ovarian cancer. 253–260 (2015).

179. Geis, T. *et al.* HIF-2alpha-dependent PAI-1 induction contributes to angiogenesis in hepatocellular carcinoma. *Exp. Cell Res.* **331**, 46–57 (2014).

180. Lee, C., Lee, C. & Huang, T. Plasminogen Activator Inhibitor-1 : The Expression , Biological Functions , and Effects on Tumorigenesis and Tumor Cell Adhesion and Migration. (2004).

181. Schmitt, M. *et al.* Cancer therapy trials employing level-of-evidence-1 disease forecast cancer biomarkers uPA and its inhibitor PAI-1. 617–634 (2011).

182. Look, M. P. *et al.* Pooled Analysis of Prognostic Impact of Urokinase-Type Plasminogen Activator and Its Inhibitor PAI-1 in 8377 Breast Cancer Patients. **94**, (2002).

183. Knoop, A. *et al.* Prognostic significance of urokinase-type plasminogen activator and

Bibliography

plasminogen activator inhibitor-I in primary breast cancer. **77**, 932–940 (1998).

184. Niki, M. New prognostic biomarkers and therapeutic effect of bevacizumab for patients with non-small-cell lung cancer. 91–99 (2017).

185. Harbeck, N., Schmitt, M., Meisner, C., Friedel, C. & Untch, M. Ten-year analysis of the prospective multicentre Chemo-N0 trial validates American Society of Clinical Oncology (ASCO) -recommended biomarkers uPA and PAI-1 for therapy decision making in node-negative breast cancer patients q. 1–11 (2013). doi:10.1016/j.ejca.2013.01.007

186. Mazzoccoli, G. *et al.* ARNTL2 and SERPINE1: Potential biomarkers for tumor aggressiveness in colorectal cancer. *J. Cancer Res. Clin. Oncol.* **138**, 501–511 (2012).

187. Robert, C. *et al.* Expression of Plasminogen Activator Inhibitors 1 and 2 in Lung Cancer and Their Role in Tumor Progression 1. **5**, 2094–2102 (1999).

188. Haven, N. Plasminogen Activator Inhibitor-1 is an Independent Poor Prognostic Factor For Survival in Advanced Stage Epithelial Ovarian Cancer Patients. **454**, 449–454 (1998).

189. Palmirotta, R. *et al.* Prognostic value of pre-surgical plasma PAI-1 (plasminogen activator inhibitor-1) levels in breast cancer. *Thromb. Res.* **124**, 403–408 (2009).

190. Watanabe, R. *et al.* Plasma Levels of Total Plasminogen Activator Inhibitor-I (PAI-I) and tPA / PAI-1 Complex in Patients With Disseminated Intravascular Coagulation and Thrombotic Thrombocytopenic Purpura. 229–233

191. Ferroni, P. *et al.* Plasma Plasminogen Activator Inhibitor-1 (PAI-1) Levels in Breast Cancer – Relationship with Clinical Outcome. **1162**, 1153–1161 (2014).

192. Chen, H., Peng, H., Liu, W., Sun, Y. & Su, N. Silencing of plasminogen activator inhibitor-1 suppresses colorectal cancer progression and liver metastasis. *Surgery* 1–10 doi:10.1016/j.surg.2015.04.053

193. Divella, R. *et al.* Tr a n s l a t i o n a l O n c o l o g y Circulating Levels of PAI-1 and Are Predictive of Poor Prognosis in HCC Patients Undergoing TACE 1. *TRANON* **8**, 273–278 (2015).

194. Fina, Æ. *et al.* High expression of cathepsin B and plasminogen activator inhibitor type-

Bibliography

1 are strong predictors of survival in glioblastomas. 745–754 (2009). doi:10.1007/s00401-009-0592-2

195.   Iwadate, Y., Hayama, M., Adachi, A. & Matsutani, T. High Serum Level of Plasminogen Activator Inhibitor-1 Predicts Histological Grade of Intracerebral Gliomas. **418**, 415–418 (2008).

196.   Hjortland, G. O., Bjørnland, K., Pettersen, S., Emilsen, E. & Nesland, J. M. Modulation of glioma cell invasion and motility by adenoviral gene transfer of. 301–309 (2003).

197.   Yu, K. A. R. V & Zagorujko, S. E. I. Increased expression of uPA , uPAR , and PAI-1 in psoriatic skin and in basal cell carcinomas. *Arch. Dermatol. Res.* **309**, 433–442 (2017).

198.   Hirahata, M. *et al.* PAI-1, a target gene of miR-143, regulates invasion and metastasis by upregulating MMP-13 expression of human osteosarcoma. *Cancer Med.* **5**, 892–902 (2016).

199.   Pavón, M. A. *et al.* Enhanced cell migration and apoptosis resistance may underlie the association between high SERPINE1 expression and poor outcome in head and neck carcinoma patients. *Oncotarget* **6**, 29016–29033 (2015).

200.   Zhang, W. *et al.* Endothelial cells promote triple-negative breast cancer cell metastasis via PAI-1 and CCL5 signaling. 276–288 doi:10.1096/fj.201700237RR

201.   Omori, K., Hattori, N., Senoo, T., Takayama, Y. & Masuda, T. Inhibition of Plasminogen Activator Inhibitor- 1 Attenuates Transforming Growth Factor- β -Dependent Epithelial Mesenchymal Transition and Differentiation of Fibroblasts to Myofibroblasts. 1–18 (2016). doi:10.1371/journal.pone.0148969

202.   Wang, X. *et al.* Oxymatrine inhibits the migration of human colorectal carcinoma RKO cells via inhibition of PAI-1 and the TGF- β 1 / Smad signaling pathway. 747–753 (2017). doi:10.3892/or.2016.5292

203.   Lin, X. *et al.* Biochemical and Biophysical Research Communications PAI-1 / PIAS3 / Stat3 / miR-34a forms a positive feedback loop to promote EMT-mediated metastasis through Stat3 signaling in Non-small cell lung cancer. *Biochem. Biophys. Res. Commun.* 1–7 (2017). doi:10.1016/j.bbrc.2017.10.014

204.   Hanekom, G. S., Stubbings, H. M. & Kidson, S. H. The active fraction of plasmatic plasminogen activator inhibitor type 1 as a possible indicator of increased risk for

Bibliography

metastatic melanoma. **26**, 50–59 (2002).

205. Degryse, B. *et al.* The low density lipoprotein receptor-related protein is a motogenic receptor for plasminogen activator inhibitor-1. *J. Biol. Chem.* **279**, 22595–604 (2004).

206. Zhou, A., Huntington, J. A., Pannu, N. S., Carrell, R. W. & Read, R. J. How vitronectin binds PAI-1 to modulate fibrinolysis and cell migration. **10**, 541–544 (2003).

207. Boccaccio, C. & Comoglio, P. M. Review A Functional Role for Hemostasis in Early Cancer Development. 8579–8583 (2005). doi:10.1158/0008-5472.CAN-05-2277

208. Morita, Y. *et al.* Inhibitory Role of Plasminogen Activator Inhibitor-1 in Invasion and Proliferation of HLE Hepatocellular Carcinoma Cells. 747–752 (1999).

209. Chen, S., Henry, D. O., Reczek, P. R. & Wong, M. K. K. Plasminogen activator inhibitor-1 inhibits prostate tumor growth through endothelial apoptosis. **7**, 1227–1237 (2008).

210. Li, S. *et al.* Plasminogen activator inhibitor-1 in cancer research. *Biomed. Pharmacother.* **105**, 83–94 (2018).

211. Fersching, D. M. I. *et al.* Apoptosis-related Biomarkers sFAS , MIF , ICAM-1 and PAI-1 in Serum of Breast Cancer Patients Undergoing Neoadjuvant Chemotherapy. **2058**, 2047–2058 (2012).

212. Alberti, C. *et al.* Ligand-dependent EGFR activation induces the co-expression of IL-6 and PAI-1 via the NFkB pathway in advanced-stage epithelial ovarian cancer. *Oncogene* 4139–4149 (2012). doi:10.1038/onc.2011.572

213. Kasza, A. *et al.* Pro-Inflammatory Cytokines Regulate the Expression of Components Of Plasminogen Activation System in U373MG Astrocytoma Cells. **1**, 187–190 (2001).

214. Lueore, C. L., Fujii, S., Wun, T., Sobel, B. E. & Billadello, J. J. Regulation of the Expression of Type 1 Plasminogen Activator Inhibitor in Hep G 2 Cells by Epidermal Growth Factor". 15845–15848 (1988).

215. Wilkins-port, C. E. *et al.* PAI-1 is a Critical Upstream Regulator of the TGF- β 1 / EGF-Induced Invasive Phenotype in Mutant p53 Human Cutaneous Squamous Cell Carcinoma. **2007**, 8–10 (2007).

216. Kawarada, Y. *et al.* TGF-β induces p53/Smads complex formation in the PAI-1 promoter to activate transcription. *Sci. Rep.* **6**, 1–13 (2016).

Bibliography

217. Sundqvist, A., Zieba, A., Vasilaki, E., Hidalgo, C. H. & So, O. Specific interactions between Smad proteins and AP-1 components determine TGF b -induced breast cancer cell invasion. 1–10 (2012). doi:10.1038/onc.2012.370

218. Pan, X. *et al.* Molecular and Cellular Endocrinology The mechanism and significance of synergistic induction of the expression of plasminogen activator inhibitor-1 by glucocorticoid and transforming growth factor beta in human ovarian cancer cells. *Mol. Cell. Endocrinol.* **407**, 37–45 (2015).

219. Lang, D. S. *et al.* Transforming Growth Factor-Beta Signaling Leads to uPA / PAI-1 Activation and Metastasis : A Study on Human Breast Cancer Tissues. 727–732 (2014). doi:10.1007/s12253-014-9753-2

220. Xu, G., Chakraborty, C. & Lala, P. K. Restoration of TGF- b regulation of plasminogen activator inhibitor-1 in Smad3-restituted human choriocarcinoma cells. **294**, 1079–1086 (2002).

221. Magnussen, S. N. *et al.* Cleavage of the urokinase receptor (uPAR) on oral cancer cells : regulation by transforming growth factor – β 1 (TGF- β 1) and potential effects on migration and invasion. 1–16 (2017). doi:10.1186/s12885-017-3349-7

222. Humbert, L. & Lebrun, J. TGF-beta inhibits human cutaneous melanoma cell migration and invasion through regulation of the plasminogen activator system. *Cell. Signal.* **25**, 490–500 (2013).

223. Konrad, L., Scheiber, J. A., Schwarz, L., Schrader, A. J. & Hofmann, R. Regulatory Peptides TGF- β 1 and TGF- β 2 strongly enhance the secretion of plasminogen activator inhibitor-1 and matrix metalloproteinase-9 of the human prostate cancer cell line PC-3. *Regul. Pept.* **155**, 28–32 (2009).

224. Albo, D. *et al.* Thrombospondin-1 and Transforming Growth Factor Beta- 1 Upregulate Plasminogen Activator Inhibitor Type 1 in Pancreatic Cancer. **69722**, 411–417 (1999).

225. Dimova, E. Y. *et al.* Transcriptional regulation of plasminogen activator inhibitor-1 expression by insulin-like growth factor-1 via MAP kinases and hypoxia-inducible factor-1 in HepG2 cells. **1**, (2005).

226. Tacchini, L., Matteucci, E., Ponti, C. De & Desiderio, M. A. Hepatocyte growth factor signaling regulates transactivation of genes belonging to the plasminogen activation

Bibliography

system via hypoxia inducible factor-1 . **290**, 391–401 (2003).

227. Tienari, J., Alanko, T. & Lehtonen, E. The expression and localization of urokinase-type plasminogen activator and its type 1 inhibitor are regulated by retinoic acid and fibroblast growth factor in human teratocarcinoma cells. **2**, 285–297 (1991).

228. Spence, M. J., Strei, R., Day, D. & Ma, Y. Oncostatin-M Induces Tissue-Type Plasminogen Activator and Plasminogen Activator Inhibitor-1 in Calu-1 Lung Carcinoma Cells 1. **18**, 26–34 (2002).

229. Lman, M. O., Nadia, E. & Enveniste, B. CXCL12-Mediated Induction of Plasminogen Activator Inhibitor-1 Expression in Human CXCR4 Positive Astroglioma Cells. **32**, 573–577 (2009).

230. Physiology, C. Plasminogen Activator Inhibitor 1 Promotes Immunosuppression in Human Non-Small Cell Lung Cancers by Enhancing TGF-B1 Expression in Macrophage. 2201–2211 (2017). doi:10.1159/000486025

231. Strong, A. L. _et al._ Leptin produced by obese adipose stromal / stem cells enhances proliferation and metastasis of estrogen receptor positive breast cancers. _Breast Cancer Res._ 1–16 (2015). doi:10.1186/s13058-015-0622-z

232. Kruithop, E. K. O., Lahm, H., Schuster, W., Tada, M. & Sordat, B. Modulation of the plasminogen activation system by inflammatory cytokines in human colon carcinoma cells. 846–852 (1996).

233. Mohr, C. _et al._ miR-145-dependent targeting of Junctional Adhesion Molecule A and modulation of fascin expression are associated with reduced breast cancer cell motility and invasiveness M Go. 6569–6580 (2010). doi:10.1038/onc.2010.386

234. Villadsen, S. B. _et al._ The miR-143/-145 cluster regulates plasminogen activator inhibitor-1 in bladder cancer. _Br. J. Cancer_ **106**, 366–374 (2012).

235. F, F. T. miR-93/106b and Their Host Gene,. **26**, 1028–1042 (2014).

236. Borjigin, N. _et al._ Biochemical and Biophysical Research Communications TLS-CHOP represses miR-486 expression , inducing upregulation of a metastasis regulator PAI-1 in human myxoid liposarcoma. _Biochem. Biophys. Res. Commun._ **427**, 355–360 (2012).

237. Inhibitor-, P. A. _et al._ miR-30b , Down-Regulated in Gastric Cancer , Promotes

Bibliography

Apoptosis and Suppresses Tumor Growth by Targeting. **9**, 1–12 (2014).

238. Moskalev, E. A. *et al.* Early Epigenetic Downregulation of microRNA-192 Expression Promotes Pancreatic Cancer Progression. 4149–4160 (2016). doi:10.1158/0008-5472.CAN-15-0390

239. Miyagawa, R. *et al.* Increased expression of plasminogen activator inhibitor type-1 (PAI-1) in HEPG2 cells induced by insulin mediated by the 3 0 -untranslated region of the PAI-1 gene and its pharmacologic implications. **1**, 144–150

240. Anfosso, F., Hospitalier, C. & Timone, U. Plasminogen Activator Inhibitor-1 Synthesis in the Human Hepatoma Cell Line Hep G2 Metformin Inhibits the Stimulating Effect of Insulin. 2185–2193

241. Heaton, J. H. & Gelehrter, T. D. Glucocorticoid Induction of Plasminogen Activator and Plasminogen Activator-Inhibitor Messenger RNA in Rat Hepatoma Cells PAI-1 tPA. 349–355 (1989).

242. Ulthoff, G. A. M. & Ayer, C. H. B. Irradiation-Induced Regulation of Plasminogen Activator Inhibitor Type-1 and Vascular Endothelial Growth Factor in Six Human Squamous Cell Carcinoma Lines.,*. **76**, 574–582 (2010).

243. Fujimoto, J., Hori, M., Ichigo, S. & Tamaya, T. Sex Steroids Regulate the E x p r e s s i o n of P l a s m i n o g e n Activator Inhibitor- 1 (PAI- 1) and its m R N A in Uterine E n d o m e t r i a l C a n c e r Cell Line Ishikawa. **59**, 1–8 (1996).

244. Schilling, D. *et al.* hypoxia and irradiation in human head and neck carcinoma cell lines. **1**, 1–11

245. Lee, Y. *et al.* Plasminogen activator inhibitor-1 as regulator of tumor-initiating cell properties in head and neck cancers. 895–904 (2016). doi:10.1002/HED

246. Masuda, T. *et al.* SK-216 , an Inhibitor of Plasminogen Activator Inhibitor-1 , Limits Tumor Progression and Angiogenesis. **12**, 2378–2389 (2013).

247. Fox, S. B. *et al.* Plasminogen activator inhibitor-1 as a measure of vascular remodelling in breast cancer. 236–243 (2001).

248. Ã, M. M. *et al.* Plasminogen activator inhibitor-1 (Pai-1) blockers suppress intestinal polyp formation in Min mice. **29**, 824–829 (2008).

Bibliography

249. Brooks, T. D., Wang, S. W. & Bru, N. XR5967 , a novel modulator of plasminogen activator inhibitor-1 activity , suppresses tumor cell invasion and angiogenesis in vitro. 37–44 doi:10.1097/01.cad.0000109802.38926.03

250. Nakatsuka, E., Sawada, K., Nakamura, K. & Yoshimura, A. Plasminogen activator inhibitor-1 is an independent prognostic factor of ovarian cancer and IMD-4482 , a novel plasminogen activator inhibitor-1 inhibitor , inhibits ovarian cancer peritoneal dissemination. **8**, 89887–89902 (2017).

251. Blake, C. M., Sullenger, B. A., Lawrence, D. A., Fortenberry, Y. M. & Al, B. E. T. Antimetastatic Potential of PAI-1 − Specific RNA Aptamers. **19**, (2009).

252. Fortenberry, Y. M., Brandal, S. M., Carpentier, G., Hemani, M. & Pathak, A. P. Intracellular Expression of PAI-1 Specific Aptamers Alters Breast Cancer Cell Migration , Invasion and Angiogenesis. 1–21 (2016). doi:10.1371/journal.pone.0164288

253. Kubala, M. H. & DeClerck, Y. A. The plasminogen activator inhibitor-1 paradox in cancer: a mechanistic understanding. *Cancer Metastasis Rev.* (2019). doi:10.1007/s10555-019-09806-4

254. Kim, D., Langmead, B. & Salzberg, S. L. HISAT : a fast spliced aligner with low memory requirements. *Nat. Methods* (2015). doi:10.1038/nmeth.3317

255. Li, H. *et al.* The Sequence Alignment/Map format and SAMtools. *Bioinformatics* **25**, 2078–2079 (2009).

256. Liao, Y., Smyth, G. K. & Shi, W. FeatureCounts: An efficient general purpose program for assigning sequence reads to genomic features. *Bioinformatics* **30**, 923–930 (2014).

257. Love, M. I., Huber, W. & Anders, S. Moderated estimation of fold change and dispersion for RNA-seq data with DESeq2. *Genome Biol.* **15**, 1–21 (2014).

258. Krämer, A., Green, J., Pollard, J. & Tugendreich, S. Causal analysis approaches in ingenuity pathway analysis. *Bioinformatics* **30**, 523–530 (2014).

259. Onder, T. T. *et al.* Loss of E-cadherin promotes metastasis via multiple downstream transcriptional pathways. *Cancer Res.* **68**, 3645–3654 (2008).

260. Olson, a, Sheth, N., Lee, J. S., Hannon, G. & Sachidanandam, R. RNAi Codex: a portal/database for short-hairpin RNA (shRNA) gene-silencing constructs. *Nucleic Acids*

Bibliography

Res. **34**, D153–D157 (2006).

261. Onder, T. T. *et al.* Chromatin-modifying enzymes as modulators of reprogramming. *Nature* **483**, 598–602 (2012).

262. Bagci-Onder, T. *et al.* Real-time imaging of the dynamics of death receptors and therapeutics that overcome TRAIL resistance in tumors. *Oncogene* **32**, 2818–2827 (2012).

263. Weng, Y. *et al.* In-Depth Proteomic Quantification of Cell Secretome in Serum-Containing Conditioned Medium. *Anal. Chem.* **88**, 4971–4978 (2016).

264. Aydin, O., Aksoy, B., Akalin, O. B., Bayraktar, H. & Alaca, B. E. Time-resolved local strain tracking microscopy for cell mechanics. *Rev. Sci. Instrum.* **87**, (2016).

265. Ii, S. & Iv, S. Methods of Digital Video Microscopy for Colloidal Studies. *J. Colloid Interface Sci.* **310**, 298–310 (1996).

266. Bagci-Onder, T., Wakimoto, H., Anderegg, M., Cameron, C. & Shah, K. A dual PI3K/mTOR inhibitor, PI-103, cooperates with stem cell-delivered TRAIL in experimental glioma models. *Cancer Res.* **71**, 154–163 (2011).

267. Kamikubo, Y., Neels, J. G. & Degryse, B. Vitronectin inhibits plasminogen activator inhibitor-1-induced signalling and chemotaxis by blocking plasminogen activator inhibitor-1 binding to the low-density lipoprotein receptor-related protein. *Int. J. Biochem. Cell Biol.* **41**, 578–585 (2009).

268. Kunz-Schughart, L. A., Freyer, J. P., Hofstaedter, F. & Ebner, R. The use of 3-D cultures for high-throughput screening: The multicellular spheroid model. *J. Biomol. Screen.* **9**, 273–285 (2004).

269. Giese, A. *et al.* Dichotomy of Astrocytoma Migration and Proliferation. **282**, 275–282 (1996).

270. Article, O. Plasminogen activator inhibitor-1 and vitronectin expression level and stoichiometry regulate vascular smooth muscle cell migration through physiological collagen matrices. 1847–1854 (2010). doi:10.1111/j.1538-7836.2010.03907.x

271. Freytag, J. *et al.* PAI-1 Regulates the Invasive Phenotype in Human Cutaneous Squamous Cell Carcinoma. *J. Oncol.* **2009**, 963209 (2009).

Bibliography

272. Hsu, J. B., Chang, T., Lee, G. A., Lee, T. & Chen, C. Identification of potential biomarkers related to glioma survival by gene expression profile analysis. *BMC Med. Genomics* **11**, 1–18 (2019).

273. Patil, V. & Mahalingam, K. Comprehensive analysis of Reverse Phase Protein Array data reveals characteristic unique proteomic signatures for glioblastoma subtypes. *Gene* **685**, 85–95 (2019).

274. Providence, K. M., Kutz, S. M., Staiano-Coico, L. & Higgins, P. J. PAI-1 gene expression is regionally induced in wounded epithelial cell monolayers and required for injury repair. *J. Cell. Physiol.* **182**, 269–280 (2000).

275. Providence, K. M. *et al.* Epithelial monolayer wounding stimulates binding of USF-1 to an E-box motif in the plasminogen activator inhibitor type 1 gene. *J. Cell Sci.* **115**, 3767–3777 (2002).

276. Providence, K. M. & Higgins, P. J. PAI-1 expression is required for epithelial cell migration in two distinct phases of in vitro wound repair. *J. Cell. Physiol.* **200**, 297–308 (2004).

277. Zhang, Q. *et al.* Crosstalk of Hypoxia-Mediated Signaling Pathways in Upregulating Plasminogen Activator Inhibitor-1 Expression in Keloid Fibroblasts. *J. Cell. Physiol.* **199**, 89–97 (2004).

278. Oda, T. *et al.* PAI-1 deficiency attenuates the fibrogenic response to ureteral obstruction. *Kidney Int.* **60**, 587–596 (2001).

279. Wu, D. M. *et al.* MircoRNA-1275 promotes proliferation, invasion and migration of glioma cells via SERPINE1. *J. Cell. Mol. Med.* 4963–4974 (2018). doi:10.1111/jcmm.13760

280. Codó, P. *et al.* Control of glioma cell migration and invasiveness by GDF-15. *Oncotarget* **7**, Epub ahead of print (2016).

281. Maziveyi, M. & Alahari, S. K. Cell matrix adhesions in cancer : The proteins that form the glue. **8**, 48471–48487 (2017).

282. Akkawi, S., Nassar, T., Tarshis, M., Cines, D. B. & Higazi, A. A.-R. LRP and alphavbeta3 mediate tPA activation of smooth muscle cells. *Am. J. Physiol. Heart Circ. Physiol.* **291**, H1351–H1359 (2006).

Bibliography

283. Czekay, R. P. & Loskutoff, D. J. Plasminogen activator inhibitors regulate cell adhesion through a uPAR-dependent mechanism. *J. Cell. Physiol.* **220**, 655–663 (2009).

284. Pavón, M. A. *et al.* uPA/uPAR and SERPINE1 in head and neck cancer: role in tumor resistance, metastasis, prognosis and therapy. *Oncotarget* **7**, 57351–57366 (2016).

285. Fink, T., Kazlauskas, A., Poellinger, L., Ebbesen, P. & Zachar, V. Identification of a tightly regulated hypoxia-response element in the promoter of human plasminogen activator inhibitor-1. *Blood* **99**, 2077–2083 (2002).

286. Stupp, R. *et al.* Cilengitide combined with standard treatment for patients with newly diagnosed glioblastoma with methylated MGMT promoter (CENTRIC EORTC 26071-22072 study): a multicentre, randomised, open-label, phase 3 trial. *Lancet. Oncol.* **15**, 1100–1108 (2014).

287. Foekens, B. J. A. *et al.* in Primary Breast Cancer. **12**, 1648–1658 (2019).